Instituto de Bioquímica Vegetal y Fotosíntesis

Departamento de Bioquímica Vegetal y Biología Molecular

Universidad de Sevilla - CSIC

The function of plant chloroplast redox systems in adaptation to light

Trabajo realizado para optar al grado de Doctora por la Universidad de Sevilla por la licenciada

Belén Naranjo Río-Miranda

Septiembre, 2015

Directores de la Tesis

Dr. Francisco Javier Cejudo Fernández

Catedrático de Bioquímica y Biología Molecular

Dra. Anna Marika Lindahl

Científico Titular del Consejo Superior de Investigaciones Científicas

AGRADECIMIENTOS

El trabajo presentado en esta tesis ha sido realizado en el Instituto de Bioquímica Vegetal y Fotosíntesis (Universidad de Sevilla-CSIC) gracias a la concesión de una ayuda Predoctoral de Formación de Personal Investigador por el Ministerio de Economía y Competitividad (BES-2011-045543).

Me gustaría agradecer a mis directores de tesis la posibilidad de haber realizado este trabajo. Al Dr. Javier Cejudo, la confianza depositada en mí habiéndome permitido formarme en su grupo, así como su valiosa aportación de ideas y su disponibilidad. A la Dra. Anna Lindahl, su incesante apoyo en todo este periodo, su implicación en los experimentos realizados y sus buenos consejos.

A mis compañeros de laboratorio, tanto presentes, Mari Cruz, Juan, Vicky y Valle, como pasados, Manolo, Bea, Julia y Leo, que han hecho de éste un sitio agradable. Gracias Juan y Leo por todas las dudas resueltas y Vicky y Valle por vuestra compañía, risas y apoyo, que facilitan el trabajo.

Agradecer también a Julia, Paula y Bea que me ayudaron a empezar en el IBVF. A las personas que he conocido en este centro y con quienes he compartido tantos desayunos, comidas y buenos momentos. Y a Leo y Sandy, que siempre han estado ahí.

A la gente de París, donde tan a gusto estuve. Kathleen y Catherine por ayudarme con todo y por supuesto Anja, a quien agradezco también todos sus consejos y su preocupación por mí.

A esas personas que he ido conociendo gracias a la ciencia en distintos momentos y que me han motivado a seguir. Carlos, Isa, M. Valle, Nerea, Blanca, Cristina…

A Jr, con quien todo empezó y tanto he aprendido.

A Laura, Hugo, Tasia, Nacho, María, Ana… mis amigos de siempre, que desde hace ya muchos años sé que están ahí y me alegra saber que puedo contar con ellos.

A Jerome, esto no hubiese sido lo mismo sin él, por su paciencia y cariño.

A mis abuelos, que tanto se han preocupado por mí.

Y por supuesto, a mis padres y hermanos, por su paciencia y apoyo incondicional, que me ayudan a tomar decisiones y avanzar, gracias por ser como sois y estar siempre ahí.

INDEX

INDEX

INDEX

FIGURES

TABLES

ABBREVIATIONS

ABA	Abscisic acid
ADP	Adenosine diphosphate
ATP	Adenosine triphosphate
Ax	Antheraxanthin
cDNA	Complementary DNA
CEF	Cyclic electron flow
Chl	Chlorophyll
CDS	Coding sequences
CTAB	Cetyltrimethylammonium bromide
Cyt	Cytochrome
DNA	Deoxyribonucleic acid
DTT	Dithiothreitol
ECS	Electrochromic shift
EDTA	Ethylenediaminetetraacetic acid
EPR	Electron paramagnetic resonance
ETR	Electron transport rate
FAD	Flavin adenine dinucleotide
FBPase	Fructose 1,6-bisphosphatase
Fd	Ferredoxin
FNR	Ferredoxin-$NADP^+$ reductase
FPLC	Fast protein liquid chromatography
FQR	Ferredoxin-plastoquinone reductase
FR	Far red
FTR	Ferredoxin-thioredoxin reductase
g	Gram
g	Standard gravity
h	Hour
HEPES	4- (2-hydroxyethyl) -1-piperazineethanesulfonic acid
HL	High light
HPLC	High-performance liquid chromatography
HRP	Horseradish peroxidase
IPTG	Isopropyl-β-thio galactopyranoside
kDa	Kilodalton
l	Litre
LEF	Linear electron flow
LHC	Light harvesting complex
m	Metre
M	Molar
min	Minute
MMPEG	Methyl-polyethylene glycol-maleimide
NADPH	Nicotinamide adenine dinucleotide phosphate
NCBI	National Center for Biotechnology Information
NDH	Nicotinamide adenine dinucleotide dehydrogenase
NPQ	Non-photochemical quenching
NTR	NADPH-dependent thioredoxin reductase
PAGE	Polyacrylamide gel electrophoresis

PAM	Pulse-amplitude modulation fluorometer
PAR	Photosynthetically active radiation
PC	Plastocyanin
PCR	Polymerase chain reaction
PEF	Pseudocyclic electron flow
PET	Photosynthetic electron transport
Pi	Inorganic phosphate
PIF	Post-illumination fluorescence
pmf	Proton motive force
PQ	Plastoquinone
Prx	Peroxiredoxin
PSI	Photosystem I
PSII	Photosystem II
Phe	Pheophytin
qE	Energy-dependent quenching
qI	Photoinhibition quenching
qP	Photochemical quenching
qT	State transition quenching
RC	Reaction centre
RNA	Ribonucleic acid
RT-qPCR	Real-time quantitative PCR
ROS	Reactive oxygen species
s	Second
SD	Standard deviation
SDS	Sodium dodecyl sulphate
SE	Standard error
SP	Saturation pulse
T-DNA	Transfer DNA
TAIR	The *Arabidopsis* Information Resource
TCA	Trichloroacetic acid
TL	Thermoluminescence
Trx	Thioredoxin
v/v	Volume/volume
VDE	Violaxanthin de-epoxidase
Vx	Violaxanthin
ZE	Zeaxanthin epoxidase
Zx	Zeaxanthin
w/v	Weight/volume
wt	Wild type
ΔpH	Proton gradient
4-POBN	4-pyridyl-1-oxide-N-tert-butylnitrone

NITROGENOUS BASES

A	Adenine
C	Cytosine
G	Guanine
T	Thymine

AMINO ACIDS

A	Ala	Alanine	L	Leu	Leucine
R	Arg	Arginine	K	Lys	Lysine
N	Asn	Asparagine	M	Met	Methionine
D	Asp	Aspartic acid	F	Phe	Phenylalanine
C	Cys	Cysteine	P	Pro	Proline
E	Glu	Glutamic acid	S	Ser	Serine
Q	Gln	Glutamine	T	Thr	Threonine
G	Gly	Glycine	W	Trp	Tryptophan
H	His	Histidine	Y	Tyr	Tyrosine
I	Ile	Isoleucine	V	Val	Valine

INTRODUCTION

1. INTRODUCTION

1.1. Plants and life

Plants, along with algae and cyanobacteria, belong to the group of photosynthetic organisms. They are responsible for the current life conditions on Earth. Due to their ability to use light energy for reduction and fixation of carbon dioxide to carbohydrates, a process referred to as photosynthesis, plants are a source of energy and organic material for the rest of the organisms. Moreover, since the ultimate source of electrons is water, molecular oxygen is evolved and this photosynthesis is known as oxygenic.

Oxygenic photosynthesis plays an essential role for the aerobic life on Earth. This process is critical for maintaining oxygen levels in the atmosphere and has allowed the development of the existing life forms. Atmospheric dioxygen, which is a by-product of photosynthesis, is used in cellular respiration and other biological oxidation processes. In addition, photosynthetic organisms constitute an essential machinery for reducing the levels of carbon dioxide in the atmosphere.

From the scientific point of view, these are some of the reasons why plants are interesting subjects of study. Moreover, understanding how this process, optimized over billions of years, works might contribute to the development of technology for renewable energy sources.

1.2. The photosynthetic process in higher plants

During photosynthesis light energy is converted into chemical energy that is used to fix carbon dioxide into carbohydrates. Focusing on the oxygenic photosynthesis of higher plants, the process can be divided into two phases:

- Photochemical reactions: photosynthetic electron transport and photophosphorylation.
- Carbon assimilation: Calvin-Benson cycle.

These reactions take place in different parts of the chloroplast. Photochemical reactions occur in the thylakoid membranes, while carbon assimilation reactions are located in the stroma.

1.2.1. Photochemical reactions: photosynthetic electron transport and photophosphorylation

The first steps of photosynthesis, the harvesting of light and its conversion into chemical energy, are carried out by four multisubunit membrane-protein complexes: photosystem I (PSI) and II (PSII), cytochrome b_6f (Cyt b_6f) and ATP synthase. PSI, PSII and Cyt b_6f, besides other cofactors, are involved in the transport of electrons from water to $NADP^+$ (linear electron transport or Z-scheme) with the associated production of a proton motive force (pmf) (Figure 1). The ATP synthase catalyses generation of ATP coupled to the proton gradient formed across the thylakoid membrane during photosynthetic electron transport (PET) (Figure 1).

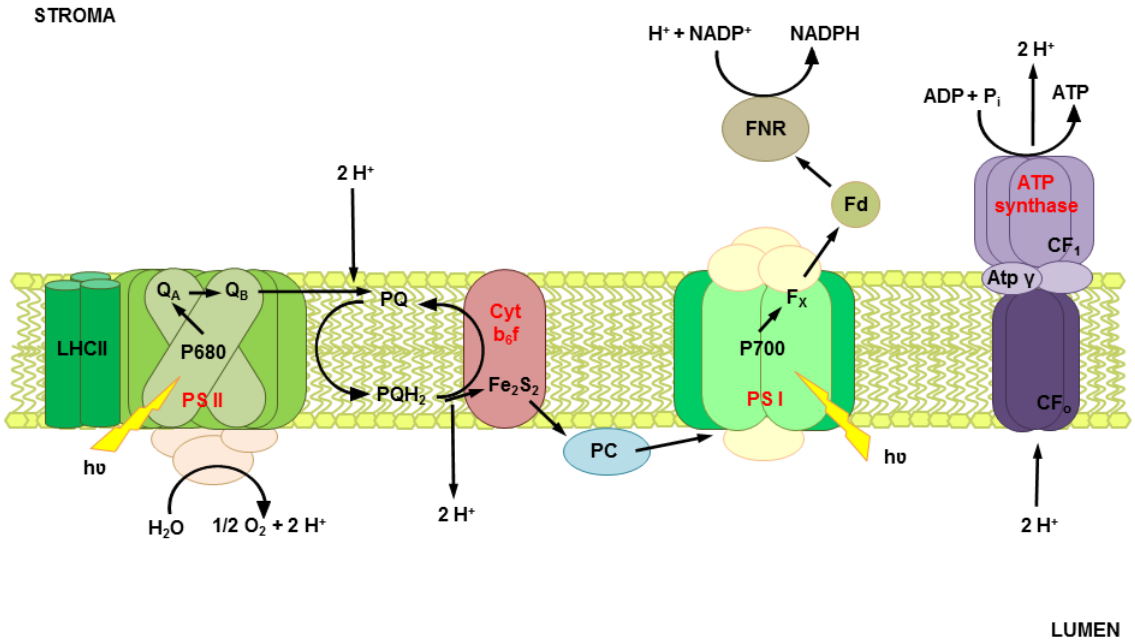

Figure 1. Linear electron transport and photophosphorylation. Photosystem I (PSI) and II (PSII), cytochrome b_6f (Cyt b_6f) and other elements such as plastoquinone (PQ) and plastocyanin (PC) molecules are involved in the transfer of electrons from H_2O to $NADP^+$ producing NADPH. The ATP synthase catalyses generation of ATP coupled to the proton gradient formed during photosynthetic electron transport (photophosphorylation). Light energy is captured by pigments in the light harvesting complexes (LHC) associated to PSI and PSII.

The entire process is light-dependent and, thus, several types of pigments bound to photosystems I and II allow the uptake of light energy by absorbing photons at different wavelengths in the visible part of the electromagnetic spectrum. The most abundant pigment is chlorophyll (Chl), a tetrapyrrole with a magnesium atom at the centre of the ring and a hydrophobic phytyl chain. In plants, there are two kinds of chlorophylls, *a* and *b* (Chl *b* is synthesized from the *a*-form by conversion of a methyl- to a formyl group), and their maximum absorbance in the red region of the visible spectrum are at 665 and 653 nm, respectively. Other pigments present in photosynthetic organisms are carotenoids that absorb light of lower wavelengths than chlorophylls, about 480 nm, and comprise the carotenes and the xanthophylls. The carotenoids act not only as accessory pigments harvesting light, but also as structural components having a protective role against photodamage.

Photosynthetic pigments together with a group of various pigment-binding proteins constitute the antenna, or light-harvesting complex (LHC). Light energy captured is transferred to the reaction centres (RC), where it is converted to electrical energy through charge separation. Each photosystem is composed of the RC and the surrounding LHC. Depending on the maximum absorbance wavelength the RC chlorophylls are referred to as P700, in PSI, or P680, in PSII. The Cyt b_6f complex provides a connection for transfer of electrons between both photosystems.

Photosystem II

PSII is a complex where the light-driven splitting of water takes place producing the concomitant reduction of the plastoquinone (PQ) pool. The PQs are membrane-soluble electron carrier intermediates, which transfer reducing equivalents to the next membrane complex, Cyt b_6f.

The LHC of PSII (LHCII), responsible for light-absorption, contains chlorophylls *a*, *b* and carotenoids attached to different chlorophyll *a*/*b*-binding proteins (Lhcb proteins). The minor Lhcb proteins (CP24, CP26 and CP29) are present as monomers and bind approximately 12 Chl molecules. The major Lhcb proteins (Lhcb 1, 2 and 3) can form mixed trimers, which together bind 24 Chl *a*, 18 Chl *b* and 12 carotenoids per trimer (Nevo et al., 2012; Nelson and Junge, 2015).

The number of monomeric and trimeric LHCII associated to each reaction centre of PSII may vary, resulting in an extensive and flexible antenna supercomplex important not only for light absorption, but also for stacking of thylakoid membranes. In fact, LHCII is the most abundant membrane protein in nature. Moreover, the dynamic increases and decreases in its size, play an important role in the long-term adaptation to light intensity and protection of the photosynthetic apparatus against photooxidative damage (Nevo *et al.*, 2012).

The reaction centre of PSII consists of two homologous proteins, D1 and D2, associated with a dimer of Chl *a* (P680). This complex also contains pheophytin (Phe) and PQ molecules, Q_A and Q_B, as electron transport components and the cytochrome b_{559}, which along with β-carotene bound to D2, is involved in protection against photoinduced damage (Barber, 2006). The PSII core multiprotein complex consists of the PSII reaction centre with the addition of two chlorophyll *a*-containing proteins, CP43 and CP47, and a few nuclear-encoded subunits, such as PsbH and PsbS (Nixon et al., 2010).

The D1 protein binds the cofactors of the active branch of the reaction centre and it is subjected to a rapid light-dependent turnover. Because of the oxidizing environment created by the excitation of P680 during illumination, D1 frequently suffers light-induced damage and needs to be continuously replaced by a newly synthesized protein.

The electron transport starts when light induces a charge separation in PSII. The Chl *a* dimer present in the reaction centre is excited (P680*) by a photon and gives the excited electron to the first acceptor, Phe, which rapidly reduces the plastoquinone Q_A that subsequently gives the electron to Q_B, which is the final and more stable acceptor of PSII. After reducing Phe, the oxidised P680 ($P680^+$) produced has a very high redox potential and is oxidising enough to take electrons from water with the concomitant release of oxygen.

The cleavage of water that provides electrons and protons for the photosynthetic process, takes place in the thylakoid lumen of the chloroplast and it is carried out by the oxygen-evolving complex, which forms part of PSII. This complex is linked to P680 by Tyr Z, a redox-active tyrosine residue of the D1 protein. The splitting of water is a four-electron process, so that absorption of four photons is necessary. For each molecule of

O_2 released, four electrons are withdrawn and accumulated to reduce the chlorophyll molecule one by one. This phenomenon takes place at the Mn-Ca cluster of the complex, where four manganese atoms reduce $P680^+$ going through five intermediate S-states (S_0-S_4), which is known as the S-state cycle (Barber, 2006).

There are several extrinsic proteins (PsbO, PsbP, PsbQ) attached to the luminal side of PSII that play a protective role preventing reductants other than water from having access to the high potential molecules generated at the catalytic site of water splitting.

Quinones are highly lipophilic molecules, allowing a rapid lateral diffusion within the lipid bilayer of the thylakoid membrane. The plastoquinone Q_B is loosely bound to PSII and after receiving two electrons from Q_A, it takes up two protons from the stroma and the resultant form, a plastoquinol (PQH_2), is displaced from its binding site in PSII by another oxidised PQ. PQH_2 leaves PSII and reduces the next complex, the Cyt b_6f.

Cytochrome b_6f

The Cyt b_6f is an integral membrane protein complex with plastoquinol-plastocyanin oxidoreductase activity. Electrons from plastoquinol are transferred to Cyt b_6f and then to PSI with plastocyanin (PC) as electron transfer intermediate. This complex is uniformly distributed in the thylakoid membrane and provides a connection between PSII and PSI. It includes, beside the polypeptides cytochrome f and b_6, with heme-binding sites, a third redox protein with a Fe_2S_2 prosthetic group (Rieske iron-sulphur centre) coordinated by cysteine (Cys) and histidine (His) residues, a quinone-binding protein (subunit IV) and some peripheral proteins necessary for assembly and stability of the complex (Baniulis *et al.*, 2008).

Electrons from plastoquinol can follow two pathways at the Cyt b_6f. The high potential pathway drives electrons through the Rieske iron-sulphur subunit and cytochrome f to PC, while the low potential pathway involves the Cyt b_6 and acts as a Q-cycle, returning the second electron from plastoquinol to the PQ-pool, allowing the net transport of two protons from the stromal side to the lumen, which helps driving the ATP synthesis (Baniulis *et al.*, 2008). Electrons from Cyt b_6f are rapidly transferred to

PSI by a pool of PC, a soluble copper-containing protein with high mobility located in the thylakoid lumen.

Photosystem I

PSI is the last complex in the electron transport chain. It accepts electrons from a pool of plastocyanin to reduce ferredoxin (Fd) located on the stromal side of the thylakoid. The plastocyanin-ferredoxin oxidoreductase activity of PSI is dependent on light. The light energy is captured by the light harvesting complex bound to PSI (LHCI), which binds chlorophylls *a* and *b* and carotenoids. The LHCI complex consists of two heterodimers formed by the antenna proteins Lhca1-4 and Lhca2-3. Each of these proteins binds approximately 15 chlorophyll *a* or *b* molecules, besides some carotenoids (Nevo *et al.*, 2012).

The reaction centre of PSI is constituted by a dimer of chlorophyll *a* (P700) bound to the PSI protein subunits PsaA (the active branch) and PsaB, together with other electron acceptors, including the Fe_4S_4 clusters (F_X, F_A, F_B) and phylloquinone molecules (Nelson and Junge, 2015). When P700 is photoexcited, it oxidizes the PC arriving from Cyt b_6f, transferring its electron to the first stable acceptor, F_X (A_2), via Chl *a* (A_0) and phylloquinone (A_1). F_A and F_B are secondary electron acceptors bound to the stromal subunit PsaC, which acts as intermediates between F_X and Fd. Ultimately, $NADP^+$ is reduced in a reaction catalysed by ferredoxin-$NADP^+$ reductase (FNR). Since Fd is a one-electron carrier, FNR must receive electrons from two Fd molecules before a molecule of $NADP^+$ can be reduced.

ATP synthase

The CF_oCF_1-ATP synthase is a multiprotein complex located in the stroma lamellae of the thylakoid membrane that catalyses the synthesis of ATP from ADP and inorganic phosphate (P_i) using the proton gradient formed across this membrane during PET. This process is referred to as photophosphorylation. The accumulation of protons in the lumen, during the light phase of photosynthesis, occurs as water is cleaved in PSII, and during the Q-cycle, in Cyt b_6f.

The ATP synthase consists of two components, one of them soluble and peripheral to the membrane, CF_1, and the other, CF_o, is integral. Both parts are constituted by different subunits: $a_1b_2c_{10\text{-}15}$ (CF_o) and $\alpha_3\beta_3\gamma_1\delta_1\varepsilon_1$ (CF_1). There is a rotational movement of the γ subunit against the $\alpha_3\beta_3$ core during catalytic reactions. CF_1 possesses ATP hydrolytic activity (CF_1-ATPase) when the proton gradient is not available for ATP synthesis. Therefore, the regulation of the ATP synthase enzyme is essential to achieve an efficient ATP synthesis and to avoid futile ATP hydrolysis. In addition to other regulatory mechanisms, e. g. inhibition by ADP, the CF_1-ATPase can be inactivated through the formation of an intrapeptide disulphide bond between two Cys residues present in the γ subunit. Conversely, the enzyme is activated through reduction of this disulphide bond (Mills et al., 1980; Hisabori et al., 2013). In dark-adapted leaves, the enzyme is found in the oxidised form (Konno *et al.*, 2012). The inactivation of the enzyme in darkness seems to be critical to maintain ATP levels in the cell. In that way, the redox switch of the ATP synthase allows its regulation under transient light conditions (Hisabori *et al.*, 2013).

Alternative electron pathways

In addition to the linear electron transport described above, there is a cyclic electron flow (CEF) around PSI implying two different pathways, involving either a complex termed NDH (NAD(P)H dehydrogenase) or mediated by the PGR5 and PGRL1 (proton gradient regulation 5 and L1, respectively) proteins. In both cases, electrons from Fd (reduced by PSI) are transferred back to PQ and subsequently to Cyt b_6f and finally returned to PSI again via PC (Figure 2). Hence, the proton gradient keeps forming through the Q-cycle and, consequently, ATP synthesis takes place, which in this case is known as cyclic phosphorylation. However, during CEF there is not a net production of NADPH, water is not split and molecular oxygen is not released. The differences between these CEF pathways are in the intermediates of each one between Fd and PQ, although the mechanisms are not completely understood.

The NDH complex is responsible for part of the CEF (Shikanai *et al.*, 1998). It is not clear whether the NDH complex acts as an NADPH dehydrogenase or takes electrons from Fd directly (Johnson and Ruban, 2011; Shikanai, 2014). In addition, the formation of a supercomplex in association with PSI required for the stabilization of the

NDH complex has been found (Peng et al., 2008; Peng et al., 2009; Suorsa et al., 2009; Peng and Shikanai, 2011).

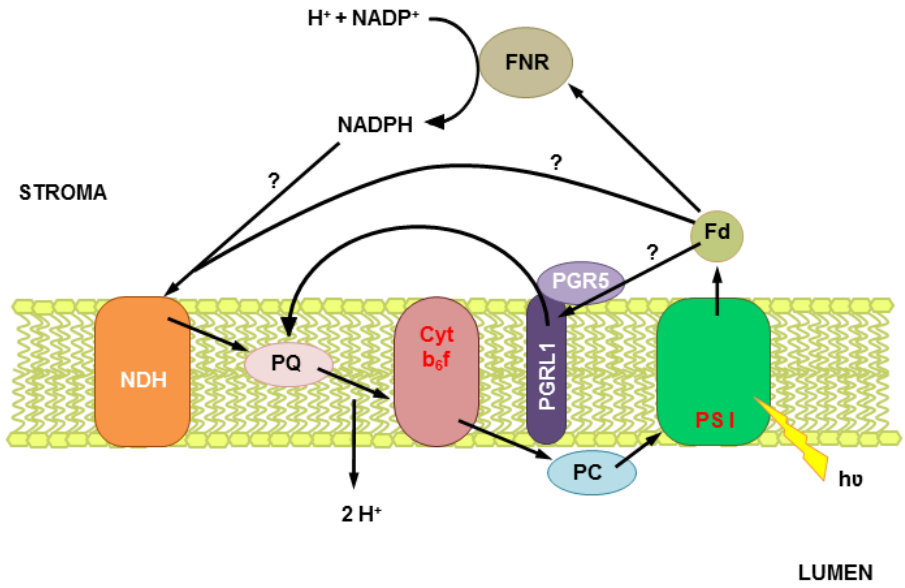

Figure 2. Cyclic electron flow. Electrons from photosystem I (PSI), trough ferredoxin (Fd), may reduce the plastoquinone (PQ) pool without net NADPH production. Two different pathways of cyclic electron flow are operative around PSI, one of them involves the NAD(P)H dehydrogenase (NDH) complex and the other is mediated by the PGR5 and PGRL1 proteins. The proton gradient keeps forming through the Q-cycle.

PGR5 is a peripheral protein located at the stromal side of thylakoids (DalCorso *et al.*, 2008), which contributes strongly to the acidification of the thylakoid lumen and it is involved in the transfer of electrons from Fd to PQ in the CEF, without NADPH oxidation (Munekage *et al.*, 2002). Consequently, *Arabidopsis pgr5* mutants, lacking the PGR5 protein, display a reduced induction of thermal dissipation under excessive light conditions - a process, which is dependent on ΔpH (Munekage *et al.*, 2002; Suorsa *et al.*, 2012). Moreover, PGR5 has been ascribed an essential role in photoprotection of PSI, since increased ΔpH leads to downregulation of PSII and Cyt b_6f resulting in a decrease of electron flow to PSI (Munekage *et al.*, 2002; Suorsa *et al.*, 2012). Recently, a novel thylakoid transmembrane protein was discovered, PGRL1, that interacts with PGR5 and is also necessary for CEF via Fd (DalCorso *et al.*, 2008). It seems that both proteins interact with PSI and Cyt b_6f to allow efficient CEF. Hence, PGRL1 acts as a

ferredoxin-plastoquinone reductase (FQR) in a PGR5-dependent manner and its activity could be controlled by thioredoxins (Trxs) (Hertle *et al.*, 2013).

It is worth highlighting that protons are translocated to the lumen through both the NDH-dependent pathway (Munekage et al., 2004; Livingston et al., 2010) and the PGR5-dependent pathway (Munekage et al., 2002; Munekage et al., 2004). In addition to generation of the proton motive force necessary for ATP synthesis, CEF might contribute to PET regulation through triggering mechanisms for excess energy dissipation as we will see below. However, the relevance of CEF in the activation of thermal energy dissipation has been debated, since any increase in CEF also involves an increase in ATP synthesis, which consumes the proton gradient (Kramer *et al.*, 2004a).

During CEF, ATP is synthetized without NADPH net production, in contrast to linear electron flow (LEF). Therefore, the balance between linear and cyclic electron transport determines the ratio between ATP and NADPH, allowing the adaptation to the demands of different metabolic pathways and the redox state of the chloroplast (Allen, 2003; Kramer *et al.*, 2004a). The PGR5/PGRL1-dependent CEF appears to function mainly in photoprotection and in balancing the ATP/NADPH ratio, whereas the NDH-dependent route is thought to be more important in preventing over-reduction of the stromal electron acceptors (Shikanai, 2007).

LEF is the predominant pathway of electrons through the thylakoid membrane, and yet, it must compete with CEF at the point where reducing equivalents enter the chain via intersystem electron carriers (Joliot and Johnson, 2011). However, the regulatory mechanisms behind the switch between LEF and CEF are still poorly understood. Moreover, reduced Fd may supply electrons not only to PQ in the CEF, but also to the enzymes FNR, to produce NADPH, ferredoxin-thioredoxin reductase (FTR), to reduce Trxs, or to other metabolic pathways (Johnson, 2011; Joliot and Johnson, 2011).

A possible control point for LEF/CEF regulation could be at the Cyt b_6f with a central position in both electron transport chains, since the association of FNR (Zhang *et al.*, 2001), PGRL1 and PGR5 (DalCorso *et al.*, 2008) with this complex has been reported. A structural model for CEF has been proposed in which electrons are trapped within these supercomplexes that associate Cyt b_6f, FNR, PGR5 and PGRL1 (cyclic configuration). When FNR is not bound to Cyt b_6f (linear configuration), electrons

would be lost for CEF and transferred to the Calvin-Benson cycle via NADPH (Joliot and Joliot, 2002; Joliot and Johnson, 2011).

There is another alternative pathway that can accept electrons from PSI, reducing molecular oxygen instead of $NADP^+$ or PQ. It is known as the pseudocyclic electron flow (PEF) or water-water cycle (Allen, 2003). This electron flux also contributes to thylakoid lumen acidification with the concomitant synthesis of ATP (pseudocyclic phosphorylation) and competes with CEF for electrons. However, since molecular oxygen is the last electron acceptor, superoxide anion radicals are produced (Mehler reaction) and therefore, subsequent enzymatic detoxification of reactive oxygen species (ROS) is required (Heber, 2002). Superoxide is converted to hydrogen peroxide by superoxide dismutases and the hydrogen peroxide, in turn, is reduced to water by ascorbate peroxidases and peroxiredoxins (Prxs) (Foyer and Noctor, 2009).

In summary, different PET pathways are possible, in each case forming a proton gradient that allows the synthesis of ATP, but differing with respect to electron acceptors downstream PSI and, consequently, the production of NADPH. The three pathways, LEF, CEF or PEF, are in competition for electrons and photosynthetic machinery. In LEF, as well as in PEF, PSII and PSI operate in series, whereas the CEF is driven by PSI alone. Although LEF represents the predominant pathway, the balance between them seems to be important to allow acclimation to different environmental conditions.

1.2.2. Carbon assimilation: The Calvin-Benson cycle

The second part of the photosynthetic process consists of CO_2 assimilation. It requires ATP and NADPH produced during the photochemical reactions and takes place in the chloroplast stroma. This process can be divided into three phases: carboxylation, reduction and regeneration. The reactions of the three phases constitute the Calvin-Benson cycle (Figure 3), also called the reductive pentose phosphate pathway.

During carboxylation, CO_2 is added to a five-carbon acceptor molecule, ribulose-1,5-bisphosphate (RuBP), producing two molecules of 3-phosphoglycerate (3-PGA), a three-carbon organic acid. This reaction is catalysed by the enzyme RuBP carboxylase-oxygenase, usually referred to as Rubisco, one of the most abundant

enzymes in nature. In addition, the oxygenase activity of Rubisco may catalyse the reaction between O_2 and a transition state of RuBP, producing 3-PGA and 2-phosphoglycolate that is metabolized through photorespiration. In the light, Rubisco is activated by the action of Rubisco activase that disrupts Rubisco-inhibitor complexes. The Rubisco activase exists in two isoforms, the largest of which is sensitive to redox regulation.

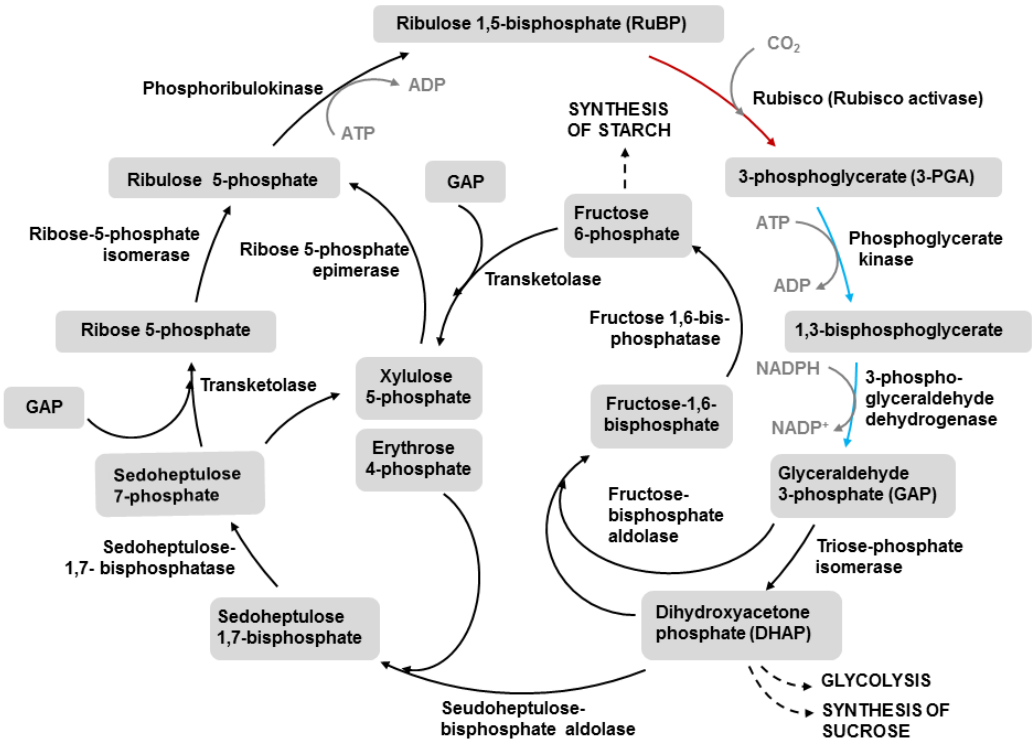

Figure 3. The Calvin-Benson cycle. Carboxylation (red arrow), reduction (blue arrows) and regeneration reactions involved in carbon assimilation which constitutes the Calvin-Benson cycle. ATP and NADPH produced during the photochemical reactions of photosynthesis are required. Adapted from (Lindahl et al., 2011).

A three-carbon sugar, the triose phosphate glyceraldehyde 3-phosphate (GAP), results from the reduction of 3-PGA. One GAP is produced for each 3-PGA, consuming one molecule each of ATP and NADPH. The conversion takes place in two consecutive enzymatic steps, the first catalysed by phosphoglycerate kinase and the second one, by the NADPH-dependent 3-phosphoglyceraldehyde dehydrogenase. GAP is a precursor for sucrose and starch synthesis through conversion into fructose-6-phosphate.

The last phase consist of regeneration of acceptor molecules converting molecules of 3-carbon into 5-carbon intermediates. Ten enzymes are involved and one ATP is consumed for the production of three RuBP from five GAP. One triose represents the net gain of carbon to the plant.

1.3. Light acclimation

Since plants are sessile organisms, their acclimation to the environment is essential to survive adverse conditions. In this context, plants have evolved several mechanisms to sense and to acclimate to different abiotic stresses, among which is the excess of light.

Plants are continuously exposed to light of different qualities and quantities. Excess light means that the light absorbed by the plant exceeds its capacity for light utilization (Figure 4). In this situation, photosynthesis becomes saturated and chloroplasts accumulate elevated levels of ROS, which constitutes an important stress for cells (Foyer and Noctor, 2009). Indeed, highly reactive intermediates could cause photo-oxidative damage to proteins and inhibit photosynthesis (Aro *et al.*, 1993; Li *et al.*, 2009; Tyystjarvi, 2013).

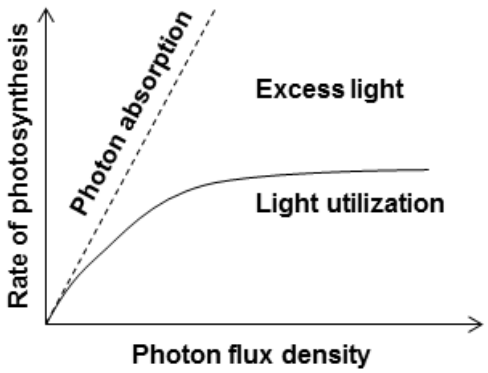

Figure 4. Photon absorption and light utilization. Under elevated photon flux (high light intensities), the photon absorption exceeds the capacity for light utilization and photosynthetic electron transport rates becomes saturated. Adapted from (Li *et al.*, 2009).

Adaptive mechanisms to cope with high light exposure may involve control of the capacity for light absorption, as well as dealing with the light energy that has already been captured. To this end, plants respond at different levels of organization; whole organism level, via leaf movements, cellular level, via chloroplast movements or controlling their number, and molecular level (Ruban *et al.*, 2012).

At the molecular level, plants have a variety of mechanisms under excess light to sense directly a high incident photon flux, using photoreceptors such as cryptochromes, or indirectly, through biochemical and metabolic signals: decrease in thylakoid lumen pH, increase in the reduction state of PQ-pool and thiol groups in chloroplast proteins, production of ROS and perturbation in chlorophyll biosynthesis (Li *et al.*, 2009). All of these signals are then translated into acclimation responses or regulatory mechanisms, such as changes in gene expression or energy dissipation, to protect against photodamage and photoinhibition.

The protective mechanisms operate on different time scale, between minutes and days and may therefore be classified into long- and short-term acclimation responses. The long-term acclimation responses comprise regulation of photosynthetic components, activity of metabolic pathways and antioxidant defence, predominantly by modifying nuclear gene expression, which involves a retrograde signalling between chloroplast and nucleus (Dietz, 2015). Many genes related to light harvesting and antioxidant functions change their expression under high light conditions, such as *ELIP* or *APX* genes, which encode light-stress related proteins belonging to the LHC family and ascorbate peroxidase, respectively (Li et al., 2009; Dietz, 2015). The levels of ELIP and APX proteins increase in response to high irradiance, whereas LHCB is decreased. Long-term adaptation processes mainly lead to alterations of the antenna size depending on the incoming light intensities.

The induction or repression of these excess light-dependent genes is indirectly regulated by the PQ redox state. The excess of light absorption by PSII leads to an overreduction of the PQ-pool that is sensed via Cyt b_6f by kinases, such as STN7 and STN8, which are involved in phosphorylation of LHCII and PSII (Adamiec *et al.*, 2008; Li *et al.*, 2009). Moreover, the ROS generation associated to excess light also regulates gene expression, especially singlet oxygen and H_2O_2 trigger specific transcriptional responses (op den Camp et al., 2003; Vanderauwera et al., 2005; Li et al., 2009). Other

genes regulated by high light are those encoding transcription factors and enzymes involved in tetrapyrrole synthesis. Excess light might have different effects on the accumulation of chlorophyll precursors depending on specific conditions (Li *et al.*, 2009).

Short-term responses that allow plants to rapidly adapt to variations of light intensity are related with the dissipation of the excess energy absorbed by PSII as heat, a phenomenon known as non-photochemical quenching (NPQ). This subject will be discussed below (see 1.3.2.).

1.3.1. Reactive oxygen species production and PSII photoinhibition

Excess light is associated with enhanced generation of ROS in chloroplasts such as hydrogen peroxide (H_2O_2), superoxide (O_2^-), hydroxyl radical ($OH^\cdot$) and singlet oxygen ($^1O_2$). The decrease in photosynthetic efficiency associated with PSII damage, is called photoinhibition.

The major source of ROS generated in chloroplasts is the PET. Electron transfer to molecular oxygen at the acceptor side of PSI can drive the formation of superoxide radicals (Mehler reaction) and, in subsequent reactions, hydrogen peroxide and hydroxyl radicals (Foyer and Noctor, 2009). Moreover, the main ROS responsible for oxidative stress during photosynthesis is considered to be singlet oxygen produced in the reaction centre of PSII (Jahns and Holzwarth, 2012).

The excited state of chlorophyll (Chl*) allows conversion of the excitation energy into an electrochemical potential via charge separation, but if the energy is not efficiently used, the excited chlorophyll can give rise to a triplet state (spontaneous spin change) that corresponds to a lower energy excited state (Figure 5) (Krieger-Liszkay *et al.*, 2008; Ruban *et al.*, 2012). Under excess light, when the PQ-pool is in a highly reduced state and electron donation from P680 to Q_A is inhibited (reaction centres are closed), the chlorophyll triplet state (^{3}Chl*) can be generated also by charge recombination involving a back-flow of electrons from Phe^- to $P680^+$ (Krieger-Liszkay *et al.*, 2008).

The chlorophyll triplet state can react with molecular oxygen (O_2) to produce singlet oxygen ($^1O_2$) (Figure 5), which is considered the most important ROS

responsible for photoinhibition. $^1O_2$ can react with proteins, pigments, nucleic acids and lipids. Therefore, in PSII, $^1O_2$ may damage the reaction centre protein D1 and also cause pigment bleaching (Tyystjarvi, 2013). However, $^1O_2$ is also a signal affecting gene expression and enzyme activation reactions required for maintenance of the components of PSII (Krieger-Liszkay *et al.*, 2008).

In the antenna, where chlorophyll is more abundant than in reaction centres, the excess energy of the excited state is quenched by carotenoids that are close enough and avoid $^1O_2$ production, in contrast to reaction centres where this is not possible because of the location of β-carotenes (Krieger-Liszkay *et al.*, 2008).

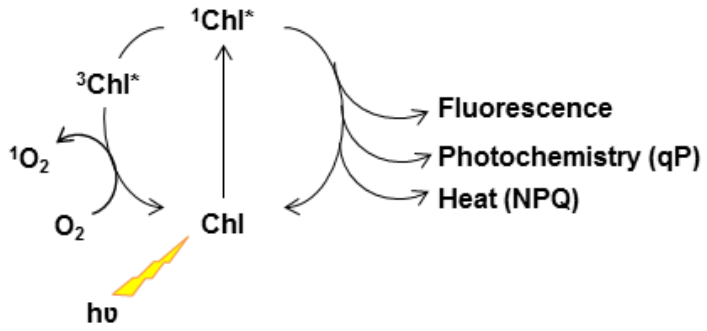

Figure 5. Chlorophyll *a* excitation and relaxation. Light energy absorbed by chlorophylls associated with PSII can be used to drive photochemistry or can be dissipated as chlorophyll fluorescence or heat, coming back the excited chlorophyll (^{1}Chl*) to its basal state (Chl). If the energy is not efficiently used, ^{1}Chl* can give rise to a triplet state (^{3}Chl*) that may react with molecular oxygen (O_2) to produce singlet oxygen ($^1O_2$). Adapted from (Muller *et al.*, 2001).

To avoid accumulation of damaged D1 protein and progressive loss of PSII activity, this protein is subject rapid turnover allowing the removal of the non-functional protein and the insertion of a newly synthesised copy (Aro *et al.*, 1993; Krieger-Liszkay *et al.*, 2008; Tyystjarvi, 2013). After triggering D1 degradation by $^1O_2$ or even a long-lived $P680^+$ radical that oxidizes the nearest pigments (Ruban *et al.*, 2012), PSII is disassembled and the inhibited PSII reaction centre moves to the stroma thylakoids leaving the LHC in the appressed grana regions (Tyystjarvi, 2013). Thereafter, the damaged D1 protein is degraded by FtsH and Deg proteases (Nixon *et al.*, 2010) followed by synthesis *de novo* of a D1 protein that is inserted into the reaction centre

with cofactors and pigments during the reassembly process. The reconstituted and activated reaction centre moves back to the grana thylakoids (Krieger-Liszkay et al., 2008; Tyystjarvi, 2013).

Under moderate light intensities, PSII activity stays constant since even if photoinhibition lowers the number of active PSII centres, the simultaneous repair through new synthesis of D1 protein, restores it. However, very high light intensities or strong light combined with other abiotic stresses, such as cold or low CO_2 may lead to an increase in net photoinhibition (Tyystjarvi, 2013).

1.3.2. Energy dissipation during photosynthesis: Non-Photochemical Quenching

NPQ is a short-term response by which plants, and also eukaryotic algae, dissipate excess absorbed light energy as heat (Szabo *et al.*, 2005). It is necessary to balance the absorption and utilization of light energy. Therefore, under excess light, NPQ minimizes the potential for photooxidative damage, since it regulates the photosynthetic electron transport rate (ETR) (Muller *et al.*, 2001; Szabo *et al.*, 2005).

This phenomenon may be observed as quenching of chlorophyll *a* fluorescence, which is not due to photochemistry. The light absorption in LHCs results in singlet-state excitation of a chlorophyll *a* molecule (^{1}Chl*), which can return to the ground state by different pathways. Excitation energy can be re-emitted as chlorophyll fluorescence, it can be transferred to reaction centres to drive photochemistry, it can be de-excited by thermal dissipation processes or it can decay through formation of the triplet state (^{3}Chl*) (Figure 5) (Muller *et al.*, 2001). The energy, which is diverted to photochemistry or dissipated as heat, results in a fluorescence decrease, or quenching. Therefore, these processes are referred to as photochemical quenching, qP, and non-photochemical quenching, NPQ (or qN), respectively. Both types of quenching favour a shorter lifetime of ^{1}Chl* and consequently decrease the ^{3}Chl* state and ROS formation (Muller *et al.*, 2001).

Using a fluorometer, we can monitor the fluorescence yield of chlorophyll *a* (see Materials and methods), and according to relaxation times, NPQ may be divided into three different components: energy- or ΔpH-dependent quenching (qE), state transition

(qT) and photoinhibition (qI). The relaxation times are seconds, minutes and hours, respectively.

In higher plants, the state transition does not significantly contribute to NPQ, in contrast to algae. It consists of the uncoupling of LHCs from PSII mediated by phosphorylation. The STN7 kinase is involved in the phosphorylation of a fraction of LHCII proteins (Bellafiore *et al.*, 2005) which leads to their redistribution and association with PSI, resulting in reduction of the PSII antenna size and fluorescence quenching. State transitions are favoured under conditions of limiting CO_2 and high reduction level of the chloroplast (Szabo *et al.*, 2005) and their function is related to the excitation energy balance between PSII and PSI.

The mechanism of photoinhibition is an irreversible quenching that involves a long-term down-regulation of PSII. Excess light leads to enhanced photooxidative damage of the D1 protein that may exceed the rate of repair resulting in a net reduction of the photochemically active PSII centres which corresponds to an irreversible decrease in chlorophyll fluorescence (qI). Energy-dependent quenching is the major and most rapid NPQ component in plants. qE constitutes an important protective mechanism and plants with higher capacity to induce qE are more resistant to photoinhibition (Li *et al.*, 2002; Roach and Krieger-Liszkay, 2012).

Energy-dependent quenching

Energy- or ΔpH-dependent quenching is a rapidly inducible and reversible energy dissipation mechanism. qE requires the acidification of the thylakoid lumen, the presence of the PSII S subunit (PsbS) and the xanthophyll zeaxanthin (Zx) (Figure 6). Protonation of PsbS and attachment of Zx to LHCII proteins is suggested to cause a conformational change that leads to quenching of excitation energy (Muller *et al.*, 2001; Szabo *et al.*, 2005).

Under high light conditions, the enzyme violaxanthin de-epoxidase (VDE) converts violaxanthin (Vx) into Zx required for qE. Thereafter, if plants are transferred to darkness or low light conditions, Zx is converted back to Vx through zeaxanthin epoxidase (ZE) (Figure 6) (Szabo *et al.*, 2005). Either Zx or Vx are associated with

trimeric LHCII, bound at the external V1 binding site (Ruban et al., 1999; Jahns and Holzwarth, 2012). The xanthophyll cycle will be described more in detail below.

The PsbS protein, also known as the 22-kDa protein or CP22, is a member of the LHC family of proteins. PsbS is closely associated to the core of PSII and seems to act as a sensor of lumen pH. The protonated form of PsbS promotes switching of the PSII-LHCII unit from a light-harvesting state containing Vx, present in low light and darkness, to an energy-dissipating state containing Zx, present in high light (Niyogi et al., 2005; Jahns et al., 2009).

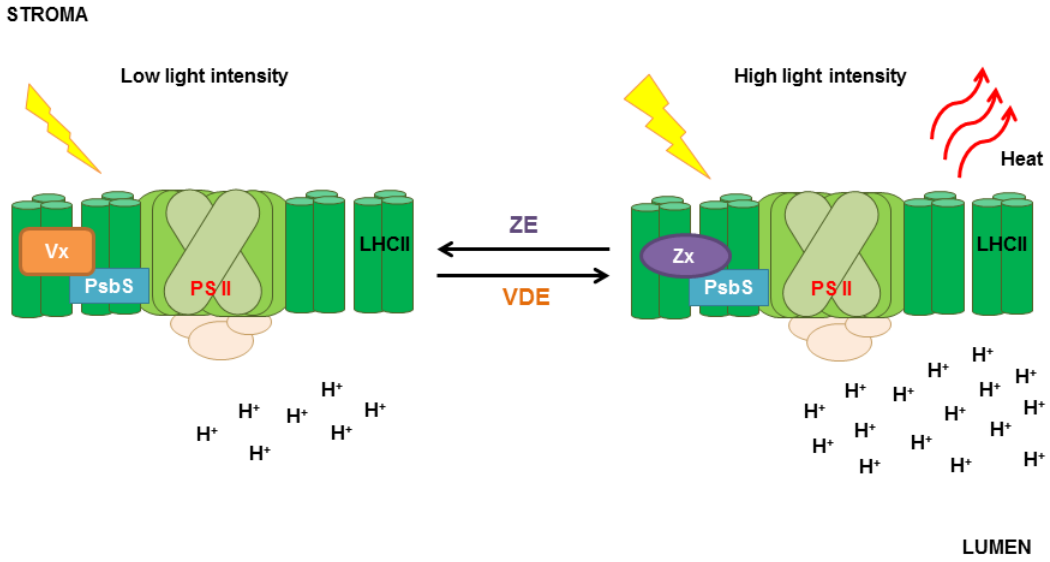

Figure 6. Energy-dependent quenching. The NPQ component dependent of energy, qE, is induced under high light conditions with the acidification of the thylakoid lumen, the presence of the PSII S subunit (PsbS) and the conversion of the xanthophyll violaxanthin (Vx) into zeaxanthin (Zx) by the action of violaxanthin de-epoxidase (VDE). The qE reversion is possible under low light conditions implying the action of zeaxanthin epoxidase (ZE) which converts Zx back into Vx.

Since ΔpH is built up during PET, a sudden decrease in the luminal pH is an immediate signal of excess light. Therefore, variations in pH allow induction or reversal of qE within seconds after a change in light intensity, which is fast enough to cope with natural light fluctuations, to which plants are exposed throughout the day (Muller *et al.*, 2001).

A decrease in luminal pH induces qE through protonation of PsbS and activation of VDE with the concomitant production of Zx. *Arabidopsis thaliana* mutants lacking VDE, npq1 mutants, have greatly reduced NPQ (Niyogi *et al.*, 1998). Similarly, mutants lacking PsbS, npq4 mutants, have hardly any NPQ (Li *et al.*, 2000). In contrast, mutants without ZE, npq2 mutants, accumulate Zx constitutively and present higher levels of NPQ at low and moderate light intensities and a more rapid induction of NPQ (Niyogi *et al.*, 1998). The increase in photoinhibition observed in mutants with deficient NPQ, such as npq4 and even npq1, is indicative of the important role of qE to attenuate photodamage (Roach and Krieger-Liszkay, 2012). In the absence of PsbS, qE can be obtained artificially with a lower pH *in vitro*. Thus, PsbS is required to shift the pK_a of qE to physiologically attainable levels of lumen pH (Johnson and Ruban, 2011). Moreover, the level of PsbS determines the extent of qE and there exists a correlation between capacity to induce qE and the amount of PsbS protein (Li *et al.*, 2002).

Zx is necessary for about 70% of the total NPQ and 80% of qE in *Arabidopsis* (Li *et al.*, 2002). Thus, in the absence of Zx, qE seems to be possible through the action of lutein bound at the L1 site of the antenna (Crouchman *et al.*, 2006; Johnson *et al.*, 2009). Zx also plays a role in the direct quenching of energy from excited chlorophyll, which constitutes an important photoprotective function independent from its function in qE. Thus, Zx acts as antioxidant in the lipid phase or protein/lipid interphase of the thylakoid membrane, preventing lipid peroxidation (Havaux and Niyogi, 1999; Johnson et al., 2007; Jahns and Holzwarth, 2012), even when unbound to proteins (Havaux et al., 2007; Dall'Osto et al., 2010). The Zx epoxidase activity is gradually inhibited after increasing high light stress, which is correlated with the down-regulation of PSII activity. The resulting high levels of Zx enhance the formation of qE and retard its relaxation (Jahns and Holzwarth, 2012).

The xanthophyll cycle

Avoiding photoinhibition under excess light is important for plant survival but it is equally important to optimise light harvesting under light-limiting conditions to permit plant growth. The rapid interchange between violaxanthin and zeaxanthin bound to LHC, allows plants to adapt efficiently to changes in light intensity. The reversible conversion of violaxanthin, Vx, to zeaxanthin, Zx, via the intermediate antheraxanthin,

Ax, is known as the xanthophyll (or violaxanthin) cycle and two enzymes are involved: violaxanthin de-epoxidase, VDE, and zeaxanthin epoxidase, ZE (Figure 7) (Jahns *et al.*, 2009).

VDE catalyses the conversion of Vx into Zx through a two-step reaction in which two epoxy groups are removed from Vx, while ZE catalyses the opposite reaction, the conversion of Zx into Vx, adding two epoxy groups to Zx, also in two steps with Ax as intermediate (Figure 7). Both enzymes are lipocalin proteins located on the opposite sides of the thylakoid membrane: VDE is located in the thylakoid lumen and ZE on the stromal side (Jahns *et al.*, 2009).

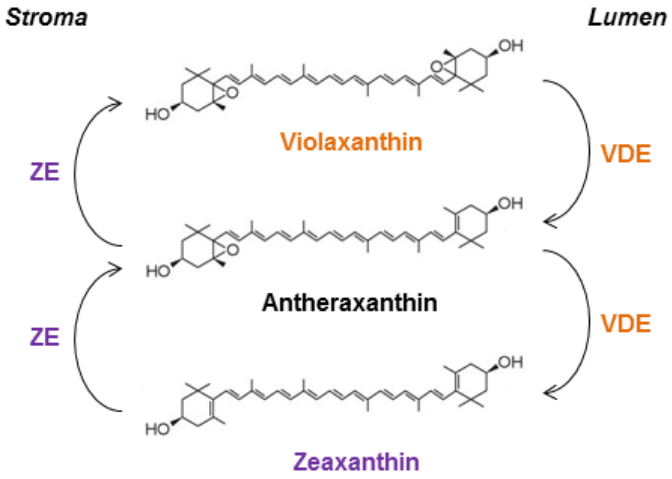

Figure 7. The xanthophyll cycle. The xanthophyll cycle consists of the reversible conversion of violaxanthin (Vx) to zeaxanthin (Zx) via the intermediate antheraxanthin (Ax). Two enzymes are involved: violaxanthin de-epoxidase (VDE), in the thylakoid lumen, and zeaxanthin epoxidase (ZE), on the stromal side. Adapted from (Szabo et al., 2005).

The activity of VDE is strictly controlled by the pH of the thylakoid lumen. The enzyme does not show any activity at pH values greater than 6.3 and shows maximum values at pH values less than 5.8 (Pfundel and Dilley, 1993). This ensures VDE activity and, subsequent Zx accumulation, only under saturating light intensities. Moreover, VDE requires ascorbate as cofactor, which is used as electron donor to the epoxide groups (Yamamoto *et al.*, 1971) and the optimal amount of ascorbate depends on pH

(Bratt *et al.*, 1995). Thus, the de-epoxidation reaction yields Zx, water and oxidised dehydroascorbate.

VDE consists of a lipocalin protein with an N-terminal cysteine-rich region and a C-terminal region enriched in glutamyl residues, both with a high degree of sequence similarity between different plants (Figure 8) (Bugos and Yamamoto, 1996). An inhibitory effect of dithiothreitol (DTT), which reduces disulphide bonds, on VDE activity has been described (Yamamoto and Kamite, 1972).

Zx accumulated at high light intensities is reconverted to Vx by ZE in low light or darkness. ZE is also a lipocalin protein with some conserved cysteines (Figure 8) (Bouvier et al., 1996; Marin et al., 1996) and therefore, potentially susceptible to be redox regulated. However, redox regulation of this enzyme has not been reported.

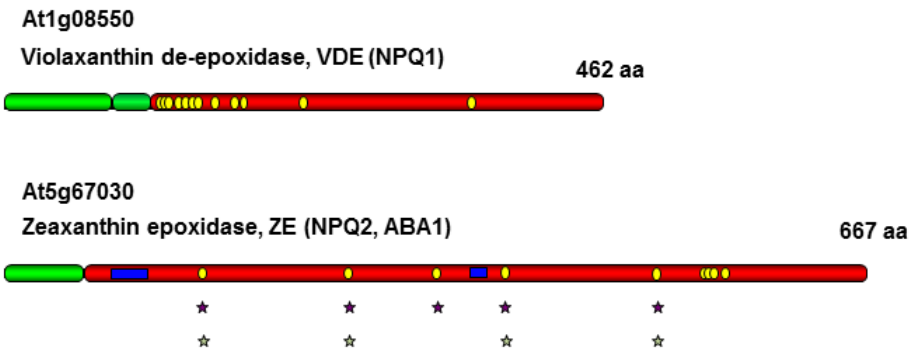

Figure 8. Domain architectures and positions of cysteines in the *Arabidopsis thaliana* VDE and ZE. Sequence information was obtained from TAIR (http://www.arabidopsis.org). Chloroplast N-terminal transit peptides are labelled in green, 113 aa in VDE and 59 aa in ZE. VDE has a bipartite transit peptide, which targets the protein to the thylakoid lumen. In red are labelled the mature proteins, in blue, the FAD-binding domains and in yellow, the cysteines. In ZE, ★ Cys are conserved in *Oryza sativa* and ☆ Cys are conserved in *Chlamydomonas reinhardtii*.

NADPH, FAD, Fd and O_2 are required as cofactors for ZE. In each reaction, one oxygen atom is incorporated into Zx using the reducing power of NADPH via reduced Fd and FAD and the optimal pH for ZE activity is 7.5 (Bouvier et al., 1996; Jahns et al., 2009).

Apart from playing several roles in photoprotection, Zx is also an intermediate in the biosynthetic pathway of abscisic acid (ABA), a plant hormone which plays an

important role in seed development and dormancy regulation, and in stress response. Thus, ZE is involved in the first step of ABA biosynthesis and this enzyme is also referred to as ABA1 in *Arabidopsis thaliana*. Mutants that accumulate Zx, show a severe reduction in ABA content. (Marin et al., 1996; Nambara and Marion-Poll, 2005)

1.4. Chloroplast redox regulation

"Redox regulation" has been defined according to (Buchanan and Balmer, 2005) as "a reversible posttranslational alteration in the properties of a protein, typically the activity of an enzyme, as a result of change in its oxidation state". These authors made a clear distinction between "redox regulation" and "terminal oxidation", which they defined as "an irreversible reaction that marks proteins for degradation" (Buchanan and Balmer, 2005) and is implicitly understood to impair protein function.

In chloroplasts a redox regulatory system has evolved that depends on the electron input from PET and thus is able to exert a light-dependent control over enzymatic activities involved in metabolic process or ROS detoxification. This system is constituted by different kinds of disulphide reductases called thioredoxins, the reducing power of which comes from Fd via FTR (Figure 9). Trxs are able to reduce cysteine disulphides in target proteins, thereby increasing or decreasing their activities (Schurmann and Buchanan, 2008).

Extra-chloroplastic plant Trxs are reduced by the NADPH-dependent thioredoxin reductase (NTR) enzymes, NTRA and NTRB. Both are present in the cytosol and in mitochondria, although NTRA is more abundant in the cytosol and NTRB is predominant in mitochondria (Reichheld *et al.*, 2005). NTRs are flavoproteins, the active form of which is a homodimer. In addition, the existence of a third kind of plant NTR present in chloroplasts has been reported (Serrato *et al.*, 2004). This enzyme, termed NTRC, includes a Trx domain and constitutes a complete NTR-Trx system in one polypeptide. Thus, taking into account the existence of NTRC in the chloroplast, redox regulation in this organelle is possible either with NADPH or Fd (Figure 9).

Redox regulation mediated by Trxs occurs via thiol-disulphide exchange reactions and implies a post-translational protein modification of cysteine residues. Trxs are able to reduce disulphide bonds between Cys (Cys-S-S-Cys) into Cys thiols (Cys-

SH), which leads to a structural change of the enzyme that modifies its catalytic capability. Disulphide bonds may be intramolecular, if the Cys are within the same polypeptide, or intermolecular, between Cys of different proteins. The formation of thiol groups through disulphide reduction is a reversible reaction, as thiolate Cys are susceptible to oxidation, which results in disulphide formation (Figure 10) (Buchanan and Luan, 2005; Lindahl et al., 2011). Protein Cys differ in their reactivity, and not all Cys are susceptible to modification. It is common to find proteins with redox-active cysteines in the chloroplast forms of the enzymes that are absent in their cytoplasmic homologues (Schurmann and Buchanan, 2008).

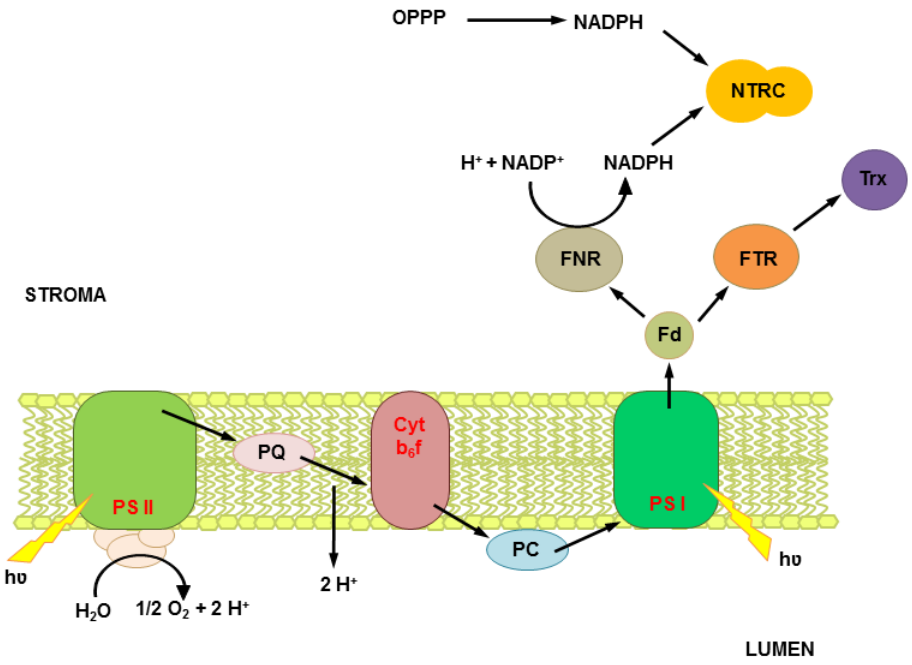

Figure 9. Chloroplast redox regulation. In chloroplasts, thioredoxin (Trx) becomes reduced with electrons from photosynthetic electron transport (PET) through ferredoxin (Fd) and Fd-Trx reductase (FTR) or in the case of NTRC, with NADPH produced through PET, during the day, or the oxidative pentose phosphate pathway (OPPP), during the night.

Apart from the Fd-dependent Trxs and NTRC, there is yet another disulphide reductase system in chloroplasts involving the so-called glutaredoxins (Grxs). These Trx-like enzymes are non-enzymatically reduced by glutathione (GSH), which is previously reduced by glutathione reductases (GR), flavin-containing proteins similar to

NTR (Meyer et al., 2009; Meyer et al., 2012). However, relatively few studies have been dedicated to the functions of chloroplast Grxs.

1.4.1. The Ferredoxin-thioredoxin system

Fd is a small protein (11 kDa approximately) with a [2Fe-2S] cluster attached to the protein by four Cys ligands. It is able to reduce not only FTR, but also other Fd-dependent enzymes, such as FNR, nitrite reductase, sulphite reductase and glutamate synthase (GOGAT) (Schurmann and Buchanan, 2008).

FTR is a heterodimer of 20-25 kDa with the catalytic subunit containing a redox-active disulphide bridge and a [4Fe-4S] cluster. Reduced Fd donates electrons, one at a time, to FTR via [2Fe-2S] - [4Fe-4S] clusters, where these electrons are stored allowing FTR to reduce the disulphide bridge of a Trx with two electrons (Dai *et al.*, 2007). FTR is a versatile enzyme that efficiently reduces different kinds of Trxs.

The Fd-Trx system is characteristic for chloroplasts and is present only in oxygenic photosynthetic organisms. Electrons from PSI reduce Fd, which interacts with FTR turning a light-induced electrical signal into a thiol signal that is transmitted to one of the Trxs. Then, reduced Trxs interact with specific Cys on target proteins modifying their activities and thus, these enzymes are able to respond to different light conditions (Figure 10) (Schurmann and Buchanan, 2008).

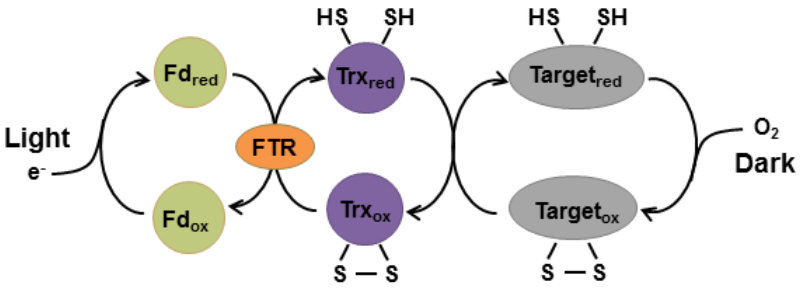

Figure 10. The ferredoxin-thioredoxin system. In light, ferredoxin (Fd) takes electrons from photosynthetic electron transport and subsequently reduces thioredoxin (Trx) by the action of Fd-Trx reductase (FTR). Trxs reduce disulphide bonds between Cys in target proteins. These reactions are reversible since thiolate Cys are susceptible to oxidation. red, reduced; ox, oxidised. Adapted from (Buchanan and Balmer, 2005).

1.4.2. Thioredoxins

Trxs are low molecular weight proteins (12-14 kDa), typically with a canonical active site sequence, WCGPC, and a characteristic fold. Trxs have oxidoreductase activity catalysing disulphide-dithiol exchange reactions with a large number of proteins (Schurmann and Buchanan, 2008).

Besides plants, Trxs are universally distributed in all types of organisms. In plants, there is a huge variety of Trxs present in the cytoplasm and in different organelles, although the most abundant are in chloroplasts. The cytosolic Trxs belong to the *h*-type which constitutes an heterogeneous group and should be divided into three subgroups (*h*1, *h*2 and *h*3) (Meyer *et al.*, 2005). In the nucleus, a form of Trx called nucleoredoxin has been found (Laughner *et al.*, 1998) and two isoforms of nucleoredoxin are encoded in the *Arabidopsis* genome. Trxs *o* (*o*1 and *o*2) are specific for mitochondria (Laloi *et al.*, 2001). In chloroplasts, five types of Trxs have been described and classified as *m*-, *f*- *x*-, *y*- (Meyer *et al.*, 2005) and *z*-type (Arsova *et al.*, 2010), in addition to other atypical Trxs, such as CDSP32 (Chloroplastic Drought-Induced Stress Protein of 32 kDa) or HCF164 (High Chlorophyll Fluorescence), which possess different redox active sites (Meyer et al., 2005; Schurmann and Buchanan, 2008).

Focusing on chloroplast Trxs, two main functions may be distinguished. On one hand, Trxs participate in protective mechanisms, as electron donors to enzymes involved in ROS detoxification, such as the 2-Cys Prx, which are Trx-dependent peroxidases able to reduce H_2O_2 by transferring electrons from Cys thiols. On the other hand, Trxs play a regulatory role, reversibly activating, or inhibiting, metabolic enzymes through reduction in the light. For example, Trxs are involved in redox regulation of carbon fixation in light, activating enzymes of the Calvin-Benson cycle (such as fructose 1,6-bisphosphatase, FBPase) and deactivating enzymes of the oxidative pentose phosphate cycle (such as glucose 6-phosphate dehydrogenase, G6PDH) (Schurmann and Buchanan, 2008). In general, based on *in vitro* studies, the *f*- and *m*-type Trxs are thought to regulate enzymes involved mainly in carbon metabolism, whereas Trxs *x*, *y* and *z* were proposed to have an antioxidant function.

Thus, among the simple Trxs, Trx *x* is the most efficient reductant for 2-Cys Prx *in vitro* (Collin *et al.*, 2003) and Prx Q seems to be the best substrate for Trx *y* (Collin *et*

al., 2004). Trx *x* is encoded by a unique gene in *Arabidopsis*, while Trx *y* exists in two isoforms. Trx *y*2 is expressed in green tissues in contrast to Trx *y*1 that is expressed mostly in non-photosynthetic organs, especially in seeds (Collin *et al.*, 2004).

Trx *z* is essential for chloroplast development by control of chloroplast gene expression depending on plastid-encoded RNA polymerase (PEP) (Arsova *et al.*, 2010). Moreover, Trx *z* is also able to reduce the 2-Cys Prx and can be reduced by other Trxs (Bohrer *et al.*, 2012).

CDSP32 might also be involved in protection against oxidative damage, reducing the 2-Cys Prx (Broin *et al.*, 2002), while HCF164, that is anchored to the thylakoid membrane and is required for assembly of Cyt b_6f, plays a role mediating the reduction of target proteins in the thylakoid lumen with reducing equivalents from the stroma (Motohashi and Hisabori, 2006).

Trx *m* was originally reported to activate the NADP-dependent malate dehydrogenase (NADP-MDH), which catalyses the reduction of oxaloacetate to malate, and Trx *f* was found to reduce the FBPase involved in the Calvin-Benson cycle. While NADP-MDH can be reduced *in vitro* by *f*-type Trxs, in addition to *m*-types, FBPase cannot be reduced by Trxs *m* (Collin *et al.*, 2003).

In *Arabidopsis* there are four Trx *m* isoforms, of which Trxs *m*1, *m*2 and *m*4 efficiently activate NADP-MDH and also reduce other enzymes, such as phosphoribulokinase and G6PDH (Schurmann and Buchanan, 2008). In addition, Trx *m1*, *m2* and *m4* are able to reduce 2-Cys Prx, as well as Prx Q (Collin et al., 2003) (Collin et al., 2004). Moreover, *Arabidopsis* Trx *m1*, *m2* and *m4*, and also Trx *x*, have been found to induce hydrogen peroxide tolerance in yeast (Issakidis-Bourguet *et al.*, 2001). However, Trx *m3* exacerbates oxidative stress in transformed yeast cells and this Trx *m* isoform is not able to reduce neither 2-Cys Prx nor NADP-MDH (Issakidis-Bourguet et al., 2001; Collin et al., 2003). Therefore, Trx *m3* appears to have a different function from that of the other Trxs *m* in *Arabidopsis*.

Since Trxs targets can be reduced by more than one type of Trx *in vitro*, although their catalytic efficiency may vary, the role of these proteins appears to be redundant and it has turned out to be difficult to determine the specificity of each. However, type-*f* Trxs seem to be the most efficient catalysts for disulphide reduction *in*

vitro of several enzymes, especially those related to carbohydrate metabolism (Schurmann and Buchanan, 2008).

In the case of Trx *f*, there are two isoforms in *Arabidopsis*, Trx *f*1and *f*2. Trx *f*1 constitutes the major form and accounts for about 96% of *f*-type Trxs (Thormahlen *et al.*, 2013). *In vitro* experiments have proved that several enzymes from the Calvin-Benson cycle are efficiently activated by Trxs *f*: FBPase, sedoheptulose 1,7-bisphosphatase (SBPase), NADP-glyceraldehyde-3-phosphate dehydrogenase (GAPDH) and phosphoribulokinase (PRK), as well as Rubisco activase and ATP synthase. Other targets of these Trxs include acetyl-CoA carboxylase (fatty acid biosynthesis), ADP-glucose pyrophosphorylase (starch biosynthesis) and α-glucan water dikinase (starch degradation) (Schurmann and Buchanan, 2008). In *Arabidopsis* plants lacking Trx *f*1, the starch accumulation decreases up to 22% (Thormahlen *et al.*, 2013). Furthermore, overexpressing Trx *f* protein in tobacco enhanced starch accumulation, which confirms the important role of *f*-type Trxs in carbon metabolism (Sanz-Barrio *et al.*, 2013).

1.4.3. NADPH-thioredoxin reductase C

NTRC is a bimodular enzyme consisting in an NTR with a joint Trx domain at the C-terminus (Serrato *et al.*, 2004), able to conjugate both Trx and NTR using NADPH as reducing equivalent. Therefore, NTRC constitutes a NTR/Trx system in one polypeptide (Alkhalfioui et al., 2007; Moon et al., 2006; Perez-Ruiz et al., 2006).

The active form of NTRC is a homodimer, using FAD as a cofactor. Electrons are transferred from NADPH to FAD, then to the adjacent redox active disulphide in the NTR domain and finally to the Trx domain containing the second reactive disulphide of NTRC. This transfer of reducing equivalents takes place inter-subunit, i.e., electrons are transferred from the NTR domain of one subunit to the Trx domain of the other (Figure 11) (Bernal-Bayard et al., 2012; Perez-Ruiz and Cejudo, 2009).

Thus, NTRC constitutes an alternative electron donor for the chloroplast redox regulation allowing the use of NADPH produced from PET, during the day, and from the oxidative pentose phosphate pathway, during the night. The relevance of this protein was demonstrated with an *Arabidopsis* NTRC knock-out mutant (*ntrc*) that presents a

severe phenotype as compared to wild-type (wt) plants (Serrato *et al.*, 2004). *ntrc* plants are stunted and chlorotic and this phenotype is dependent on the photoperiod, being more pronounced under short-day conditions. Moreover, *ntrc* shows lower CO_2 fixation rates, especially at low light intensities, abnormal chloroplast structure and is hypersensitive to different abiotic stresses, such as drought, cold, high salinity and prolonged darkness (Perez-Ruiz et al., 2006; Lepisto et al., 2009).

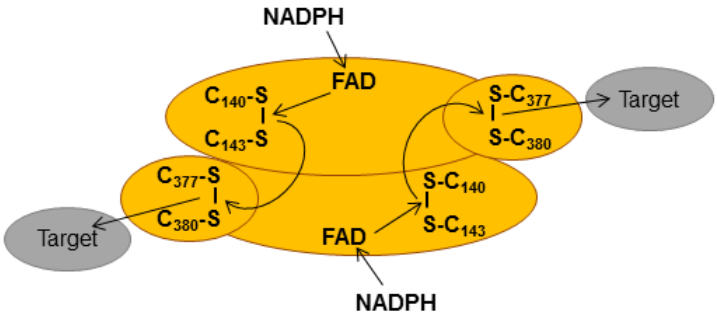

Figure 11. Proposed model for the reaction mechanism of NTRC. The minimal catalytic unit of NTRC is the dimer. Targets of NTRC are reduced via the Trx domain. Electrons are transferred from NTR to Trx domains through an inter-subunit pathway. Adapted from (Perez-Ruiz and Cejudo, 2009).

A role in protection against oxidative stress has been attributed to NTRC through reduction of 2-Cys Prx, being the most efficient electron donor of this enzyme *in vitro* and *in vivo* compared to other Trxs, such as CDSP32 and Trx *x* (Perez-Ruiz et al., 2006; Pulido et al., 2010). This also implies a role for NTRC in redox signalling (Puerto-Galan *et al.*, 2013). This function could be more important in darkness when NTRC is the only candidate as catalyst for disulphide reduction (Spinola *et al.*, 2008). In addition, other enzymes can be reduced by NTRC implying this protein in the regulation of several chloroplast processes (Cejudo *et al.*, 2012). This is also suggested from the severe growth phenotype of *ntrc* as compared to the almost wt phenotype of a mutant containing less than 5% of the 2-Cys Prx, *Δ2cp* (Pulido *et al.*, 2010).

NTRC is involved in the biosynthesis of tetrapyrroles through reduction of different enzymes, such as glutamyl-transfer RNA reductase 1 (GluTR1), Mg-protoporphyrin methyl transferase (CHLM) (Richter *et al.*, 2013) and the CHLI subunit of the Mg-chelatase complex (Perez-Ruiz *et al.*, 2014). Furthermore, the lower content

of starch in the *ntrc* mutant led to the identification of ADP-glucose pyrophosphorylase (AGPase) as an NTRC-regulated enzyme (Michalska et al., 2009; Lepisto et al., 2013). The redox state of AGPase was found to be altered in *ntrc* not only in leaf chloroplasts, but also in roots, suggesting the presence of NTRC also in heterotrophic tissues (Michalska *et al.*, 2009). The presence of NTRC in plastids of non-photosynthetic tissues as well as in chloroplasts has recently been demonstrated. Interestingly, the selective expression of NTRC in leaves is sufficient to rescue the phenotype of the *ntrc* mutant with respect to growth and pigmentation, revealing the supreme importance of chloroplast redox regulation for plant growth (Kirchsteiger *et al.*, 2012).

The co-existence of two different thiol-based light-dependent redox-signalling systems in the chloroplast (Figure 9) is intriguing and raises a number of questions. Some of theses questions relate to the presumed substrate specificities and redundancies between these systems. In addition, putative interactions and even interdependence between the NAPDH-dependent NTRC system and Fd-FTR-dependent simple module Trx systems should be taken into account. The possible implication of chloroplast redox enzymes as signalling molecules in high light acclimation was postulated several years ago (Li et al., 2009), but has so far not been proven. Recently, the involvement of Trxs in adaptation of plants to fluctuating light conditions has also been considered (Nikkanen and Rintamaki, 2014). Therefore, the specific contributions of NTRC and FTR-dependent Trxs to the possible redox regulation of light acclimation mechanisms should be determined in order to understand how plants adapt to the natural variations in their light environment.

OBJECTIVES

2. OBJECTIVES

The aim of this thesis was to elucidate the possible implication of the two distinct chloroplast redox systems in adaptation of plants to changes in light conditions and the regulation of photosynthesis. To this end, the following specific objectives were addressed:

1. To investigate the possible role of NTRC in long- and short-term acclimation to different light intensities and in protection against excess excitation.

2. To establish the relevance of *f*- type Trxs for plant growth and their function in carbon assimilation.

Part of this work has been performed during a three months stay in the laboratory of Dr. Anja Krieger-Liszkay at the Institute for Integrative Biology of the Cell (I2BC), Commissariat à l'Energie Atomique et aux Energies Alternatives (CEA) Saclay, France.

Part of the results presented in this thesis has been included in the following manuscripts:

- The chloroplast NADPH thioredoxin reductase C, NTRC, is required for efficient utilisation of light energy and control of photosynthetic electron transport in *Arabidopsis*. Belén Naranjo, Clara Mignée, Anja Krieger-Liszkay, Dámaso Hornero-Méndez, Lourdes Gallardo-Guerrero, Francisco Javier Cejudo and Marika Lindahl. Plant Cell & Environment (pending minor revisions).

- Type-*f* thioredoxins function in short-term activation of carbon metabolism after a dark-light transition but are dispensable for growth in *Arabidopsis thaliana*.

Belén Naranjo, Antonio Díaz-Espejo, Marika Lindahl and Francisco Javier Cejudo. Journal of Experimental Botany (pending minor revisions).

- Thioredoxin *f*1 and NADPH-dependent thioredoxin reductase C have overlapping functions in regulating photosynthetic metabolism and plant growth in response to varying light conditions. Ina Thormählen, Tobias Meitzel, Julia Groysman, Alexandra Öchsner, Edda von Roepenack-Lahaye, Belen Naranjo, Francisco Cejudo, and Peter Geigenberger. Plant Physiology, September 2015 (http://dx.doi.org/10.1104/pp.15.01122).

MATERIALS AND METHODS

3. MATERIALS AND METHODS

3.1. Plant material and growth conditions

Arabidopsis thaliana wild type and mutant plants (ecotype Columbia) were grown on soil in growth chambers (SANYO, Leicester, UK) under long-day (16 h light / 8 h darkness) or short-day (8 h light / 16 h darkness) conditions at a light intensity of 120 μmol quanta m^{-2} s^{-1} or in a growth chamber FITOCLIMA 700 EDTU from Aralab (Rio de Mouro, Portugal) under a photoperiod of 10 h light / 14 h darkness at different light intensities: 50 (low light), 120 (normal light), 600 (moderately high light), or 1000 μmol quanta m^{-2} s^{-1} (high light). Temperature, 22 ºC during the light and 20 ºC during the dark periods, and relative humidity (60%) were strictly controlled.

Arabidopsis mutants used in this work, previously reported, were the *ntrc* knockout mutant (Serrato et al., 2004; Perez-Ruiz et al., 2006), the *trxx* and *Δ2cp* mutants (Pulido *et al.*, 2010), and the *trxf1* mutant (Perez-Ruiz *et al.*, 2014). In addition, two new single mutants were isolated, *trxf2* (GK-020E05-013161) and *psbs* (SALK_095156), which were used to generate the double mutants *trxf1f2* and *ntrc-psbs*.

Generation of Arabidopsis mutants

A homozygous line GK-020E05-013161 with a T-DNA insertion in the *TRX f2* gene (At5g16400.1) from *Arabidopsis*, termed the *trxf2* mutant, was selected by PCR analysis of genomic DNA with the oligonucleotides described in Tables 1 and 2. This mutant was manually crossed with the *trxf1* mutant. Seeds resulting from this cross were tested for heterozygosity of the T-DNA insertions in the *TRX f1* and *TRX f2* genes. Plants were then self-crossed and double homozygous lines, denoted *trxf1f2* mutants, were identified in the progeny by PCR analysis of genomic DNA using oligonucleotides described in Tables 1 and 2. DNA extraction was performed with CTAB (Sigma) based on the protocol described by (Murray and Thompson, 1980).

The same procedure was performed with the insertion line SALK_095156, which contains the T-DNA in the second exon of the *PsbS* gene (At1g44575). Plant genotypes were analysed with oligonucleotides PsbS LP - RP (wild type allele) and Lba1 - PsbS RP (mutant allele) described in Tables 1 and 2, and homozygous *psbs*

mutants were crossed with the *ntrc* knockout mutant. The double homozygous line, *ntrc-psbs* mutant, was identified by PCR analysis of genomic DNA using oligonucleotides described in Table 1 and**Table 2**.

Table 1. DNA sequence of specific oligonucleotides used for plant genotype and/or transcript analysis in the *ntrc*, *psbs*, *ntrc-psbs*, *trxf1*, *trxf2* and *trxf1f2* knockout mutants.

Primer	DNA Sequence (5' - 3')
NtrC Fw	TCACCAACATGTGGCCC
NtrC Rv	TTCTTCATCTTCACACCCGA
PsbS LP	TGACCAGACACAATTCATTTACATC
PsbS RP	ATAAACATAAAGCCGATCCGG
TRX f1 Fw	TTCATATGTGTAGCTTAGAAACCGTTAATG
TRX f1 Rv	AAGTCGACAGAGACTGGTTCATCCG
TRX f2 Fw	TGGTCCTTGCAAAGTGATTG
TRX f2 Rv	CCCCGGTCACTTCCTTTACT
TRX f2 RP	TTCTCAATTGCCAATTCTTGC
TRX f2 LP	CTATTTCAACAATCGGGTCCC
Lba1	TGGTTCACGTAGTGGGCCATCG
LBb1.3	ATTTTGCCGATTTCGGAAC
o8409	ATATTGACCATCATACTCATTGC
Ubq Fw	GATCTTTGCCGGAAAACAATTGGAGGATGGT
Ubq Rv	CGACTTGTCATTAGAAAGAAAGAGATAACAGG

Table 2. Oligonucleotides used for plant genotype and/or transcript analysis in the *ntrc*, *psbs*, *ntrc-psbs*, *trxf1*, *trxf2* and *trxf1f2* knockout mutants. The size of the amplified DNA from the different templates is also shown.

Primer pair	Template	Product size (Kb)
NtrC Fw - Rv	*NtrC* genomic and cDNA, wild type allele	0.38/0.21
NtrC Fw - LBb1.3	*NtrC* genomic, mutant allele	~0.35
PsbS LP - RP	*PsbS* genomic, wild type allele	1.26
Lba1 - PsbS RP	*PsbS* genomic, mutant allele	~0.85
TRX f1 Fw - Rv	*TRX f1* genomic and cDNA, wild type allele	0.88/0.39
Lba1 - TRX f1 Rv	*TRX f1* genomic, mutant allele	~0.40
TRX f2 Fw - Rv	*TRX f2* genomic and cDNA	0.26/0.18
TRX f2 RP - LP	*TRX f2* genomic, wild type allele	1.05
TRX f2 RP - o8409	*TRX f2* genomic, mutant allele	~0.65
Ubq Fw - Rv	*Ubiquitin* cDNA	0.48

3.2. RNA extraction and quantitative PCR analysis

Total RNA was extracted using TRIsure RNA extraction reagent (BIOLINE) and cDNA synthesis was performed with 1 µg of total RNA using the Maxima first strand cDNA synthesis kit (Thermo Scientific) according to the manufacturer's instructions.

The content of transcripts was determined by semiquantitative-PCR (annealing temperature 55ºC, 30 cycles) and/or real time-quantitative PCR (RT-qPCR). The RT-qPCR was performed using an IQ5 real-time PCR detection system (Bio-Rad) and following a standard thermal profile: 95 ºC for 3 min, 40 cycles of 95 ºC for 10 s and 60 ºC for 30 s. Oligonucleotides used for semiquantitative-PCR were Trx *f*1 Fw - Trx *f*1 Rv, Trx *f*2 Fw - Rv and Ubq Fw - Rv described in Tables 1 and 2. Oligonucleotides used for RT-qPCR are shown in Table 3.

Table 3. DNA sequences of specific oligonucleotides used for RT-qPCR.

Primer	DNA Sequence (5' - 3')
NtrC qFw	TGAAGATGAAGAAAGAGTACCGAG
NtrC qRv	GGTGTCCTCATTTATTGGCCT
PsbS qFw	TCGTTGGTCGTGTTGCTATGA
PsbS qRv	CTTTTCCCGTCAACGCCTCA
TRX f1 qFw	CGATGATCTGGTTGCAGCG
TRX f1 qRv	CTGGTTCATCCGGAAGCAG
TRX f2 qFw	TGTAACCAAGACAACAAGCCA
TRX f2 qRv	CGGTCACTTCCTTTACTACCT
TRX x qFw	TGCTTTCGTTAAGCTCCGGT
TRX x qRv	ATCTCTTTGATTCCGCCGCA
Ubq qFw	GAAGTTCAATGTTTCGTTTCATGT
Ubq qRv	GGATTATACAAGGCCCCAAAA
18S qFw	TATAGGACTCCGCTGGCACC
18S qRv	CCCGGAACCCAAAAACTTTG

3.3. Protein extraction and Western blot analysis

Total leaf or thylakoid proteins were extracted with a buffer containing 25 mM HEPES-KOH, pH 7.4 and 10 mM $MgCl_2$ as described in (Lepisto *et al.*, 2009), the chlorophyll concentrations were measured in 80% acetone as in (Lichtenthaler, 1987) and the protein concentrations were determined following a modification of the Lowry procedure described in (Markwell *et al.*, 1978).

Proteins were resolved using SDS-PAGE gels at different acrylamide concentrations, transferred onto nitrocellulose membranes and probed with the corresponding antibody after blocking the membranes with 5% (w/v) of milk in TBS-Tween (20 mM Tris-HCl, 150 mM NaCl, 0.1% Tween-20). Signals were visualised with enhanced chemiluminescence (ECL) using the Immobilon™ Western Chemiluminescent HRP Substrate reagent (Millipore).

Antibodies against purified recombinant VDE and Trx *f*1 were raised in rabbit and used at 1:2500 and 1:1000 dilutions, respectively. Antibodies against PsbS, ZE and the ATP synthase γ subunit (AtpC) were from Agrisera (Vännäs, Sweden) and used at dilutions of 1:2000, 1:3000 and 1:5000, respectively. The antibody against FBPase was provided by Dr. M. Sahrawy, Estación Experimental del Zaidín, Granada, Spain, and the anti-Rubisco activase antibody, by Dr. A.R. Portis, USDA, Urbana, USA, and were used at dilutions of 1:5000 and 1:20000, respectively. The antibody against NtrC (Serrato *et al.*, 2004) was used at a dilution of 1:1000.

Alkylation assay with MM(PEG)$_{24}$

For alkylation experiments, leaves were ground in liquid nitrogen and 10% (v/v) trichloroacetic acid (TCA) was immediately added to quench thiol oxidation, in a relation of 350 µl 10% TCA per 100 mg of leaves. Sample aliquots of 50 - 100 µl were incubated on ice for 20 min and then centrifuged at 16200 *g* at 4 ºC for 10 min. Pellets were washed with 200 µl acetone without resuspension and centrifuged during 10 min at 16200 *g* at 4 ºC. Dry pellets were resuspended in the same initial volume (50 - 100 µl) of alkylation buffer (2% SDS, 50 mM Tris-HCl pH 7.8, 2.5% glycerol and 4 M urea) with 10 mM MM(PEG)$_{24}$ from Thermo, and incubated for protein thiol alkylation during 20 min at room temperature. Alkylated samples were heated at 70 ºC for 5 min and centrifuged briefly to remove cellular debris and starch prior to electrophoresis. Five to 10 µl of supernatants were electrophoresed and analysed by Western blot. Each MM(PEG)$_{24}$ molecule bound to a reduced Cys (-SH group), adds 1.24 kDa to the total protein mass.

3.4. Analysis of pigments

Chlorophylls

Leaf discs were weighed and incubated in 1 ml 100% methanol (2 discs of 4 mm diameter) overnight at 4°C. After extraction, chlorophyll concentrations were measured spectrophotometrically, using the equations in (Lichtenthaler, 1987), and normalized to fresh weight or leaf area.

Xanthophylls

Analysis of the contents of the xanthophylls violaxanthin, antheraxanthin and zeaxanthin was performed using HPLC as described in (Hornero-Mendez *et al.*, 2000). HPLC measurements were performed in the laboratory of Drs. Dámaso Hornero and Lourdes Gallardo, Instituto de la Grasa-CSIC (Sevilla).

Pigments were extracted by grinding 0.5 g of leaves in liquid nitrogen and resuspension in acetone. Leaf powder was first resuspended in 8 ml of 85% acetone and kept on ice for 15 min. After centrifugation during 10 min at 3700 *g* and 4 ºC, the supernatants were transferred to a new tube and the pellets were resuspended again in 2 ml of 100% acetone, centrifuged and the supernatants were pooled. One ml of each pooled extract containing 90% acetone final concentration was centrifuged at maximum speed (16200 *g*) for 10 min prior to injection of 20 µl into the HPLC system.

3.5. Determination of ABA content

The content of ABA was determined by liquid chromatography–electrospray/tandem mass spectrometry at the Servicio de Microanálisis of Universidad de Sevilla, following the method proposed by (Gomez-Cadenas *et al.*, 2002).

ABA was extracted from depetiolated leaves of plants at the end of the night or after 45 min of illumination. Two-hundred mg of tissue were homogenised and extracted in 2.5 ml of water. Samples were then centrifuged at 698 *g* during 15 min at 4 ºC. The pH of the supernatant was adjusted at 3.0 with 75 µl of 30% (v/v) acetic acid and partitioned with 1.5 ml of ethyl ether twice, recovering the organic phase after centrifugation 2 min at 698 *g*. The ethyl ether was evaporated and completely dry samples were resuspended in 250 µl of methanol and then the volumes were completed until 500 µl with water. After filtering the samples through 0.2 µm filters, 20 µl of each extract was injected into the HPLC system. Before performing the extraction, 100 ng of deuterated ABA (dABA) solution was added to the homogenised plant samples as an internal standard. ABA concentrations were obtained using a standard curve with different amounts of dABA.

3.6. Measurements of photosystem II activity: chlorophyll *a* fluorescence

Room temperature chlorophyll *a* fluorescence of PSII was measured using a pulse-amplitude modulation fluorometer (DUAL-PAM-100, Walz, Effeltrich, Germany).

Measuring fluorescence of chlorophyll *a* bound to PSII is a valuable non-invasive tool to monitor photosynthesis *in vivo*, even in attached leaves. Using a fluorometer it is possible to detect the quenching of fluorescence that exists when electrons are transferred from P680 to Q_A, also known as photochemical quenching (qP) (Baker, 2008).

Plants adapted to darkness have Q_A totally oxidised, in this case we say that reaction centres are "open", i.e., they are able to use the maximum amount of light received to reduce Q_A. Therefore, after a pulse of saturating light, Q_A reaches the maximal reduction state and reaction centres become "closed", which means that the total light received by P680 is dissipated as fluorescence. This fluorescence corresponds to the highest value possible and is referred to as maximal fluorescence (F_m). The ratio of the variable fluorescence (F_v) to maximal fluorescence (F_m), F_v/F_m, is used to determine the maximal effectiveness of PSII, where F_v is the difference between F_m and F_0, and F_0, the minimal fluorescence emitted by Chl *a* exposed only to blue measuring light (460 nm), when the reaction centres are "open" (Q_A maximally oxidised) (Figure 12). Abiotic and biotic stresses usually induce decrease in F_v/F_m due to photo-oxidative damage to PSII.

When the dark-adapted plants are illuminated with a red (653 nm) actinic light, PET starts and, subsequently, the metabolic reactions associated. This drives a continuous reduction and reoxidation of PQs. Applying saturation pulses (SPs) it is possible to determine photosynthetic performance through the maximal fluorescence achieved (F_m'). Each F_m' value corresponds to the fluorescence owing to the maximally reduced Q_A during the course of illumination with actinic light. The difference between F_m and F_m' represents the fraction of Q_A that is not being reduced and it is associated with the activation of protective mechanisms to dissipate energy (NPQ) (Figure 12). Sometimes NPQ is expressed using the Stern-Volmer equation as (F_m/F_m') - 1 (Gilmore et al., 1994; Baker, 2008). NPQ can be observed applying actinic light intensities much higher than the growth light intensity, but when both are similar, NPQ is rather

negligible. After switching off the light, depending on the recovery kinetics of the F_m values, it is possible to distinguish between the different components of NPQ: qI, qE and qT.

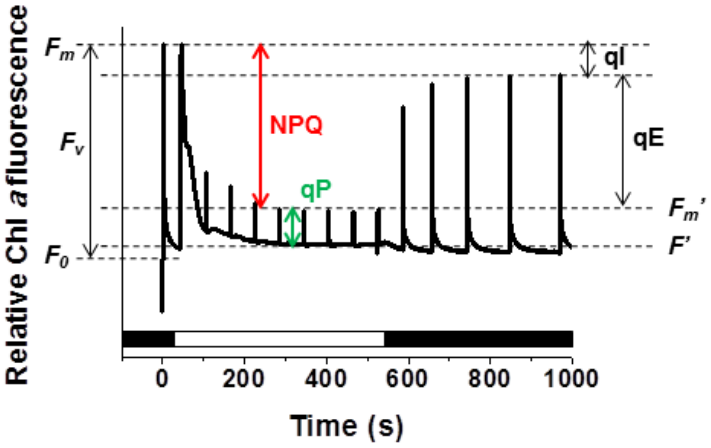

Figure 12. Chlorophyll *a* fluorescence. Applying saturating light pulses, maximum chlorophyll fluorescence values (F_m in darkness and F_m' in light) are obtained. Black and white bars indicate darkness and actinic light, respectively. The fluorescence quenching (F_m' - F') corresponds to the energy used in photochemistry, *i.e.* photochemical quenching (qP). The difference between *Fm* and *Fm'*, corresponds to the light energy absorbed that does not reach P680 (NPQ). The fluorescence maxima rapidly recovered during the subsequent dark period reflects the energy-dependent component of NPQ, qE, while the fraction remaining is the inhibitory component, qI.

Maximum quantum yield of PSII

The maximum quantum yield of PSII was assayed after incubation of plants in the dark for 30 min by calculating the ratio of the variable fluorescence, F_v, to maximal fluorescence, F_m, (F_v/F_m). F_m value was determined applying a saturation pulse of red light at 10000 μmol quanta m^{-2} s^{-1} intensity and 0.6 s duration to the dark adapted leaf.

Induction-recovery curve

Induction-recovery curves were performed using red actinic light at the intensities specified for each experiment during 8 min. Saturating pulses of red light at 10000 μmol quanta m^{-2} s^{-1} intensity and 0.6 s duration were applied every 60 s and

recovery in darkness was recorded for up to 12 min. The parameters Y(II), Y(NPQ) and Y(NO), corresponding to the respective quantum yields of PSII photochemistry, non-photochemical quenching and non-regulated basal quenching (NO), were calculated by the DUAL-PAM-100 software according to the equations in (Kramer *et al.*, 2004b).

In addition, induction-recovery curves were performed using IMAGING-PAM M-Series Chlorophyll Fluorescence System (Walz, Effeltrich, Germany) to simultaneously determine various photosynthetic parameters in the complete aerial part of plants. Dark-adapted plants were illuminated with 81 μmol quanta m^{-2} s^{-1} of actinic light during 360 s and subsequently, kept in darkness for 180 s. Saturating pulses were applied each 20 s.

Electron transport rates

Relative linear electron transport rates were measured in pre-illuminated plants applying stepwise increasing actinic light intensities up to 2000 μmol quanta m^{-2} s^{-1}. Values were calculated by the DUAL-PAM100 software.

Post-illumination fluorescence

Dark-adapted leaves (10 min in darkness) were subjected to a saturation pulse followed by 5 min of actinic light. Subsequently, post-illumination fluorescence (PIF) was measured during 5 min in darkness. The transient increase detected in chlorophyll fluorescence after actinic light illumination depends on Q_A reduction due to backflow of electrons from the stroma to the PQ-pool. PIF has been associated with CEF around PSI and is typically absent in mutants lacking the NDH-complex (Shikanai et al., 1998; Munekage et al., 2004).

3.7. Measurements of photosystem I activity: P700 absorbance

The oxidised form of P700 displays a broad absorbance peak around 800-840 nm. Thus, it is possible to analyse its redox state monitoring changes in the absorbance

of leaves at 830 nm. The P700 signal represents the difference between the transmittance signals at 830 nm and 875 nm, respectively.

In dark-adapted leaves, P700 is found reduced, the acceptor side of P700, *i.e.*, the Calvin-Benson cycle and subsequent reactions, are de-activated. Applying far red (FR) light (730 nm), that is preferentially absorbed by PSI pigments and reduces Fd, P700 is oxidised. The maximal level of oxidation (P_m) is achieved by application of a red light saturation pulse (635 nm, 10000 µmol quanta m^{-2} s^{-1} during 0.6 s) in the presence of FR illumination. The signal a few ms after the SP, corresponds to P700 fully reduced (P_0) (Figure 13).

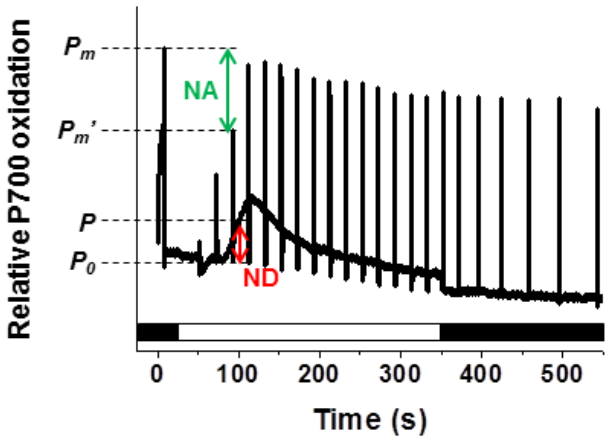

Figure 13. Oxidation of P700. In dark-adapted plants P700 is reduced. The maximal level of oxidation (P_m) is achieved by applying a saturating light pulse (SP) in the presence of far red (FR) (SP after 10 s of FR pre-illumination). Fully reduced P700 (P_0) corresponds to the signal level milliseconds after this SP. An illuminated sample displays a P700 signal denoted by *P*. Applying SPs during actinic light illumination, strong P700 oxidation (P_m') followed by full reduction (P_0) is obtained. The difference between *P* and P_0 corresponds to the fraction $P700^+$ A, which reflects a donor deficit to P700 (ND). The difference between P_m and P_m' corresponds to the fraction P700 A^-, which reflects an acceptor deficit from P700 (NA). The difference between P_m' and *P* corresponds to the fraction P700 A, which reflects the P700 pool able to perform charge separation, i.e., the PSI quantum yield, Y(I).

Under actinic light P700 is reduced by electrons coming from the PQ-pool and applying SP its ability to become reduced and oxidised can be determined. SP induces strong P700 oxidation (P_m') followed by full reduction (P_0). The PSI quantum yield depends on the redox states of P700 and of the PSI acceptors (A). The difference

between P_m and P_m' corresponds to the pool of P700 that cannot become oxidised because of a deficit at the acceptor side of PSI (P700 A^-), which is referred to as non-photochemical acceptor-side limited heat dissipation (NA) (Figure 13). The difference between *P*, the P700 signal under illumination, and P_0 corresponds to the pool of P700 that cannot become reduced because of a donor deficit ($P700^+$ A), which is referred to as non-photochemical donor-side limited heat dissipation (ND) (Figure 13). The PSI quantum yield, Y(I), is the fraction of open centres, when P700 is reduced and acceptors are oxidised (P700 A) and corresponds to the difference between P_m' and *P* (Klughammer and Schreiber, 2008).

Induction-recovery curve

The redox state of photosystem I was monitored by following changes in absorbance at 830 nm versus 875 nm using the DUAL-PAM-100. Plants were kept in the dark for 30 min and, to probe the maximum extent of P700 oxidation, a red light SP of 0.6 s at 10000 µmol quanta m^{-2} s^{-1} was applied to leaves after 10 s of FR pre-illumination. Thereafter, absorbance traces were recorded during 5 min illumination with 126 µmol quanta m^{-2} s^{-1}, 635 nm, red actinic light followed by 5 min darkness. Saturation pulses were applied every 20 s. The quantum yields of PSI photochemistry Y(I), donor side limitations Y(ND) and acceptor side limitations Y(NA) were based on saturating pulse analysis and calculated by the DUAL-PAM-100 software (Klughammer and Schreiber, 2008).

3.8. Thermoluminescence

Thermoluminescence (TL) from PSII is delayed light emission by singlet excited chlorophylls stimulated by warming of samples which have been previously illuminated either by single turnover flashed or continuous FR light at 1°C. Illumination was performed at a relatively low temperature to stabilize the charge pair formed in the light. TL results from recombination of charge pairs between positively charged carriers on the donor side of PSII and electrons on the acceptor side of PSII that produce excited P680. Thus, the S_2 and S_3 oxidation states of the Mn cluster of the oxygen evolving

complex may recombine with the primary and secondary quinone electron acceptors of PSII, Q_A and Q_B, generating the $S_2Q_A^-$, $S_2Q_B^-$ and $S_3Q_B^-$ charge pairs (Ducruet, 2003).

After a single turn-over flash, which induces one charge separation in each PSII centre, the B-band is typically observed. This band originates from $S_{2/3}Q_B^-$ recombination and has a temperature maximum at about 35 °C. The afterglow band (AG-band) is typically induced by FR illumination and has a temperature maximum at about 45 °C. The AG-band is a B-type recombination that depends on the back transfer of electrons from stroma to the acceptor side of PSII (Ducruet, 2003; Ducruet and Vass, 2009). In this back electron transfer PQH_2/Q_B^- is generated. FR illumination excites mainly PSI but does also excite PSII so that higher oxidation states of the Mn cluster (S_2/S_3) are generated (Thapper et al., 2009).

TL measurements were performed to probe the redox state of the PQ-pool in dark-adapted leaves according to the method described in (Roach and Krieger-Liszkay, 2012). The measurements were carried out with a home-built apparatus on leaf segments taken from plants dark adapted for 15 min. TL was excited with 1 single turnover flash or 30 s of FR at 1 °C. Samples were heated at a rate of 24 °C/min from 1 to 70 °C, and the light emission was recorded. Graphical and numerical data analyses were performed according to (Ducruet and Miranda, 1992).

3.9. Electrochromic pigment absorbance shift

The movement of electrons and protons through the thylakoid membrane generates a proton motive force which comprises an electric field, or transmembrane potential, ($\Delta\psi$) and a proton concentration gradient (ΔpH). The presence of the electric field has also an effect on the photosynthetic pigments modifying their spectrum (Bailleul *et al.*, 2010). The "electrochromic shift" (ECS) signal measured at 520 nm has been shown to respond linearly to changes in trans-thylakoid potential and is mainly due to carotenoids and Chl *b* (Schreiber and Klughammer, 2009). The relaxation kinetic of ECS in darkness after illumination allows determination of the two components of pmf, $\Delta\psi$ and ΔpH (Takizawa *et al.*, 2007).

The dark relaxation of ECS is studied after photosynthetic steady-state conditions where proton influx into the lumen is precisely balanced by efflux (Figure

14). Therefore, dark relaxation kinetics of ECS were measured in leaves after 15 min of actinic illumination by red LEDs (650 nm) at intensities from 12 to 940 μmol quanta m^{-2} s^{-1}. The total rapid change in ECS (tens of ms after switch off the light), termed ECS_t, should be proportional to the light-induced pmf (pmf in light minus pmf in dark). The rapid signal decline is followed by a biphasic signal increase to an apparent "dark-baseline". This slowly-reversible (tens of s) phase of ECS decay is known as inverted ECS or ECS_{inv} and is proportional to the light-induced ΔpH. The difference between ECS_t and ECS_{inv} therefore reflects the Δψ portion of light induced pmf (Takizawa *et al.*, 2007).

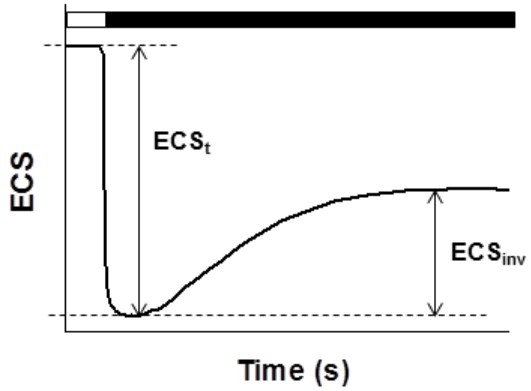

Figure 14. Dark-relaxation of electrochromic shift (ECS). After steady-state photosynthetic conditions, the rapid ECS signal decline (ECS_t) is proportional to the light-induced pmf. This relaxation is slowly reversible and the increased signal is known as inverted ECS (ECS_{inv}) which is proportional to the light-induced ΔpH. The difference between ECS_t and ECS_{inv} reflects the Δψ portion of light induced pmf.

3.10. Determination of the rate of carbon assimilation

Net CO_2 assimilation rate (A_N) was measured using an open gas exchange system Li-6400 equipped with the 6400-40 leaf chamber fluorometer (*LI-COR* Biosciences, Lincoln, NE, USA). All measurements were conducted in dark-adapted leaves at 500 μmol mol^{-1} of CO_2, constant leaf temperature of 20 ºC and vapour pressure deficit between leaf and air below 1 kPa. Before the light, at an intensity of 70 μmol quanta m^{-2} s^{-1}, was turned on in the leaf chamber, A_N was recorded for 30 min every 5 s. Then recording continued for 10 min or until equilibrium was reached.

3.11. Determination of starch content

Starch content was determined in leaves of plants grown under long-day conditions harvested before flowering (22 to 26 days-old), essentially as described in (Lin *et al.*, 1988). For starch extraction, leaves (100 to 200 mg fresh weight) harvested at the end of the day, were ground in liquid nitrogen and washed with 80% (v/v) ethanol in 10 mM HEPES pH 7.6, during 2 h at 80ºC and then washed with the same solution at room temperature until the tissue was free of pigments. Dry pellets, after centrifugation, were resuspended in 1 ml of 0.2 N KOH and heated at 100 °C for 30 min. After cooling, samples were centrifuged at 17000 *g* for 10 min and the supernatant was adjusted to pH 5.0 with 1 N acetic acid. An aliquot of 200 µl of this solution was used to determine the starch amount using the enzymatic method described by (Lin *et al.*, 1988).

3.12. Electron paramagnetic resonance

Electron paramagnetic resonance (EPR) spectroscopy allows direct detection of radicals in complex biological systems such as intact cells and tissue samples. EPR is a technique based on the absorption of electromagnetic radiation by a paramagnetic sample, *i.e.* a species with one or more unpaired electrons, when placed in a magnetic field. These absorptions only occur at very well defined frequencies (usually in the microwave region) and magnetic field combinations, which depend on the type of paramagnetic species present and its characteristics. Hence, different types of radicals (and also metal ions with unpaired electrons) will produce lines at very different regions of the scanned magnetic field and the signal is directly proportional to the concentration of the paramagnetic species (Hawkins and Davies, 2014).

Spin trapping agents are used to facilitate the detection of reactive radicals present in low concentration. This method involves the addition of a spin trap, typically a nitrone or nitroso compound to give stable and detectable nitroxide radical adducts (Hawkins and Davies, 2014).

To detect H_2O_2-derived hydroxyl radicals the spin trap 4-pyridyl-1-oxide-N-tert-butylnitrone (4-POBN) was used. Adding Fe-EDTA, $OH^{\cdot}$ radicals are produced from H_2O_2 via the so-called Fenton reaction (Mubarakshina *et al.*, 2010). Spin trapping assays were carried out using leaves from plants growing at 120 µmol quanta m^{-2} s^{-1}. A

piece of 15 - 20 mg of leaf per sample was infiltrated with a solution containing 50 mM 4-POBN, 4% ethanol, 2.5 μM Fe-EDTA, and 20 mM phosphate buffer pH 7.0. Infiltrated leaves in 250 μl of the same solution were incubated during 1 h in growth light (120 μmol quanta m^{-2} s^{-1}), moderately high light (450 μmol quanta m^{-2} s^{-1}) or darkness.

EPR spectra were recorded at room temperature in a standard quartz flat cell using an ESP-300 X-band (9.73 GHz) spectrometer (Bruker, Rheinstetten, Germany). The following parameters were used: 9.73 GHz microwave frequency, 100 kHz modulation frequency, 1 G modulation amplitude, 63 mW microwave power, 2×10^4 receiver gain, 40.96 ms time constant; number of scans, 2 (Mubarakshina et al., 2010; Roach and Krieger-Liszkay, 2012; Galzerano et al., 2014).

3.13. Cloning, expression and purification of recombinant proteins

For the expression of proteins, the coding sequences (CDS) for VDE (At1g08550) and ZE (At5g67030), without putative transit peptides (113 and 59 amino acids, respectively), were amplified from the full-length cDNA by PCR using gene-specific oligonucleotides, which included restriction sites for cloning into the pQE-30 vector (Qiagen Sciences, Germantown, MD, USA). The sequences of these oligonucleotides were as follows (Table 4).

Table 4. Oligonucleotides used to amplify the complete coding sequences (CDS) of mature proteins VDE (At1g08550) and ZE (At5g67030). Oligonucleotides include restriction sites (underlined at the DNA sequence).

Primer	DNA Sequence (5' - 3')
VDE Fw (BamH1)	GAGGATCCGTTGATGCACTTAAA
VDE Rv (PstI)	AACTGCAGCCTGACCTTCCTGAT
ZE Fw (BamH1)	AAGGATCCGCGGCGACG
ZE Rv (HindIII)	GCAAGCTTAGCTGTCTGAAGTAA

cDNA sequences amplified with oligonucleotides described in Table 4, using iProof High Fidelity enzyme (BIO-RAD), were ligated into the pGEMt vector

(Promega). *Escherichia coli* DH5α cells were transformed by heat shock (30 min on ice, 2 min at 42 ºC and 5 min on ice) with the ligation product, to obtain a high number of copies of the plasmid. The constructions were extracted with a plasmid DNA purification kit, DNA-Spin (Intron biotechnology), according to the manufacturer's instructions. All cDNAs had both strands sequenced and were restricted with the corresponding enzymes, *Bam*H1 and *Pst*I or *Hind*III to introduce the VDE or ZE sequences into the pQE-30 expression vector.

Proteins were overexpressed from pQE-30 in *Escherichia coli* XL1-Blue cells (transformed by heat shock), using 0.5 mM IPTG. VDE expression was induced during 4 h at 25 ºC and ZE, over-night at 25 ºC.

After breaking cells using sonication or French press, the recombinant proteins, containing a His-tag at the N-terminus, were purified by nickel-affinity chromatography. ZE was purified using an ÄKTA prime FPLC system (GE Healthcare, Buckinghamshire, UK) with Hi-Trap chelating columns, 1 ml (GE-Healthcare), and 20 mM phosphate buffer pH 7.4 containing 200 mM NaCl and 10% glycerol. An elution gradient was applied from 40 to 500 mM imidazole (ZE eluted at ~ 250 mM imidazole). VDE was not soluble and therefore, was purified from inclusion bodies with 6 M urea in 20 mM Tris-HCl pH 8.0 and 500 mM NaCl buffer using Ni-NTA Agarose resin (Qiagen). Protein was eluted with 500 mM imidazole. Quantification of proteins was determined using the Bio-Rad protein assay.

Purified recombinant rice NTRC was prepared as in (Serrato *et al.*, 2004), but using nickel- instead of copper-affinity chromatography. Trx *x* and BAS1 (2-Cys Prx) were purified as in (Perez-Ruiz *et al.*, 2006), and *Arabidopsis* Trx *f*1 according to (Perez-Ruiz *et al.*, 2014).

Escherichia coli cultures were grown in LB medium (10 g/l NaCl, 5 g/l yeast extract, 10 g/l tryptone). For solid media, LB was supplemented with 15 g/l agar and 100 µg/ml ampicillin was added for selection of strains containing pGEMt and pQE30 vectors. In some cases, 0.1 mM X-Gal was added to select positive colonies with pGEMt containing inserts and 2% glucose to repress pQE30 basal expression.

3.14. NTRC *in vitro* activity

In vitro alkylation assays

Purified recombinant proteins in 10 mM phosphate buffer pH 7.4 were incubated during 20 min at room temperature in different combinations and in the presence of $CuCl_2$, H_2O_2, DTT or NADPH. Some of these proteins were previously treated with $CuCl_2$ or DTT during 20 min at room temperature and then dialyzed using Amicon Ultra-0.5 filters (Millipore) to remove the reagents. After the reactions, proteins were precipitated using 10% TCA and then alkylated with 10 mM $MM(PEG)_{24}$ as described above for tissue samples. Twenty µl of alkylated protein samples were subjected to SDS-PAGE under reducing conditions and stained with Coomassie Brilliant Blue.

Determination of NADPH concentration

The reduction of 1 mM $NADP^+$ to NADPH by 2, 5 or 10 µM NTRC was determined following absorbance increase at 340 nm during 20 min in 250 µl of 100 mM K_3PO_4 solution pH 7.0. One mM DTT or 0.1 mM DTT in the presence of 20 µM Trx *f*1 was used as electron donor. The concentration of NADPH was determined using the extinction coefficient for NAD(P)H at 340 nm (ε_{340} = 6220 M^{-1} cm^{-1}).

3.15. Bioinformatic methods

Sequences of genes and proteins were obtained from the *Arabidopsis* database TAIR (The *Arabidopsis* Information Resource) (http://www.arabidopsis.org) and the Universal Protein Resource, Uniprot (http://www.uniprot.org/).

Oligonucleotides were designed using the Primer-BLAST application from the National Center for Biotechnology Information, NCBI (http://blast.ncbi.nlm.nih.gov/Blast.cgi). To analyse mutant plants, the T-DNA Express tool from Salk Institute was also used (http://signal.salk.edu/cgi-bin/tdnaexpress).

The search for nucleotide or amino acid sequence similarity with the sequences available in databases was made using the BLAST application from NCBI

(http://blast.ncbi.nlm.nih.gov/Blast.cgi). Multiple sequence alignment of DNA or protein sequences was performed with the Clustal Omega tool from the European Bioinformatic Institute (EMBL-EBI) (http://www.ebi.ac.uk/Tools/msa/clustalo/).

The presence of signal peptide was analysed by the SignalP (http://www.cbs.dtu.dk/services/SignalP/) and ChloroP (http://www.cbs.dtu.dk/services/ChloroP/) servers.

To determine the restriction sites of DNA sequences, the Webcutter application (http://rna.lundberg.gu.se/cutter2/) was used.

Gel bands were quantified with the Scion Image program (Scion corporation).

Statistical analyses were performed with the SPSS program from IBM.

RESULTS

4. RESULTS

4.1. The role of NTRC in light acclimation and energy utilisation

4.1.1. The sensitivity of the *ntrc* mutant to high irradiances

Chloroplast Trxs seem to be crucial for plant adaptation to environmental changes (Nikkanen and Rintamaki, 2014). Their involvement in light acclimation as redox sensors regulating the plant response to high light has been proposed (Li *et al.*, 2009). However, the possible redox regulatory mechanisms of light acclimation still remain unclear.

The NTRC protein constitutes a chloroplast redox regulatory system that is dependent on NADPH (Serrato *et al.*, 2004). Plants lacking NTRC are hypersensitive to different abiotic stresses, and the retarded growth phenotype of the *ntrc* mutant is more severe under abiotic stresses including drought, high salinity (Serrato *et al.*, 2004), heat (Chae *et al.*, 2013) or prolonged darkness (Perez-Ruiz *et al.*, 2006). Moreover, NTRC is the most relevant reductant for the chloroplast 2-Cys Prxs (Moon et al., 2006; Perez-Ruiz et al., 2006; Alkhalfioui et al., 2007; Puerto-Galan et al., 2013), which has been recently reported to be required to avoid photoinhibition upon transfer from low to high irradiances (Awad *et al.*, 2015). In this context, we have studied the possible involvement of NTRC in plant acclimation to high light intensities.

To study long-term acclimation to high light, we examined the growth of *ntrc* and wild type plants at different light intensities, from 50 up to 1000 μmol quanta m^{-2} s^{-1}, under a photoperiod of 10 h light / 14 h darkness. Elevated light intensities did not further compromise the growth of *ntrc* plants (Figure 15A). The rosettes of mutant plants maintained their proportions to those of wild type plants even at higher light intensities, and the rosette weight of the *ntrc* mutant was approximately 10-fold lower than wild type plants independently of light intensity (Figure 15B). Regarding the amount of total chlorophyll per leaf area, mutant plants had about 60% of the values of wild type plants at all light intensities examined (Figure 15C).

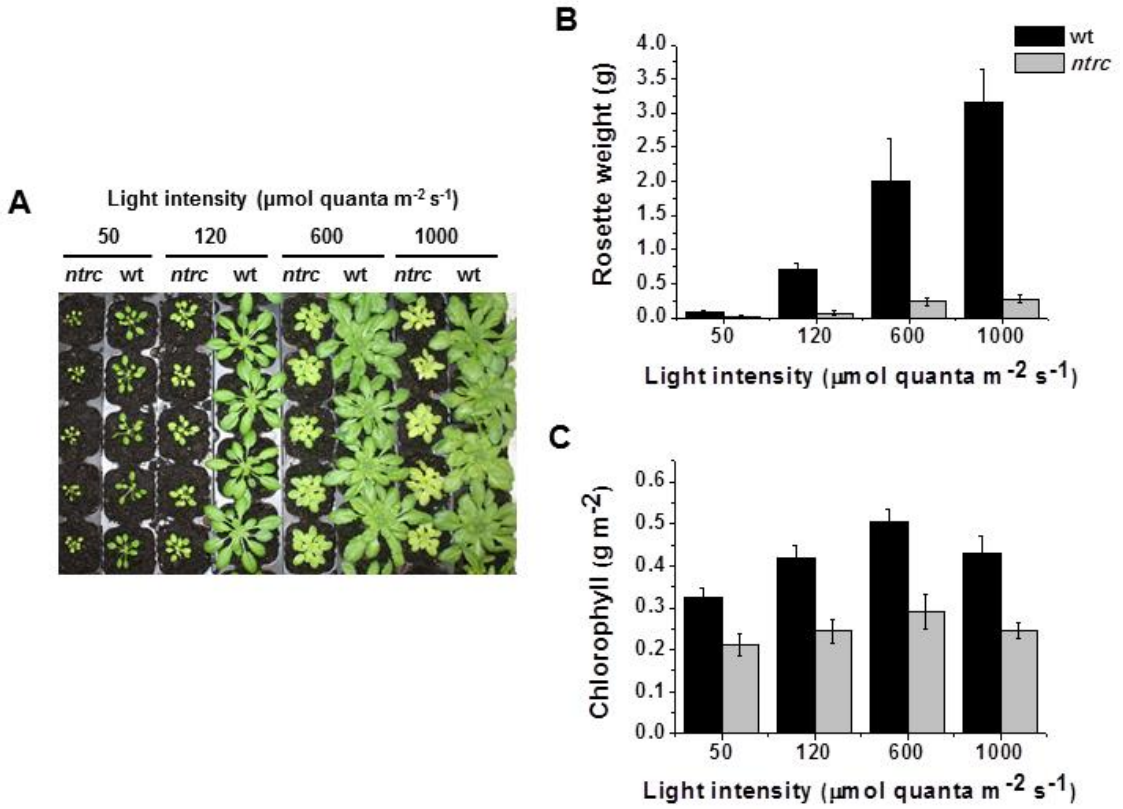

Figure 15. Tolerance of *Arabidopsis* wild type and *ntrc* knockout mutant plants to different irradiances. Plants were grown under a photoperiod of 10 h light / 14 h darkness at 50, 120, 600, or 1000 µmol quanta m^{-2} s^{-1} intensity during 5 weeks. **A)** Wild type (wt) and *ntrc* mutant plants grown at the respective light intensities. **B)** Fresh weight of rosettes. Each data point is the mean of 10 to 20 plants and SDs are presented as error bars. **C)** Content of total chlorophylls *a* and *b* determined in leaf discs. Each data point is the mean of discs from 10 plants ± SDs.

To test short-term tolerance to high light, plants grown at a light intensity of 120 µmol quanta m^{-2} s^{-1} were transferred to 800 µmol quanta m^{-2} s^{-1} and the integrity of PSII was assayed as variable fluorescence normalised to maximal fluorescence (F_v/F_m). F_v/F_m measurements were made at the end of the night and each three hours during the day. Before the transfer to high light *ntrc* plants had an F_v/F_m ratio of about 0.78, which is slightly lower than the typical 0.83 of wild type plants (Figure 16A). After three hours of illumination at 800 µmol quanta m^{-2} s^{-1} these values had decreased to 0.74 and 0.76, respectively. Comparing the differences between F_v/F_m ratio in 800 µmol quanta m^{-2} s^{-1} with the initial one (120 µmol quanta m^{-2} s^{-1}) (Figure 16), the results indicate that the *ntrc* mutant does not suffer increased damage to PSII, although the repair rate in the dark appears to be deficient.

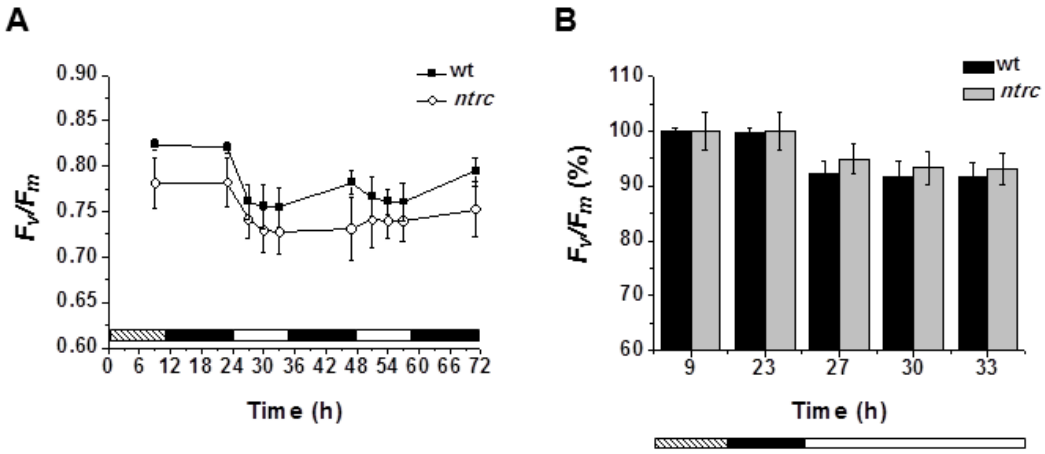

Figure 16. Tolerance of *ntrc* plants to photoinhibition. Plants were grown under a photoperiod of 10 h light / 14 h darkness. **A)** Five-weeks old plants grown at 120 μmol quanta m^{-2} s^{-1} light intensity were transferred to an intensity of 800 μmol quanta m^{-2} s^{-1}. Time 0 corresponds to the beginning of the last day in normal light. Each data point is the mean of the F_v/F_m values measured from 12 plants (3 leaves from each) and SDs are presented as error bars. **B)** F_v/F_m values at the end of the night (23 h) and during the first day at 800 μmol quanta m^{-2} s^{-1} (27, 30 and 33 h) presented as percentage of the respective F_v/F_m values at the end of the last day in normal light (9 h).

Detached leaves vacuum-infiltrated with or without lincomycin, which inhibits the synthesis of chloroplast proteins and, therefore, impedes D1 protein turnover, were exposed to 450 μmol quanta m^{-2} s^{-1} light intensity. These assays confirmed that there is no significant difference in sensitivity to photoinhibition between mutant and wild type plants, although in the presence of lincomycin after 3 and 4 hours a slight difference was observed (Figure 17).

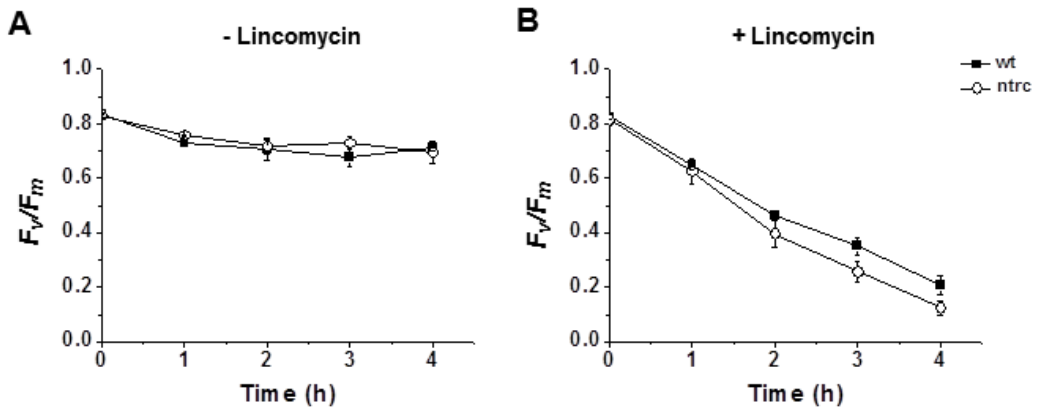

Figure 17. Photoinhibition in the presence of lincomycin. Leaves from 5-weeks old plants grown at 120 μmol quanta m^{-2} s^{-1} light intensity under short photoperiod, were infiltrated with 2 mM lincomycin or water and transferred to a light intensity of 450 μmol quanta m^{-2} s^{-1}. Photoinhibition was assayed by chlorophyll fluorescence as F_v/F_m in untreated **(A)** and lincomycin-treated **(B)** leaves. Prior to measurements, leaves were kept in the dark for 10 min. During light incubation, infiltrated leaves were floated on water or lincomycin solution. Each data point is the mean of the F_v/F_m values measured from 4 leaves and SDs are indicated by error bars.

Under high light conditions the increase in formation of superoxide anion leads to enhanced production of hydrogen peroxide and hydroxyl radicals (Foyer and Noctor, 2009; Li et al., 2009). Taking into account that NTRC is an important source of electrons for one of the most abundant chloroplast peroxidases, the 2-Cys Prx (Moon et al., 2006; Perez-Ruiz et al., 2006; Alkhalfioui et al., 2007), we examined the content of peroxides in plants at their growth light intensity (120 μmol quanta m^{-2} s^{-1}) and after exposure to moderate high light (450 μmol quanta m^{-2} s^{-1}) or darkness. To this end, leaves infiltrated with 4-POBN/ethanol in the presence of Fe-EDTA were immersed in the same solution while illuminated during 1 h and EPR spectra of the 4-POBN/α-hydroxyethyl adducts were recorded (Figure 18A). Notably, *ntrc* plants had 40% higher content of peroxide-derived hydroxyl radicals than the corresponding wild type controls at growth light intensity, but not at higher light intensity (Figure 18B). This would speak against a function of NTRC in peroxide detoxification at high irradiances.

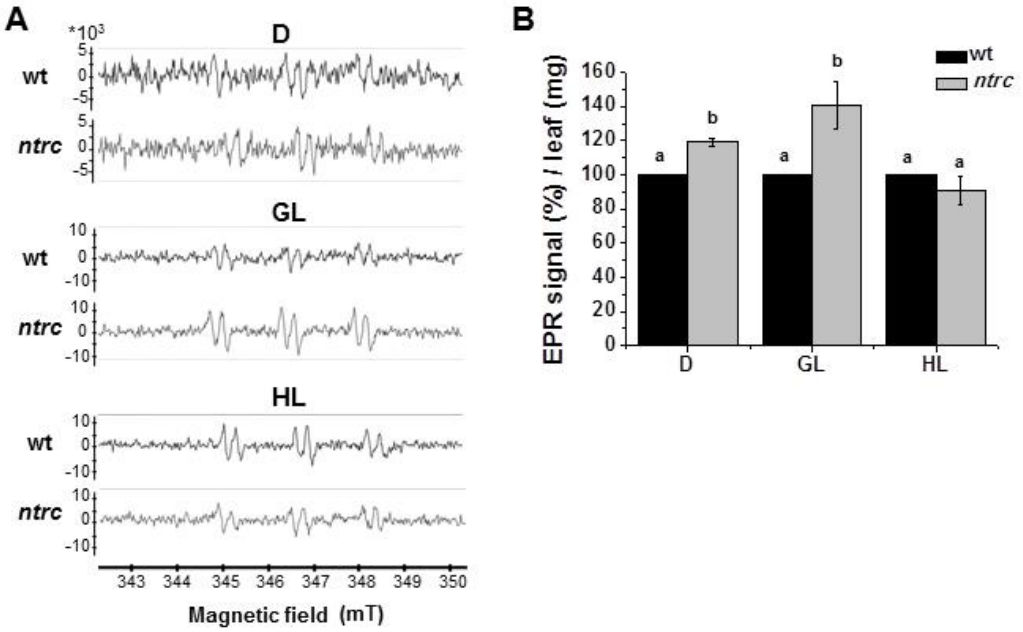

Figure 18. Hydrogen peroxide content in leaves from wild type and *ntrc* mutant plants. Hydrogen peroxide in wild type and *ntrc* mutant leaves from short-day plants after 1 h in the dark, D, growth light, GL (120 μmol quanta m^{-2} s^{-1}), and in high light, HL (450 μmol quanta m^{-2} s^{-1}). The presence of peroxide-derived hydroxyl radicals was shown by indirect spin trapping with 4-POBN/ethanol in the presence of Fe-EDTA. **A)** Typical electron paramagnetic resonance (EPR) spectra of the 4-POBN/α-hydroxyethyl adducts are shown. **B)** Relative content of hydroxyl radicals based on EPR signals from experiments, such as in (A). The signal from the *ntrc* mutant is expressed as % of the corresponding wt control sample ± SE. Darkness, n = 5; growth light, n = 8; high light, n = 4. Significantly different values according to Student's t-test are marked with different letters ($p < 0.05$).

4.1.2. Acclimation to high light: PSII energy dissipation

Protection against excess light in plants lacking NTRC

To measure the ability of the *ntrc* mutant to adapt to a sudden increase in light intensity, chlorophyll fluorescence was monitored during illumination of dark-adapted leaves with actinic light followed by darkness (Figure 19). The intensity of the actinic light in this experiment, 278 μmol quanta m^{-2} s^{-1}, was about twice the growth light of these plants. The saturating light pulse-induced peaks of maximal fluorescence during illumination (F_m') were smaller than the maximal fluorescence in the dark-adapted state (F_m) for both wild type and *ntrc* mutant plants (Figure 19). This shows that the mutant is capable of responding adequately to an increase in light intensity by inducing NPQ.

During the subsequent dark period, fluorescence maxima were recovered in both wild type and mutant plants with similar kinetics (Figure 19).

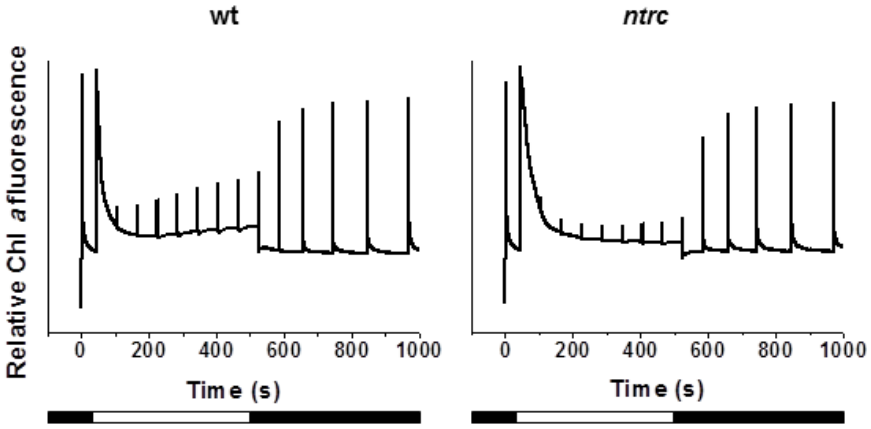

Figure 19. Chlorophyll fluorescence in wild type and *ntrc* mutant plants. Induction and recovery curves with 278 μmol quanta m^{-2} s^{-1} intensity actinic light. Attached leaves of 5-weeks old plants grown at 120 μmol quanta m^{-2} s^{-1} light intensity under a photoperiod of 10 h light and 14 h darkness were used. Following 30 min dark incubation and determination of F_0 and F_m, actinic light was turned on and saturating pulses were applied every 60 s. After 8 min illumination, measurements were continued for another 10 min in the dark. White and black bars below graphs indicate periods of illumination with actinic light and darkness, respectively.

At actinic light intensities lower than growth light intensity NPQ is normally not observed, except shortly after the onset of light due to transient acidification of the thylakoid lumen (Kalituho *et al.*, 2007). This was confirmed in the fluorescence curves recorded for the wild type plants (Figure 20A). In contrast, the *ntrc* mutant displayed extensive NPQ during the entire illumination period, as revealed by the dramatic reduction of the F_m' values (Figure 20A). This response is abnormal and distinguishes plants lacking NTRC from wild type plants. In order to compare quantitatively the photosynthetic performance of these plants during induction and recovery, the respective quantum yields of NPQ, PSII photochemistry and non-regulated, or basal, energy dissipation (NO) were analysed according to (Kramer *et al.*, 2004a). At 75 μmol quanta m^{-2} s^{-1} actinic light the fraction of total energy dissipated through NPQ in the *ntrc* mutant plants was as high as 0.5 under steady state photosynthesis, whereas the corresponding value for wild type plants was close to 0.05 (Figure 20B). Accordingly,

the effective quantum yield of PSII in the light was more than four times lower in the mutant as compared to wild type plants, while NO did not differ (Figure 20B).

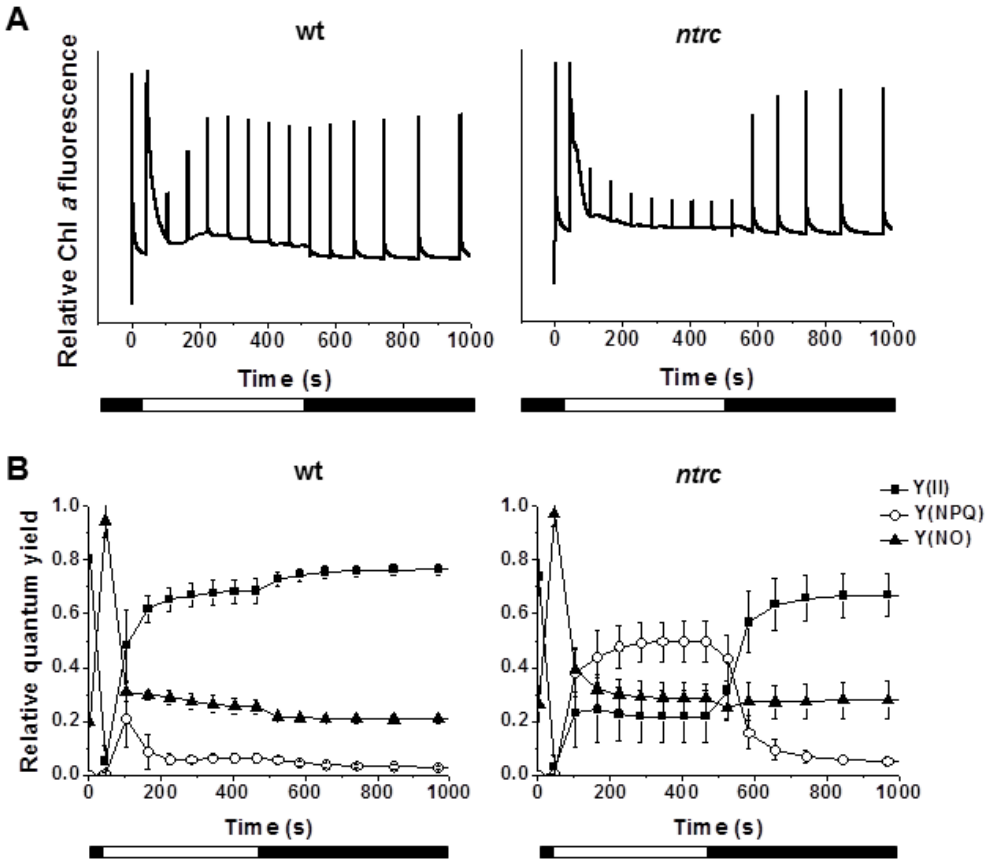

Figure 20. PSII activity and NPQ in wild type and *ntrc* mutant plants. Attached leaves of 5-weeks old plants grown at 120 µmol quanta m^{-2} s^{-1} light intensity under a photoperiod of 10 h light and 14 h darkness were used. **A)** Induction and recovery curves applying 75 µmol quanta m^{-2} s^{-1} intensity actinic light. **B)** Quantum yields of NPQ, Y(NPQ), PSII photochemistry, Y(II), and non-regulated energy dissipation, Y(NO), based on experiments such as in (A). Each data point is the mean of the values from 4 plants and SDs are indicated by error bars. White and black bars below graphs indicate periods of illumination with actinic light and darkness, respectively.

It should be noted that these experiments were performed using plants grown under short-day conditions with 10 h light and 14 h darkness. Since some features of the *ntrc* mutant phenotype depend on the day length during growth (Perez-Ruiz et al., 2006; Lepisto et al., 2009; Lepisto et al., 2013), we also measured chlorophyll fluorescence of plants grown under long-day (16 h light / 8 h dark) photoperiod. However, *ntrc* mutant

plants grown under long photoperiods also displayed exceptionally high and persisting NPQ at low light intensities (Figure 21).

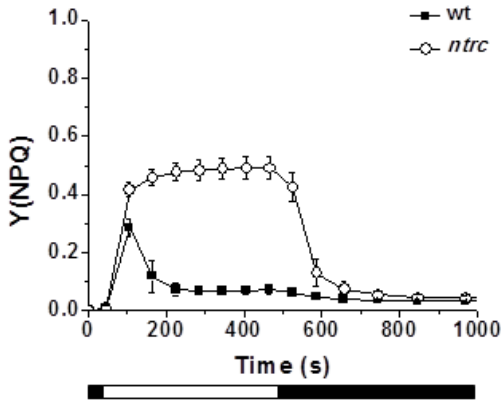

Figure 21. NPQ in wild type and *ntrc* mutant plants grown under long-day conditions. Chlorophyll fluorescence was measured using 3-weeks old plants grown at 120 μmol quanta m^{-2} s^{-1} light intensity under a photoperiod of 16 h light and 8 h darkness. Prior to measurements plants were kept in the dark for 30 min. Actinic light at 75 μmol quanta m^{-2} s^{-1} was turned on and saturating pulses were applied every 60 s. After 8 min the actinic light was switched off and measurements were continued for another 10 min. White and black bars below graphs indicate periods of illumination with actinic light and darkness, respectively. The quantum yields of NPQ were calculated and each data point is the mean of the Y(NPQ) from 4 leaves and SDs are presented as error bars.

Chlorophyll fluorescence imaging showed that the high-NPQ phenotype is particularly pronounced in the young expanding leaves of *ntrc* plants and that there is variegation within single leaves (Figure 22).

High light acclimation in *ntrc* plants in relation to the 2-Cys Prx activity

NTRC is known to be an important electron donor to chloroplast 2-Cys Prxs (Perez-Ruiz *et al.*, 2006; Pulido *et al.*, 2010) and, since ROS are involved in the regulation of various responses to excess light (Li *et al.*, 2009), we addressed the relevance of this function for the control of NPQ. A severe knock-down mutant with minimal levels of 2-Cys Prxs, the *Δ2cp* mutant (Pulido *et al.*, 2010), was examined for its capacity to induce NPQ as a function of light intensity and compared to *ntrc* and

wild type plants. In addition, mutant plants devoid of the chloroplast Trx *x* (Pulido *et al.*, 2010) were included in these experiments, since Trx *x* has been proposed as an alternative electron donor for 2-Cys Prxs (Collin *et al.*, 2003).

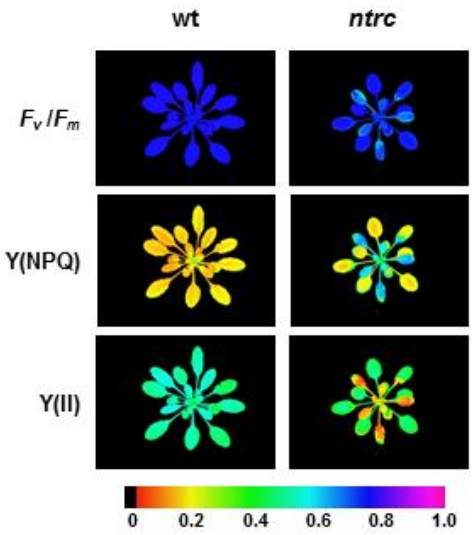

Figure 22. Fluorescence imaging. False-colour images representing F_v/F_m in wild type and *ntrc* mutant plants grown under short day conditions at 120 µmol quanta m^{-2} s^{-1} and the respective Y(NPQ) and Y(II) after 3 min of 81 µmol quanta m^{-2} s^{-1} intensity illumination. Induction-recovery curves were performed using IMAGING-PAM Chlorophyll Fluorescence System (Walz). F_v/F_m values were determined in dark-adapted plants. Subsequently, plants were illuminated with 81 µmol quanta m^{-2} s^{-1} of actinic light during 6 min and saturating pulses were applied each 20 s. Images of *ntrc* plants have been enlarged to facilitate viewing.

Plants were grown at four different light intensities and fluorescence induction-recovery curves were recorded using three actinic light intensities for each set of plants. The yields of NPQ for the *Δ2cp* and *trxx* mutants were similar to those of wild type plants (Figure 23), except *Δ2cp* plants grown at high light intensities, which had less NPQ under lower actinic light. In contrast, the yields of NPQ for the *ntrc* mutant were higher under all conditions tested (Figure 23). This indicates that the effect that NTRC exerts on NPQ is not related to reduction of 2-Cys Prx.

To compare the photosynthetic performance of these plants, the relative rates of linear PET were analysed by chlorophyll fluorescence using gradually increasing intensities of actinic light up to 2000 µmol quanta m^{-2} s^{-1} (Figure 24). Wild type plants

adapted to higher light intensities had higher linear PET rates, but the electron transport for the *ntrc* mutant remained extremely slow at all intensities examined. The electron transport rates of plants deficient in Trx *x* and 2-Cys Prx were comparable to those of the wild type (Figure 24A). The yields of NPQ in these experiments were always higher for *ntrc* plants, particularly at lower light intensities (Figure 24B). In contrast, the *Δ2cp* plants grown at high light intensities displayed considerably less NPQ under low actinic light.

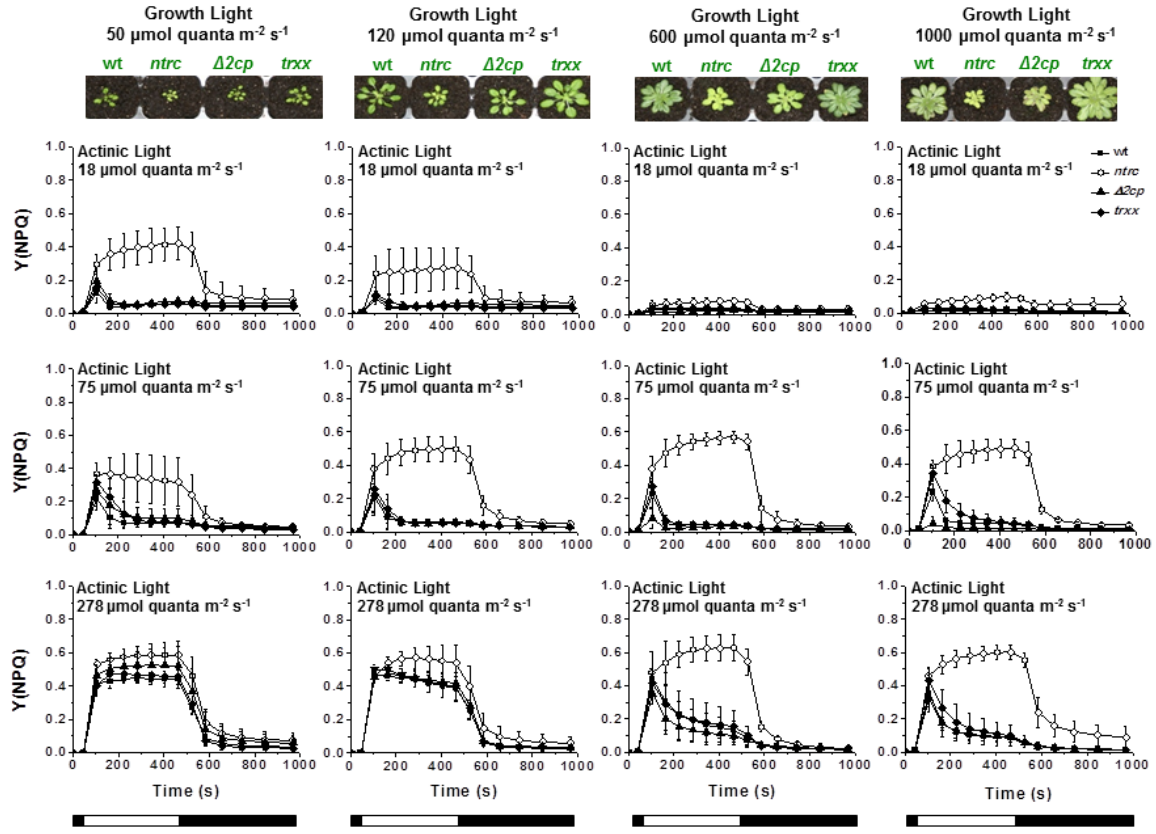

Figure 23. NPQ in wild type and *ntrc*, *Δ2cp* and *trxx* mutant plants grown under different irradiances. Chlorophyll fluorescence was measured using attached leaves of 5-weeks old plants grown at 50, 120, 600 and 1000 µmol quanta m^{-2} s^{-1} under a photoperiod of 10 h light / 14 h darkness. Plants were kept in the dark for 30 min prior to measurements. Three different actinic light intensities of 18, 75 and 278 µmol quanta m^{-2} s^{-1} were used and saturating pulses were applied every 60 s. Quantum yields of NPQ, Y(NPQ), were calculated from saturating pulse analyses. White and black bars below graphs indicate periods of illumination with actinic light and darkness, respectively. Each data point is the mean of the Y(NPQ) from 4 plants and SDs are indicated by error bars.

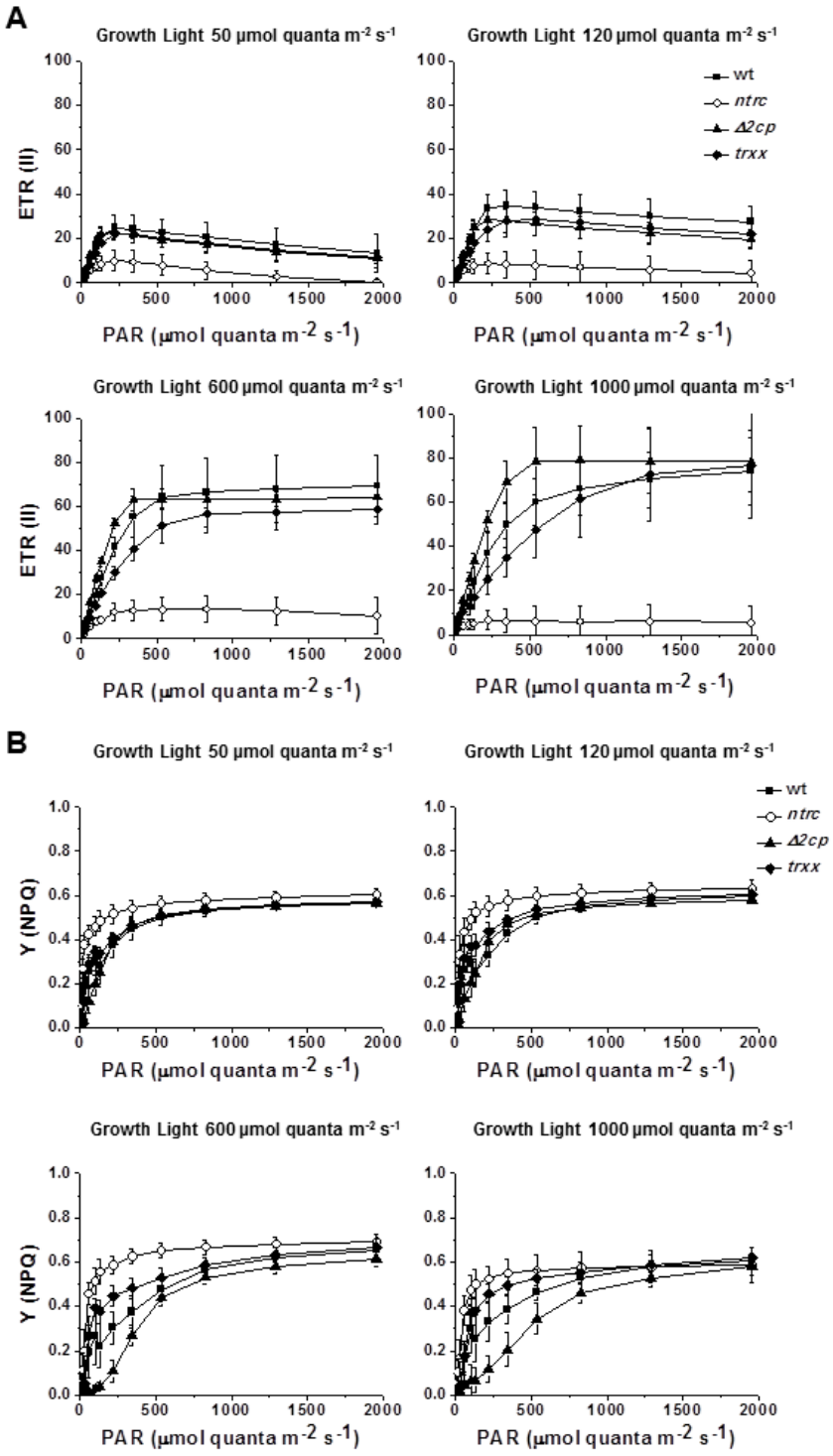

Figure 24. Linear electron transport and NPQ as function of light intensity in wild type and *ntrc*, *Δ2cp* and *trxx* mutant plants grown under different irradiances. Attached leaves of plants grown at 50, 120, 600 and 1000 µmol quanta m^{-2} s^{-1} for 5 weeks under a photoperiod of 10 h light and 14 h darkness were used for chlorophyll fluorescence. **A)** Relative electron transport rates of PSII, ETR(II), were determined during stepwise increasing photosynthetically active radiation (PAR). **B)** The quantum yields of NPQ, Y(NPQ), were determined during the same curves than (A). Each data point is the mean of the values from 8 plants and SDs are presented as error bars.

Characterisation of the component of NPQ regulated by NTRC

As we have seen, the unusually high NPQ present in the *ntrc* mutant shows rapid kinetics characteristic for the energy-dependent component, qE, of NPQ (Figure 20). It is rapidly activated, remains constant during illumination and is rapidly reverted in darkness. Therefore, we have studied the factors contributing to the qE process in *ntrc* mutant plants.

The PsbS protein is a subunit of PSII required for induction of the qE component of NPQ (Li *et al.*, 2009), and transgenic plants overexpressing PsbS have higher NPQ (Li et al., 2002; Roach and Krieger-Liszkay, 2012). To search for a possible alteration of the PsbS levels, we examined the expression of PsbS in the *ntrc* mutant. However, the levels of the PsbS protein were similar in mutant and wild type plants (Figure 25). The presence of the xanthophyll zeaxanthin is another determinant for formation of NPQ, while violaxanthin is inactive in this process (Jahns et al., 2009; Jahns and Holzwarth, 2012). Therefore, we analysed the levels of VDE, the enzyme responsible for the conversion of violaxanthin to zeaxanthin, but found that the quantities of VDE did not differ between *ntrc* mutant and wild type plants (Figure 25). Similarly, ZE, which catalyses the conversion of zeaxanthin back to violaxanthin, was equally abundant in *ntrc* mutant and wild type plants (Figure 25). Hence, there is no evidence for changes in gene expression that could contribute to explaining the observed differences in NPQ.

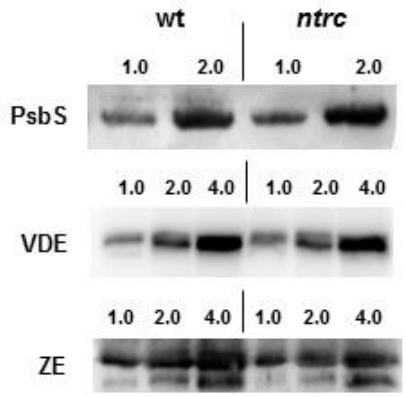

Figure 25. Levels of PsbS, VDE and ZE proteins in wild type and *ntrc* mutant plants. Proteins extracted from leaves of plants grown at 120 µmol quanta m^{-2} s^{-1} light intensity were analysed by protein gel immunoblot. Numbers above each lane indicate the quantity of chlorophyll in µg.

Although the amounts of the enzymes VDE and ZE do not differ between plants lacking NTRC and wild type plants, the possibility remains that their activities may be altered. Therefore, the levels of the xanthophyll cycle pigments violaxanthin, antheraxanthin and zeaxanthin were measured in wild type and *ntrc* mutant plants grown at 120 μmol quanta m^{-2} s^{-1}. Samples were collected at the end of the night and following the onset of light during a normal day/night cycle. As expected, wild type leaves displayed only a minor increase in the content of antheraxanthin and zeaxanthin 20 min after turning on the light, which reverted after 40 min of illumination (Figure 26). Then, as the light was turned off and after an additional 90 min of darkness, the original violaxanthin levels were nearly completely recovered in wild type leaves. In contrast, the *ntrc* mutant showed ten-fold higher levels of zeaxanthin throughout the 40 min of illumination (Figure 26). This implies that the high NPQ of *ntrc* plants at normal light intensities corresponds to the qE component and is a direct consequence of excess zeaxanthin and antheraxanthin, despite wild type levels of VDE and ZE. Therefore, NTRC seems to be regulating the activity of some of these enzymes involved in the xanthophyll cycle, either regulating their redox states or their activation through lumen acidification.

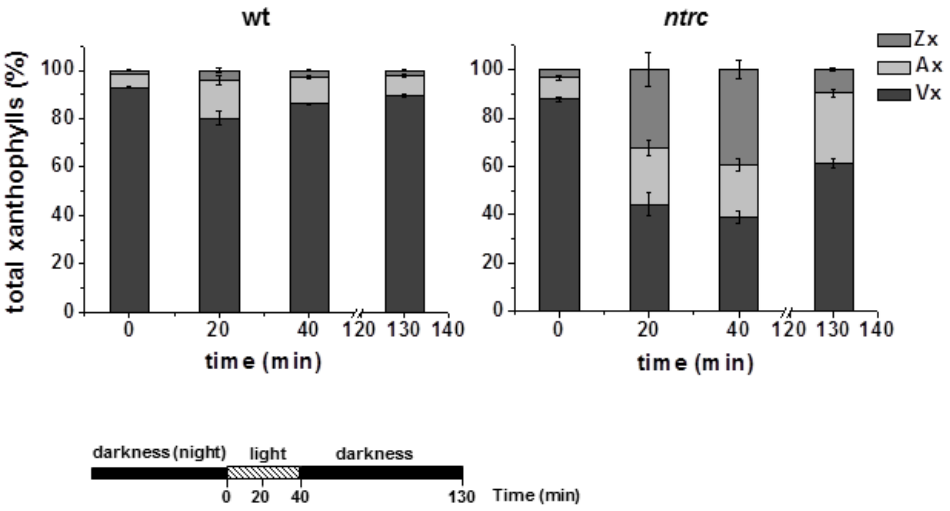

Figure 26. Xanthophyll cycle pigments in wild type and *ntrc* mutant plants. Pigments were extracted from leaves of plants grown at 120 μmol quanta m^{-2} s^{-1} light intensity and the levels of violaxanthin (Vx), antheraxanthin (Ax) and zeaxanthin (Zx) were determined. Leaves were harvested just before the onset of light in the morning (0 min) and after 20 and 40 min of illumination with normal light. Thereafter, plants were kept in the dark for another 90 min and samples were taken again (130 min). Values are the mean (n = 3) ± SD of the xanthophyll levels determined in leaves from 3 plants.

It is known that the activity of VDE, necessary to form zeaxanthin, depends on ΔpH (Pfundel and Dilley, 1993) and is inhibited by DTT (Yamamoto and Kamite, 1972). Therefore, we examined the NPQ levels in *ntrc* upon treatment of leaves with the thiol-reducing agent DTT, or the uncoupler nigericin, abolishing the trans-thylakoid proton gradient (Ruban *et al.*, 2012) (Figure 27). Treatment with nigericin *in vivo* reduced markedly the NPQ in *ntrc* plants (Figure 27A), as well as the treatment with DTT (Figure 27B). The titration showed that incubation with 2 mM DTT could reduce the yield of NPQ to wild type levels (Figure 27C). Concomitantly, the effective quantum yield of PSII in the light increased significantly in the mutant leaves upon incubation with DTT (Figure 27D). Taken together, the effects of nigericin and DTT and the elevated zeaxanthin levels indicate that the energy-dependent quenching qE is permanently activated under low-light conditions in *ntrc* plants.

The redox state of the xanthophyll cycle enzymes VDE and ZE *in vivo*

Since treatment of *ntrc* mutant leaves with DTT reverts the characteristic NPQ phenotype, it is conceivable that NTRC could modulate the activities of VDE and/or ZE through reduction of regulatory disulphides. VDE is known to be inhibited by disulphide reduction *in vitro* (Yamamoto and Kamite, 1972; Hall et al., 2010; Simionato et al., 2015), though the physiological meaning of this remains unknown. The *Arabidopsis* VDE contains twelve cysteines in the sequence of the mature protein and, yet, a single substitution of Cys-72 to Tyr is sufficient to abolish activity (Niyogi *et al.*, 1998). ZE contains nine cysteine residues, five of which are conserved in orthologues from monocotyledons and four are also conserved in green algae (Figure 8). Thiol-based redox regulation of ZE has not been previously reported, though ZE was found to be inhibited *in vivo* by photo-oxidative stress under high light conditions (Reinhold *et al.*, 2008).

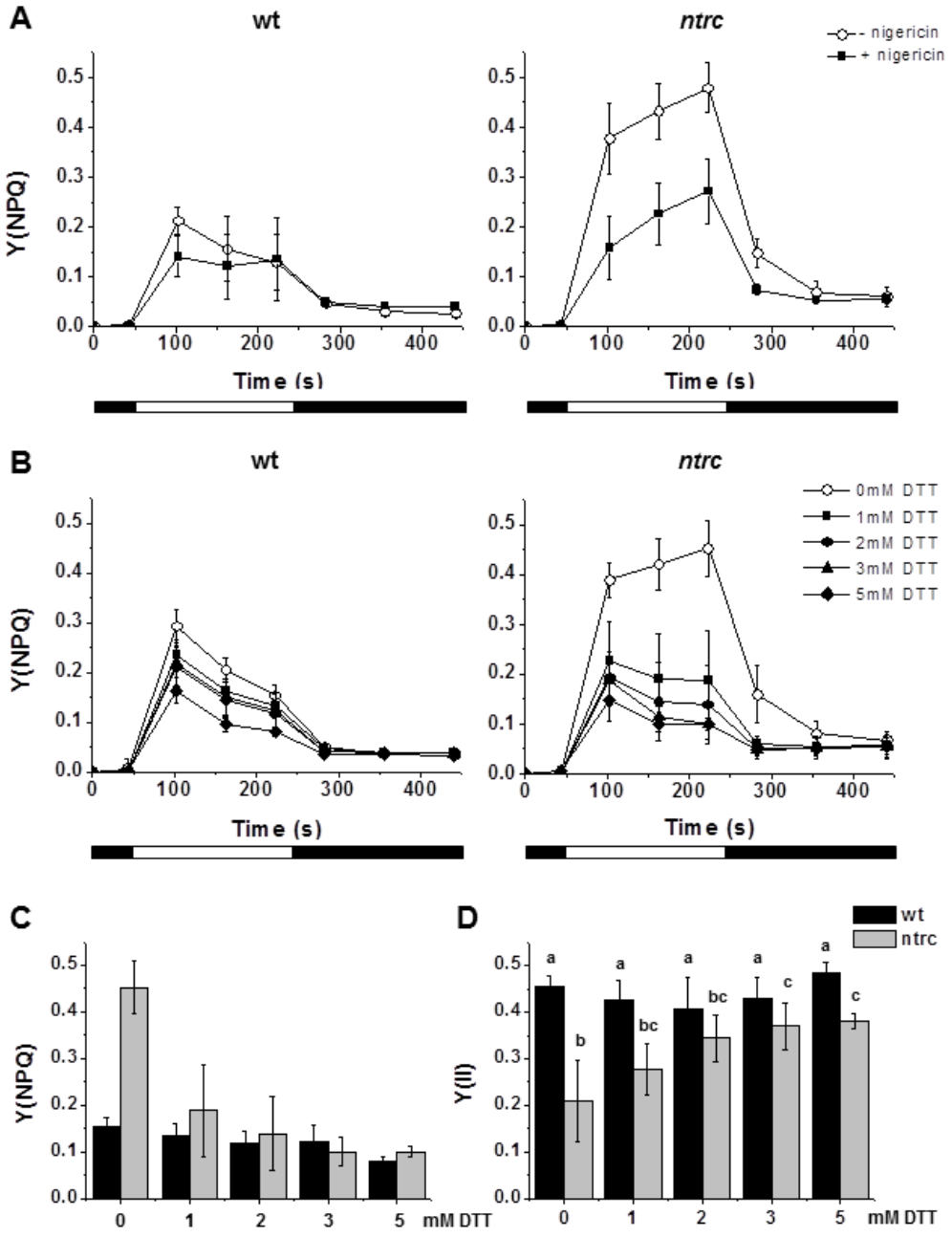

Figure 27. Effects of nigericin and DTT *in vivo* on the NPQ and PSII effective quantum yield of wild type and *ntrc* mutant plants. Leaves from 5-weeks old plants grown at 120 μmol quanta m^{-2} s^{-1} light intensity were floated on 100 μm nigericin **(A)** or DTT solutions **(B)** in the dark for three hours. Chlorophyll fluorescence was measured during 4 min illumination with actinic light at 75 μmol quanta m^{-2} s^{-1} intensity followed by 4 min darkness and the yields of NPQ were determined. **C)** Yields of NPQ in DTT-treated leaves after 3 min illumination. **D)** PSII effective quantum yields in DTT-treated leaves after 3 min illumination. Each data point is the mean of the Y(NPQ) or Y(II) from 6 leaves and SDs are presented as error bars. Significantly different values according to Tukey-test (ANOVA) in (D) are marked with different letters ($p < 0.01$).

First, we examined the redox state of VDE *in vivo* in the *ntrc* mutant and wild type plants taking advantage of the fact that reduced VDE form *in vitro* migrates slower on SDS-PAGE (Figure 28A). While the most oxidised form of VDE is somewhat more abundant in the *ntrc* mutant in the dark, there is no significant difference between the mutant and wild type VDE redox state in the light (Figure 28B). This would rule out a possible role for NTRC in reductive inactivation of VDE in the light.

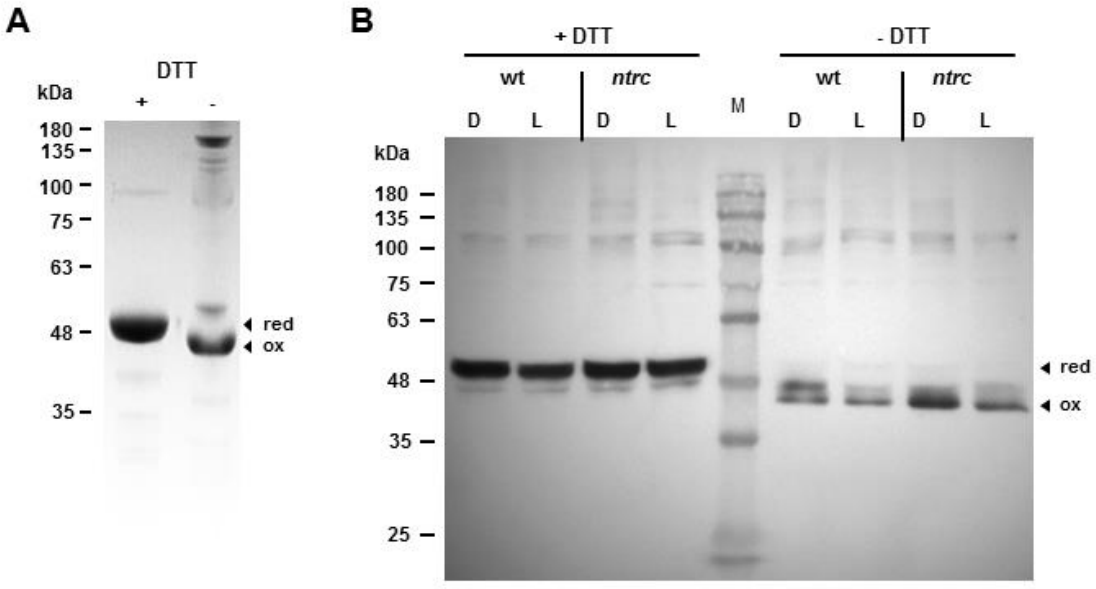

Figure 28. The redox state of VDE. A) Migration of reduced and oxidised VDE in SDS-PAGE. Purified recombinant VDE (1.7 µg) was electrophoresed in a 10% acrylamide gel in the presence and absence of 2 mM DTT and stained with Coomassie Brilliant Blue. **B)** Total leaf proteins from wild type and *ntrc* mutant plants in the dark or after 1 hour in the light at 120 µmol quanta m^{-2} s^{-1} intensity were extracted in the presence of 10% TCA to preserve the thiol redox state. Proteins were solubilised in the presence of 40 mM N-ethyl maleimide to avoid oxidation of thiols and electrophoresed in a 10% acrylamide gel in the presence or absence of DTT. VDE was detected by immunoblot analysis. D, dark; L, light; M, molecular mass protein standard; red, reduced; ox, oxidised.

Analysing the electrophoretic mobility of ZE *in vitro*, we found that the purified recombinant enzyme forms intermolecular disulphides under non-reducing conditions (Figure 29A and B) and that purified NTRC is able to catalyse the reduction of these disulphides *in vitro* (Figure 29C). In contrast, analysis of ZE *in vivo* using alkylation with $MM(PEG)_{24}$, showed that the redox state remains unchanged in darkness and

moderate light both in the wild type and the *ntrc* mutant (Figure 30). This indicates that ZE is not a target for redox regulation under normal light conditions.

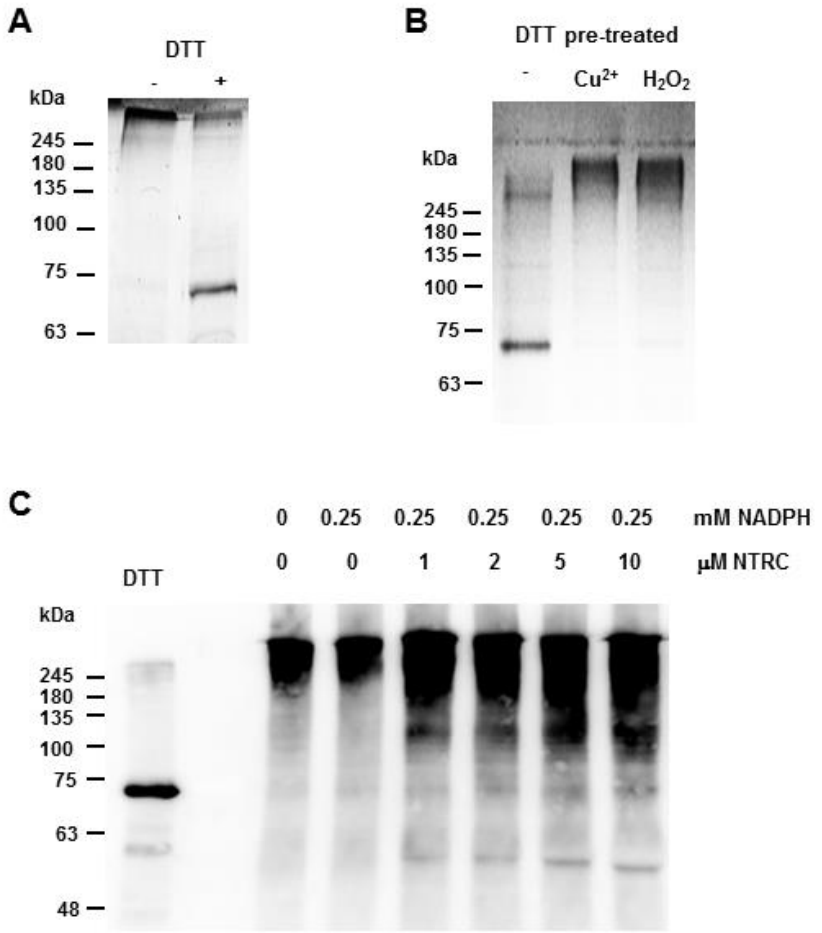

Figure 29. Reduction of ZE *in vitro*. A) Purified recombinant ZE was subjected to SDS-PAGE under non-reducing and reducing conditions. Three µg of ZE was applied on a 10% acrylamide gel in the absence and presence of 2 mM DTT and stained with Coomassie Brilliant Blue. **B)** ZE was pretreated with 5 mM DTT and reduced ZE (3 µg) was electrophoresed in the absence and presence of thiol oxidants in a 10% acrylamide gel and stained with Coomassie Brilliant Blue. $CuCl_2$ and H_2O_2, which are known to induce disulphide formation between redox-sensitive cysteines (Hansen and Winther, 2009; Lindahl et al., 2011), were added at 50 µM and 1 mM concentration, respectively. **C)** ZE (400 ng) was visualized by Western blot using anti-ZE antibody, after incubating 0.3 µM ZE for 20 min with either 2 mM DTT, without additions or with increasing concentrations of purified NTRC using NADPH as ultimate reductant.

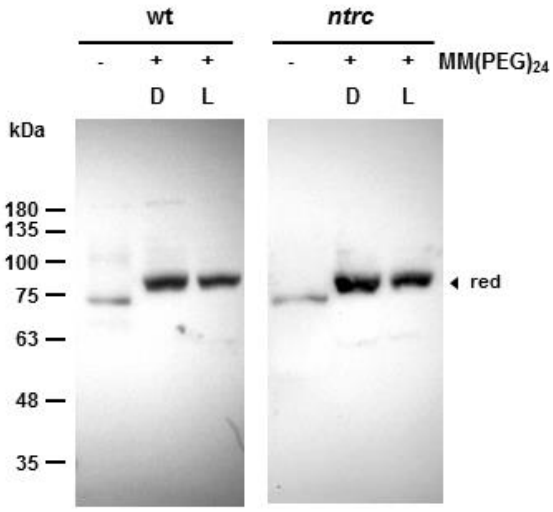

Figure 30. The *in vivo* redox state of ZE. Total leaf proteins from wild type and *ntrc* mutant plants in the dark or after 1 hour in the light at 120 μmol quanta m^{-2} s^{-1} intensity were extracted in the presence of 10% TCA to preserve the thiol redox state. Protein thiols were alkylated with 10 mM $MM(PEG)_{24}$ during solubilisation for SDS-PAGE and electrophoresed in a 10% acrylamide gel in the presence of DTT. ZE was detected by immunoblot. The left lanes of each gel contain control samples without alkylation. D, dark; L, light; red, reduced.

ABA content

ABA is a plant hormone which plays an important role in stress response in addition to seed germination and plant development. Since ZE, also known as ABA1, is involved in the first step of ABA biosynthesis (Nambara and Marion-Poll, 2005), we have measured the levels of ABA in *ntrc* plants grown under long- and short-photoperiod. The ABA content in long-day grown plants was lower than in plants grown under short-day conditions, but no differences were found according to Student's t-test between wild type and *ntrc* plants and between dark and light conditions (Table 5).

Table 5. ABA content in wild type and *ntrc* plants in different conditions. ABA was extracted from depetiolated leaves of plants grown at 120 μmol quanta m^{-2} s^{-1} intensity under short- and long-day conditions, at the end of the night (dark) or after 45 min of illumination with growth light. ABA content was determined by liquid chromatography and related to fresh leaf weight (fw). Each value is the mean of 3 extractions.

		Short-day		Long-day	
		ABA (pmol g^{-1} fw)	± SD	**ABA (pmol g^{-1} fw)**	± SD
Dark	wt	**27,01**	1,51	**16,37**	0,95
	ntrc	**26,95**	0,18	**17,45**	0,53
Light	wt	**26,98**	1,10	**18,25**	0,56
	ntrc	**27,00**	0,39	**17,86**	0,45

The trans-thylakoid proton gradient in *ntrc* plants

It is well known that VDE is regulated by luminal pH. When the pH in the thylakoid lumen decreases below 6, the protein is activated through a conformational change leading to production of zeaxanthin (Pfundel and Dilley, 1993; Arnoux et al., 2009). Therefore, the high qE accompanied by high zeaxanthin levels observed in the *ntrc* mutant, could be a consequence of an excessive acidification of the thylakoid lumen in these plants under low light conditions.

In this context we have studied the proton gradient (ΔpH) formed across the thylakoid membrane at different light intensities in plants lacking NTRC, based on electrochromic shift (ECS_{inv}) (Takizawa *et al.*, 2007). At light intensities lower than growth light, ΔpH was consistently higher in the *ntrc* mutant with respect to wild type plants (Figure 31B). However, at higher light intensities, ΔpH in *ntrc* was lower than in wild type (Figure 31A). This result is in agreement with the NPQ response, which is more pronounced in plants lacking NTRC under low light intensities (Figure 23).

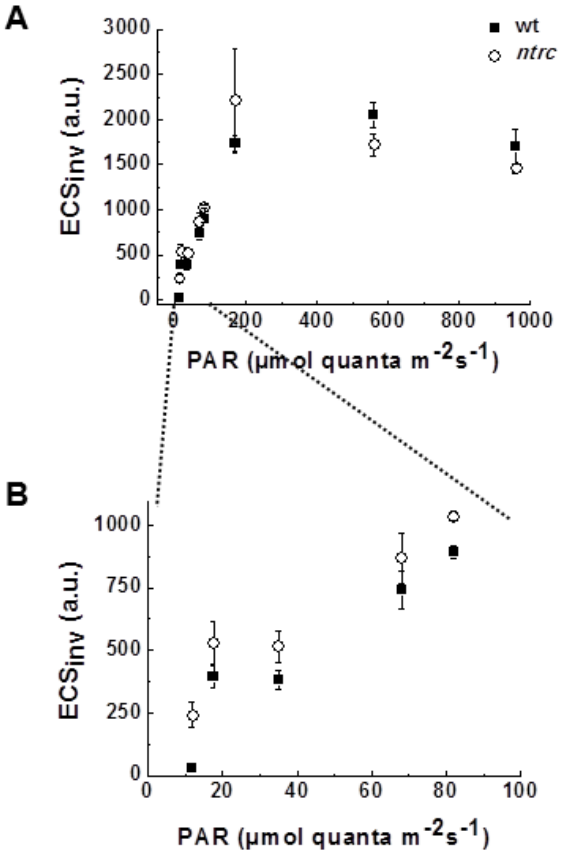

Figure 31. Electrochromic shift in wild type and *ntrc* plants at different light intensities. Plants grown at 120 µmol quanta m^{-2} s^{-1} under short-day photoperiod. Dark relaxation of ECS was measured in leaves after photosynthetic steady-state conditions, 15 min of actinic illumination by red LEDs (650 nm) at different photosynthetically active radiations (PAR). Intensities were from 12 to 940 µmol quanta m^{-2} s^{-1}. **A)** The graph shows the recovery phase of the ECS decay, ECS_{inv}, after the light-dark transition which is proportional to the trans-thylakoid proton gradient formed during photosynthesis. **B)** Zoom in the part of the curve (A) up to 100 µmol quanta m^{-2} s^{-1} PAR. Each value is the mean ± SE of ECS_{inv} in 3 leaves.

A relevant target for redox regulation involved in ΔpH formation, is the γ-subunit of the thylakoid ATP synthase, which is known to mediate light-induced activation of ATP synthesis (Hisabori *et al.*, 2013). A possible deficiency in the reduction of the γ-subunit would lead to a build-up of the trans-thylakoid proton gradient and enhanced NPQ. In the dark this subunit was found in the oxidised form both in the wild type and the *ntrc* mutant (Figure 32). After 1 min of illumination the γ-subunit was fully reduced in the wild type and nearly completely reduced in the *ntrc* mutant plants (Figure 32). However, a small fraction of this protein remained oxidised in *ntrc* plants. Therefore, the γ-subunit of the ATP synthase appears to be reduced by

NTRC *in vivo*, although there must be other enzymes more efficient than NTRC in reducing this subunit.

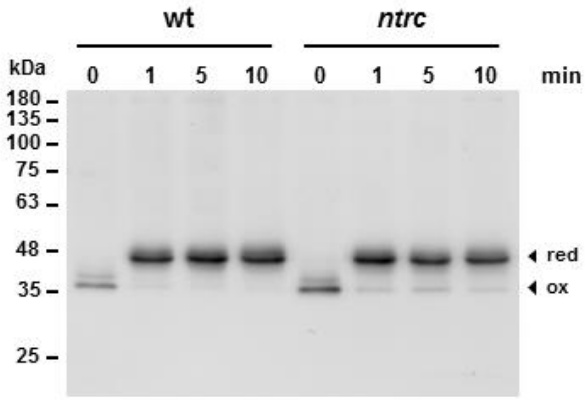

Figure 32. The *in vivo* redox state of the ATP synthase γ subunit. Total leaf proteins from wild type and *ntrc* mutant plants in the dark (0 min) and after 1, 5 and 10 min of illumination at 120 μmol quanta m^{-2} s^{-1} intensity were extracted in the presence of 10% TCA to preserve the thiol redox state. Protein thiols were alkylated with 10 mM $MM(PEG)_{24}$ prior to electrophoresis in a 10% polyacrylamide gel under non-reducing conditions and the γ subunit of the ATP synthase was detected by immunoblot. red, reduced; ox, oxidised.

Isolation and analysis of a *ntrc-psbs* double mutant

Since the PsbS protein is necessary for induction of the qE component of NPQ (Li *et al.*, 2000), a double mutant lacking both NTRC and PsbS presumably would be devoid of qE and, thus, would provide useful insight into the nature of the NPQ of the *ntrc* mutant. Furthermore, such a double mutant would permit establishing the specific impact of qE on the *ntrc* mutant phenotype. The *Arabidopsis ntrc-psbs* double mutant was obtained by manual crossing of the corresponding single mutants and the absence of the two proteins NTRC and PsbS was confirmed by Western blot analysis (Figure 33).

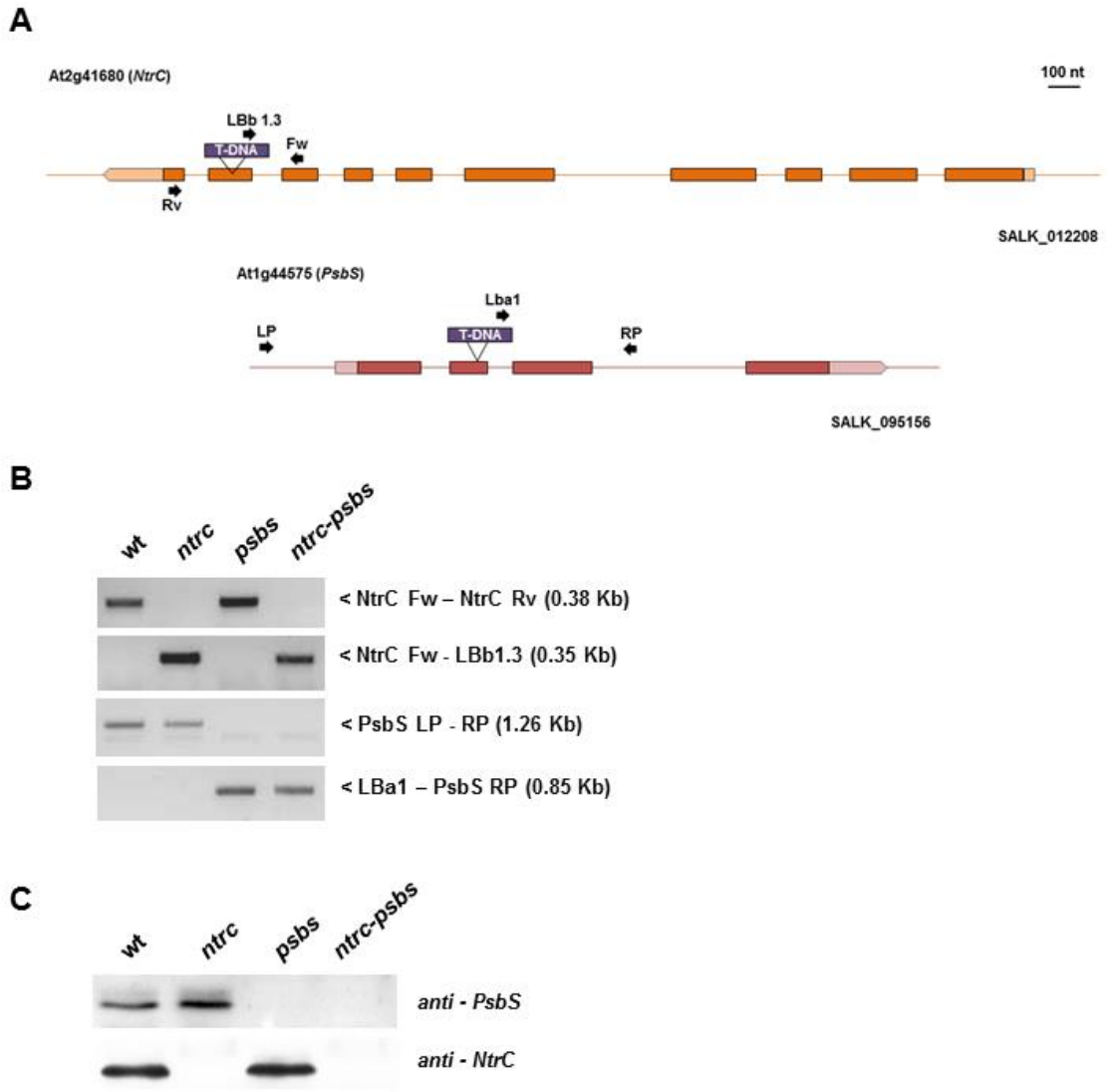

Figure 33. Isolation of a *psbs* knockout mutant and *ntrc-psbs* double knockout mutant. A) The SALK_012208 line contains a T-DNA insertion in the ninth exon of the *NtrC* gene (At2g41680). The SALK_095156 line contains a T-DNA insertion in the second exon of the *PsbS* gene (At1g44575). Sequence information was obtained from TAIR (http://www.arabidopsis.org). **B)** The presence of the T-DNA insertions was tested by PCR using as template genomic DNA isolated from wild type plants, the insertion line SALK_095156 (*psbs* mutant) and from the cross between the homozygous *psbs* mutant and the *ntrc* knockout mutant. Oligonucleotide positions are indicated in (A) and detailed in Tables 1 and 2. **C)** The absence of NTRC and/or PsbS protein was verified in extracts from leaves by Western blot using antibodies against PsbS and NTRC. Samples corresponding to 2 μg chlorophyll were loaded in each lane.

When plants were grown at moderate light intensity (120 μmol quanta m^{-2} s^{-1}) for 10 weeks under short-day photoperiod (8 h light / 16 h darkness), the double mutant

plants were larger and had higher chlorophyll content than the single *ntrc* mutant (Figure 34). The rosette weight and chlorophyll content of *ntrc-psbs* mutant plants were twice as high as compared to those of *ntrc* plants (Figure 34C and D).

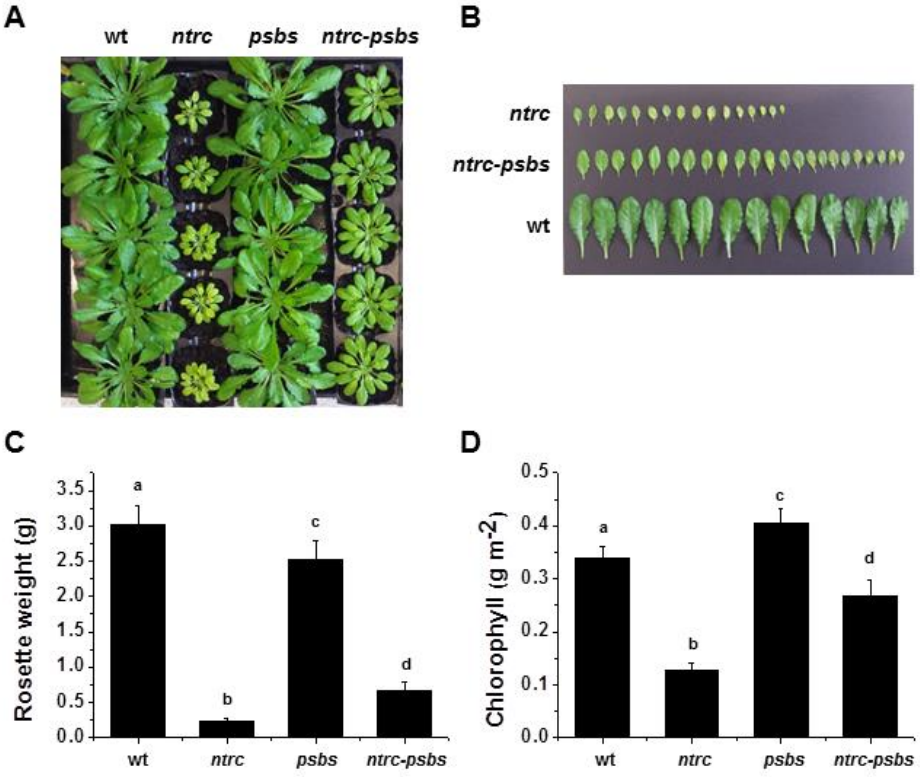

Figure 34. Growth and chlorophyll content of the *ntrc-psbs* double mutant. A) Plants grown for 10 weeks at 120 μmol quanta m^{-2} s^{-1} light intensity under a photoperiod of 8 h light / 16 h darkness. **B)** The largest rosette leaves from representative plants of wild type, *ntrc* and the *ntrc-psbs* mutant. **C)** Fresh weight of rosettes from 10-weeks old plants. Each data point is the mean of 8 to 12 plants and SDs are presented as error bars. Significantly different values according to Student's t-test are indicated with different letters ($p < 0.01$). **D)** Content of total chlorophylls *a* and *b* determined in leaf discs from 10-weeks old plants. Each data point is the mean of 12 discs from different plants. Significantly different values according to Tukey-test (ANOVA) are indicated with different letters ($p < 0.01$).

Chlorophyll fluorescence imaging indicated that the *ntrc-psbs* mutant has low NPQ similar to the *psbs* simple mutant and the effective PSII quantum yield is higher in *ntrc-psbs* than in the *ntrc* mutant (Figure 35). Furthermore, less difference in the effective PSII quantum yield was observed between leaves of the double mutant than in *ntrc* (Figure 35).

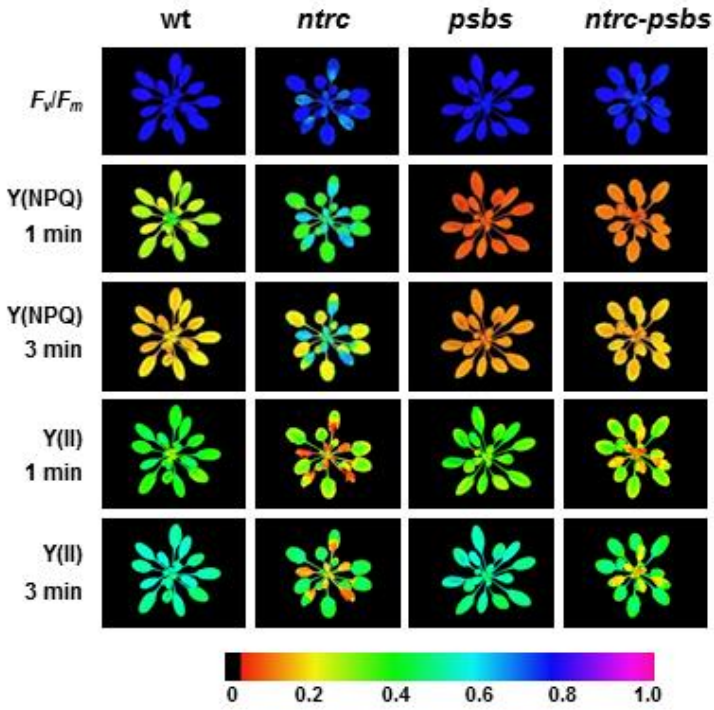

Figure 35. Fluorescence imaging of the *ntrc-psbs* double mutant. False-colour images representing F_v/F_m in wild type and *ntrc* mutant plants and the respective Y(NPQ) and Y(II) after 3 min of 81 µmol quanta m^{-2} s^{-1} intensity illumination. Induction-recovery curves were performed using IMAGING-PAM Chlorophyll Fluorescence System (Walz). F_v/F_m values were determined in plants grown under short day conditions at 120 µmol quanta m^{-2} s^{-1}. Subsequently, plants were illuminated with 81 µmol quanta m^{-2} s^{-1} of actinic light during 6 min and saturating pulses were applied each 20 s to obtain PSII quantum yields. Images of *ntrc* plants have been enlarged to facilitate viewing.

Measurements of chlorophyll fluorescence showed that qE is missing in the *psbs* mutant and the *ntrc-psbs* double mutant (Figure 36A). Interestingly, the effective PSII quantum yield was higher in plants lacking both NTRC and PsbS than in plants lacking only NTRC (Figure 36B). The higher degree of basal non-regulated energy dissipation in the double mutant (Figure 36C) accounts for the lower effective PSII quantum yield as compared to the wild type and *psbs* simple mutant (Figure 36B). The linear electron transport rates at growth light and low light intensities were significantly higher in the *ntrc-psbs* double mutant than in the *ntrc* mutant (Figure 37). However, the double mutant was hypersensitive to high irradiances similarly to the *psbs* simple mutant (Figure 37).

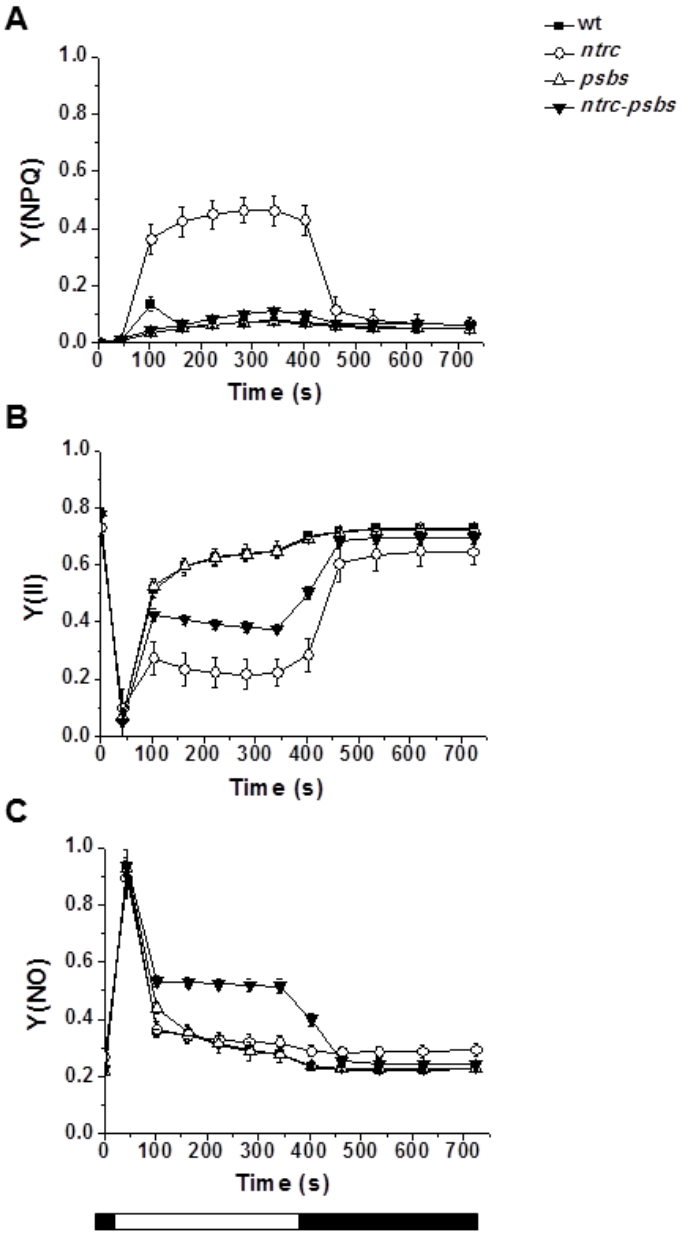

Figure 36. Photosystem II quantum yield of the *ntrc-psbs* double mutant. Chlorophyll fluorescence was measured with a pulse-amplitude modulation fluorometer using plants grown for 5 weeks at 120 μmol quanta m^{-2} s^{-1} light intensity under a photoperiod of 10 h light / 14 h darkness. Plants were dark-adapted for 30 min before measurements. Induction-recovery curves were performed with actinic light of 75 μmol quanta m^{-2} s^{-1} intensity and saturating pulses applied every 60 s. After 6 min of illumination, the actinic light was switched off and measurements were continued for another 6 min. White and black bars indicate periods of illumination with actinic light and darkness, respectively. **A)** Quantum yields of NPQ, Y(NPQ). **B)** Quantum yields of PSII photochemistry, Y(II). **C)** Quantum yields of basal non-regulated energy dissipation, Y(NO). Values are the means of 6 measurements ± SD.

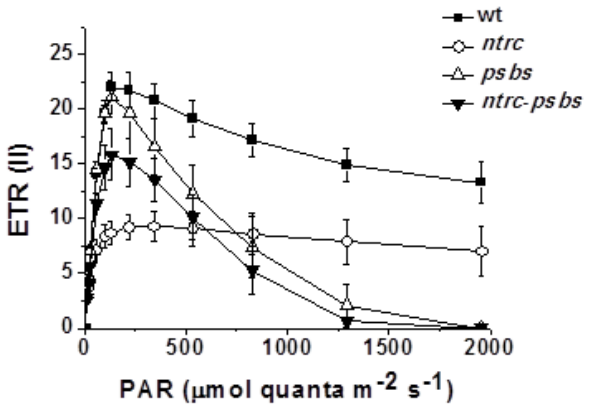

Figure 37. Electron transport rate of the *ntrc-psbs* double mutant. Relative linear electron transport rates ETR(II) were determined by chlorophyll fluorescence as a function of actinic light intensity in pre-illuminated leaves of plants grown for 5 weeks at 120 µmol quanta m^{-2} s^{-1} light intensity under a photoperiod of 10 h light / 14 h darkness. Values are the means of 6 measurements ± SD.

4.1.3. Effect of NTRC deficiency on other components of the photosynthetic electron transport chain

Photosystem I

Since the lack of NTRC strongly influences the levels of NPQ and PSII activity, we proceeded to investigate the PSI activity. Various biosynthetic processes, such as starch synthesis, are deficient in the *ntrc* mutant (Michalska *et al.*, 2009; Toivola *et al.*, 2013) and, therefore, a shortage of electron acceptors for PSI might be expected. This, in turn, could lead to activation of NPQ because of a lower ATP consumption and a concomitant proton accumulation in the lumen (Kalituho *et al.*, 2007). NTRC was previously reported to reduce and activate the small subunit of the ADP glucose pyrophosphorylase, a key enzyme in starch synthesis (Michalska *et al.*, 2009). An *Arabidopsis* mutant lacking the regulatory small subunit of the ADP glucose pyrophosphorylase, *aps1*, is devoid of leaf starch and grows poorly, except under continuous light conditions (Ventriglia *et al.*, 2008). However, *aps1* shows a pattern of NPQ identical to wild type plants (Figure 38) indicating that the role of NTRC in starch synthesis is not relevant for the increased energy dissipation.

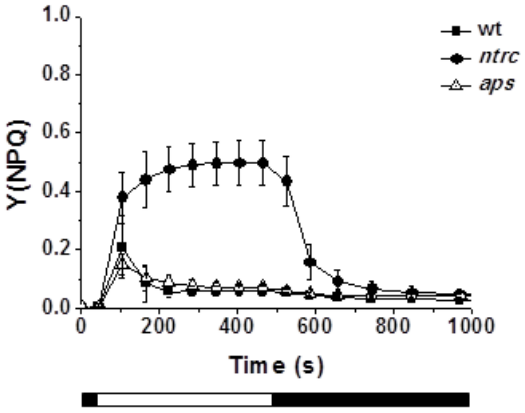

Figure 38. NPQ in the *aps1* mutant in comparison to wild type and *ntrc* plants. Chlorophyll fluorescence was measured using *aps1*, *ntrc* and wild type plants grown at 120 μmol quanta m^{-2} s^{-1} light intensity. Prior to measurements plants were kept in the dark for 30 min. Actinic light at 75 μmol quanta m^{-2} s^{-1} was turned on and saturating pulses were applied every 60 s. After 8 min the actinic light was switched off and measurements were continued for another 10 min. White and black bars indicate periods of illumination with actinic light and darkness, respectively. Each data point is the mean of the Y(NPQ) from 4 leaves and the error bars represent SDs.

Measurements of the PSI activity in wild type and *ntrc* plants through induction-recovery curves based on P700 absorbance changes showed that the redox state of P700 during illumination was affected in plants lacking NTRC (Figure 39). Analysis of the respective quantum yields of PSI activity, Y(I), donor side limitations, Y(ND), and acceptor side limitations, Y(NA), revealed the lower effective PSI quantum yield under growth light intensity in the *ntrc* mutant (Figure 40A). This turned out to be the result of limitations at the donor side of PSI in the electron transport chain during illumination (Figure 40B). In contrast, wild type and *ntrc* plants were indistinguishable with respect to acceptor side limitations (Figure 40C). Thus, the absence of NTRC leads to a deficiency in PSI activity affecting specifically the supply of electrons to this photosystem in the light. This could be a consequence of the high NPQ observed in the *ntrc* mutant that decreases the flux through the photosynthetic electron transport chain. However, the demand for electrons from PSI appears not to be altered.

In order to know if the partial recovery of PSII activity observed in the double mutant *ntrc-psbs* (Figure 36B) led to a concomitant recovery of PSI, quantum yields of this photosystem were analysed in plants lacking PsbS. Thus, PSI activity was found to be partially restored in *ntrc-psbs* plants (Figure 41A), probably due to the relief of the donor side limitations observed in the *ntrc* plants (Figure 41B). A slight increase in acceptor side limitations (Figure 41C) counteracts the complete rescue of PSI activity in the double mutant. Thus, abolishing qE in plants lacking NTRC stimulates linear PET.

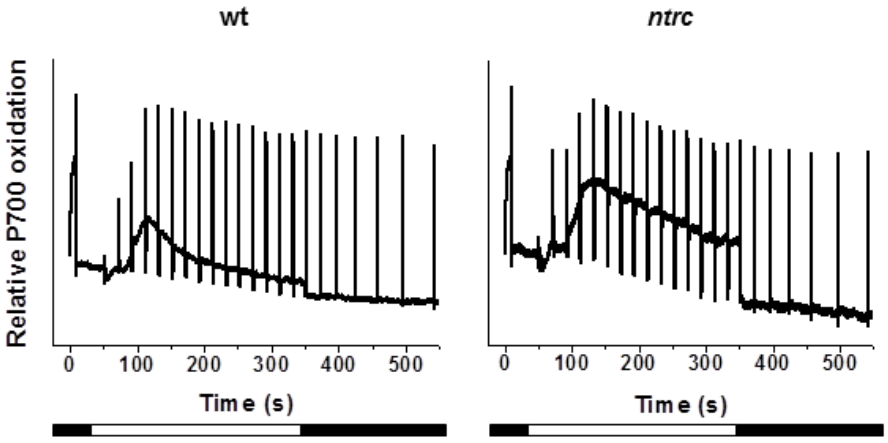

Figure 39. Redox state of the P700 in wild type and *ntrc* mutant plants. The redox state of the PSI reaction centre P700 was determined measuring the absorbance of attached leaves at 830 and 875 nm using the DUAL PAM-100. Following the initial determination of maximal oxidation of P700 with a saturating pulse after 10 s of far red light, the actinic light at an intensity of 126 μmol quanta m^{-2} s^{-1} was turned on and saturating pulses were applied every 20 s. After 5 min actinic light was switched off and measurements were continued for another 5 min. White and black bars below graphs indicate periods of illumination with actinic light and darkness, respectively.

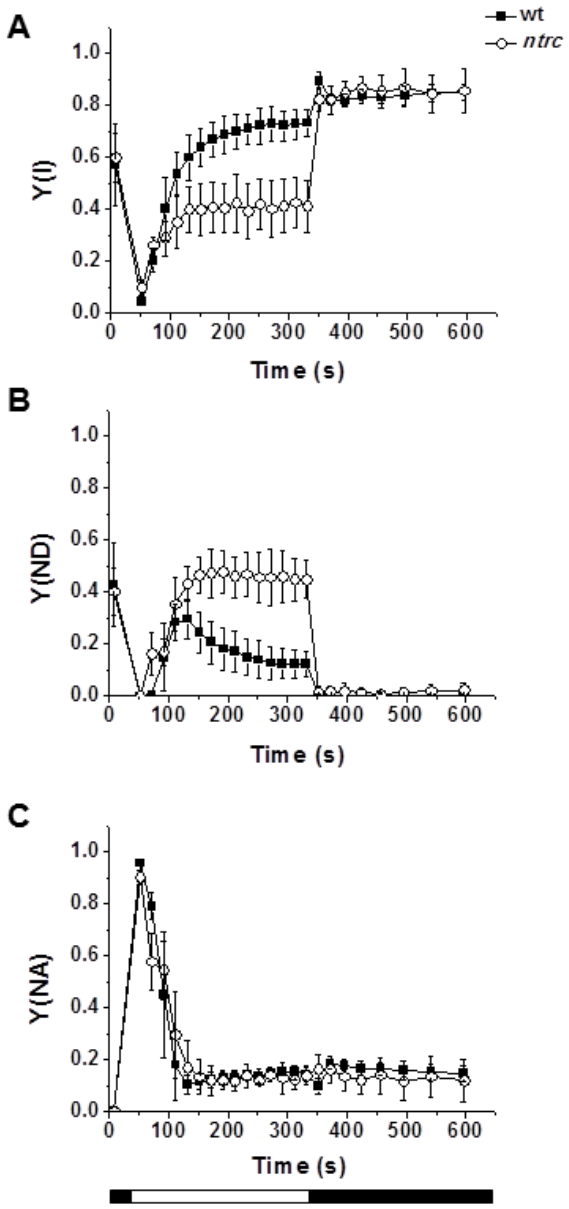

Figure 40. Activity of PSI in wild type and *ntrc* mutant plants. The redox state of the PSI reaction centre P700 was monitored through changes in absorbance at 830 nm versus 875 nm. Five-weeks old plants grown at 120 μmol quanta m^{-2} s^{-1} light intensity were kept in the dark for 30 min prior the induction-recovery curve. Following the initial determination of maximal oxidation of P700 actinic light at an intensity of 126 μmol quanta m^{-2} s^{-1} was turned on and saturating pulses were applied every 20 s. After 5 min the actinic light was switched off and measurements were continued for another 5 min. The quantum yields of PSI photochemistry, Y(I), donor side limitations Y(ND) and acceptor side limitations Y(NA) are based on saturating pulse analyses (Figure 39). White and black bars below graphs indicate periods of illumination with actinic light and darkness, respectively. Each data point is the mean of values from 6 plants and SDs are shown as error bars.

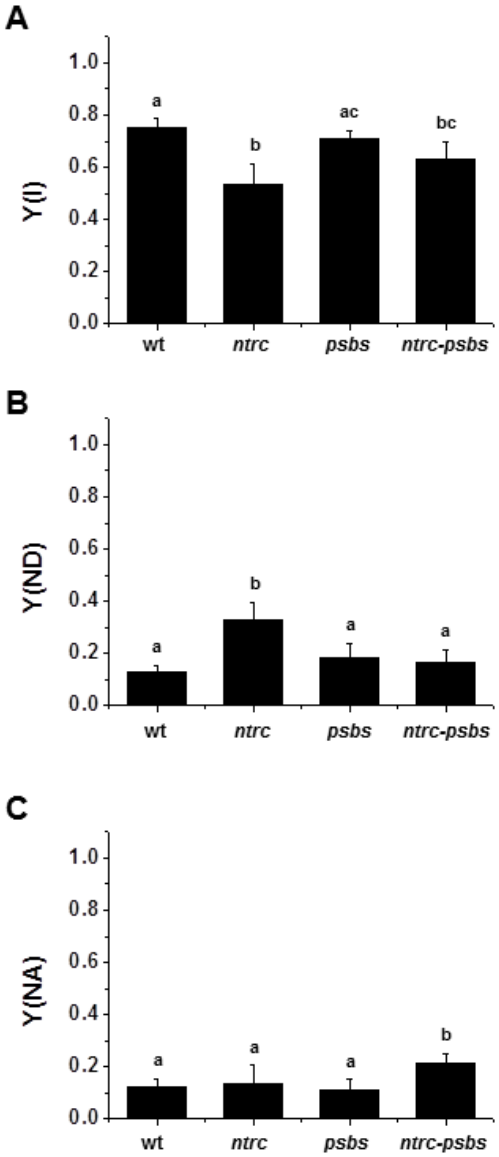

Figure 41. Activity of PSI in the double mutant *ntrc-psbs*. The quantum yields of (**A**) PSI photochemistry, Y(I), (**B**) donor side limitations, Y(ND), and (**C**) acceptor side limitations, Y(NA), are displayed after 3 min of illumination during an induction-recovery curve with 126 μmol quanta m^{-2} s^{-1} actinic light and saturating pulses every 20 s. Five-weeks old plants grown at 120 μmol quanta m^{-2} s^{-1} light intensity were used. Values are the means of 6 measurements ± SD. Significantly different values according to Tukey-test (ANOVA) are marked with different letters ($p < 0.05$).

The plastoquinone redox state

A direct consequence of high NPQ is that fewer electrons are transferred from P680 to the first electron acceptor Q_A in PSII. Hence, a more oxidised pool of PQs in the *ntrc* mutant might be expected. Therefore, we have studied the redox state of the

PQs using approaches based on post-illumination fluorescence and thermoluminescence.

In darkness, after a period of illumination, a transient increase in chlorophyll fluorescence is observed which is caused by Q_A reduction due to backflow of electrons from the stroma to the PQ-pool. This post-illumination fluorescence is related to the activity of the NADPH dehydrogenase (NDH) complex (Shikanai *et al.*, 1998). Whereas in wild type plants the rise of chlorophyll fluorescence after turning off the actinic light was only transitory, in the *ntrc* mutant this fluorescence remained high after a few minutes (Figure 42) indicating that Q_A stays more reduced in these plants after illumination.

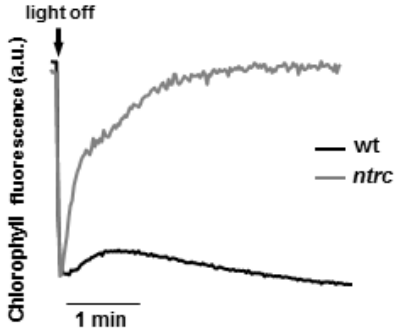

Figure 42. Post-illumination fluorescence in wild type and *ntrc* mutant plants. Dark-adapted leaves during 10 min of plants grown at 120 μmol quanta m^{-2} s^{-1} light intensity under short-day conditions were subjected to a saturation pulse followed by 5 min of actinic light at an intensity of 126 μmol quanta m^{-2} s^{-1}. Post-illumination fluorescence was measured during 5 min in darkness.

Thermoluminescence measurements constitute an alternative approach to determine the redox state of PQs. After a single turn-over flash, the expected B-band was observed in both wild type an *ntrc* plants with a maximum at about 35 °C (Figure 43A and Table 6). The AG-band induced by far red illumination had a temperature maximum at about 50 °C in wild type plants, while in *ntrc* plants it was observed at around 36 ºC (Figure 43B and Table 6). The lower temperature of the AG-band is associated with an increased back transfer of electrons to the acceptor side of PSII (Ducruet and Vass, 2009).

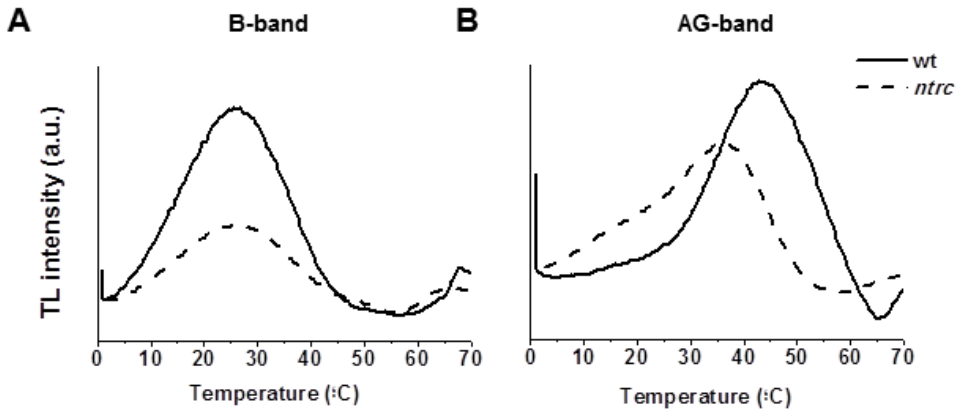

Figure 43. Measurements of thermoluminescence. Thermoluminescence was measured with a home-built apparatus on leaf segments taken from plants that were grown at 120 μmol quanta m^{-2} s^{-1} light intensity under short-day conditions and adapted to dark for 15 min. **A)** The B-band originated from $S_{2/3}Q_B^-$ recombination, was obtained after a single turn-over flash. **B)** The afterglow band (AG-band) was induced with far red illumination during 30 s. In both cases, thermoluminescence was excited at 1 °C and samples were heated at a rate of 24 °C/min from 1 to 70 °C while the light emission was recorded.

Table 6. B- and AG-band maximum temperatures. Maximum temperatures corresponding with curves such as Figure 43. Each value is the mean of at least 4 measurements.

	B-band				**AG-band**			
	T1 (ºC)	± SD	**T2 (ºC)**	± SD	**T1 (ºC)**	± SD	**T2 (ºC)**	± SD
wt	**25,50**	0,87	**35,69**	6,91	**38,64**	4,99	**50,98**	2,60
ntrc	**23,72**	0,95	**35,21**	1,95	**23,97**	5,71	**36,29**	3,51

Both experiments based on post-illumination fluorescence and thermoluminescence measurements indicate that *ntrc* plants present higher levels of reduced PQs than wild type plants, apparently caused by flow of electrons from the stroma to the PQ-pool.

4.2. The function of the *f*-type thioredoxins *in vivo*

Chloroplasts harbour a complex set of Trxs. However, their specific functions *in vivo* are not fully understood. In the case of *f*-type Trxs, extensive biochemical and proteomics studies suggest their central role in the reductive activation of most of the Calvin-Benson cycle enzymes, but so far *in vivo* studies supporting this notion are scarce. The *Arabidopsis* genome encodes two isoforms of *f*-type Trxs, *f*1 and *f*2. *Arabidopsis* knockout mutants lacking Trx *f*1 show wild type phenotype with respect to growth (Thormahlen *et al.*, 2013). Therefore, the loss of Trx *f*1 might be compensated for either by Trx *f*2 still present in the mutant, which was estimated to comprise about 5% of the total content of *f*-type Trxs in wild type plants, or additional chloroplast redox systems. Thus, to address this possibility and whether or not the *f*-type Trxs are essential for plant growth, we have generated *Arabidopsis* plants devoid of *f*-type Trxs.

4.2.1. Generation of plants lacking *f*-type Trxs

To generate a double knockout mutant of *Arabidopsis* lacking both Trx *f*1 and Trx *f*2, the *Arabidopsis* line (GK-020E05-013161), with a T-DNA insertion at the AT5G16400.1 locus encoding Trx *f*2, was isolated and manually crossed with the Trx *f*1 knockout mutant (SALK_128365.45.75.x) (Figure 44A), which was previously reported (Perez-Ruiz *et al.*, 2014). Plants homozygous for both T-DNAs were selected by PCR analysis of genomic DNA (Figure 44B). The double mutant, here termed *trxf1f2*, was effectively devoid of both Trx *f*1 and Trx *f*2 as shown by the lack of transcripts of the two genes, based on semiquantitative PCR and qRT-PCR analysis (Figure 45A and B), and the lack of the corresponding polypeptides, as shown by Western blot with an anti-Trx *f* antibody (Figure 45C). Different intensities of the signals observed in Western blot analysis of the *trxf1* and *trxf2* single mutants (Figure 45C) confirmed that Trx *f*1 is much more abundant than Trx *f*2.

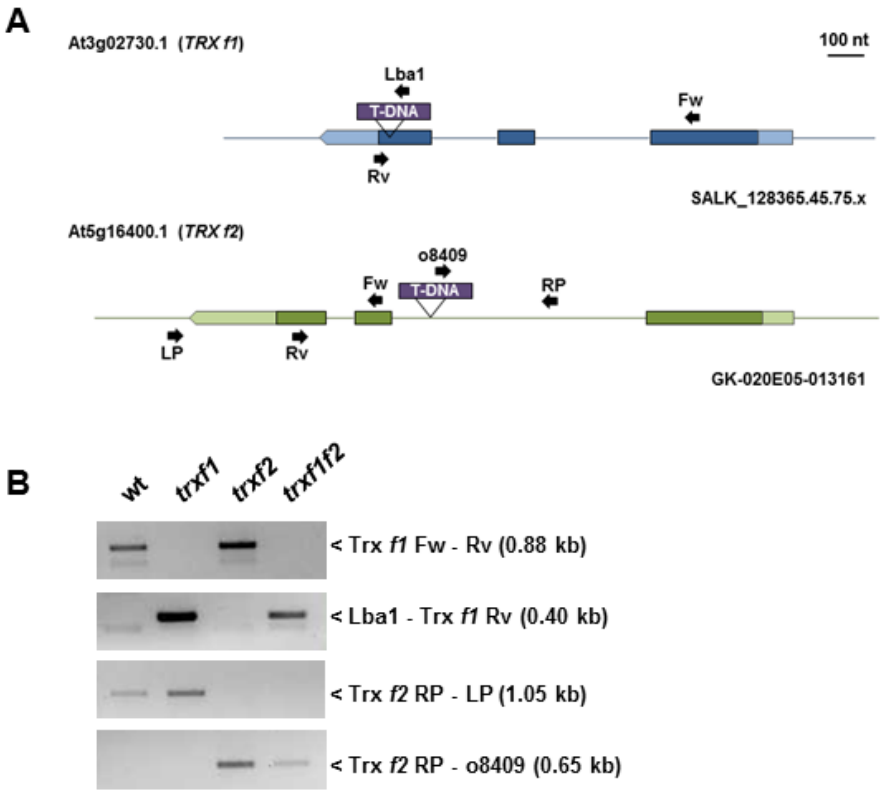

Figure 44. Identification of *Trx f*-deficient mutants. A) The SALK_128365.45.75 line contains a T-DNA insertion in the third exon of the *TRX f1* (At3g02730.1) gene. The GK-020E05-013161 line contains a T-DNA insertion in the first intron of the *TRX f2* (At5g16400.1) gene. Sequence information was obtained from TAIR (http://www.arabidopsis.org). **B)** The presence of the T-DNA insertions was tested by PCR using as template genomic DNA isolated from wild type and mutant plants (*trxf1*, *trxf2* and *trxf1f2*). Oligonucleotides are signalled in (A) and detailed in Tables 1 and 2.

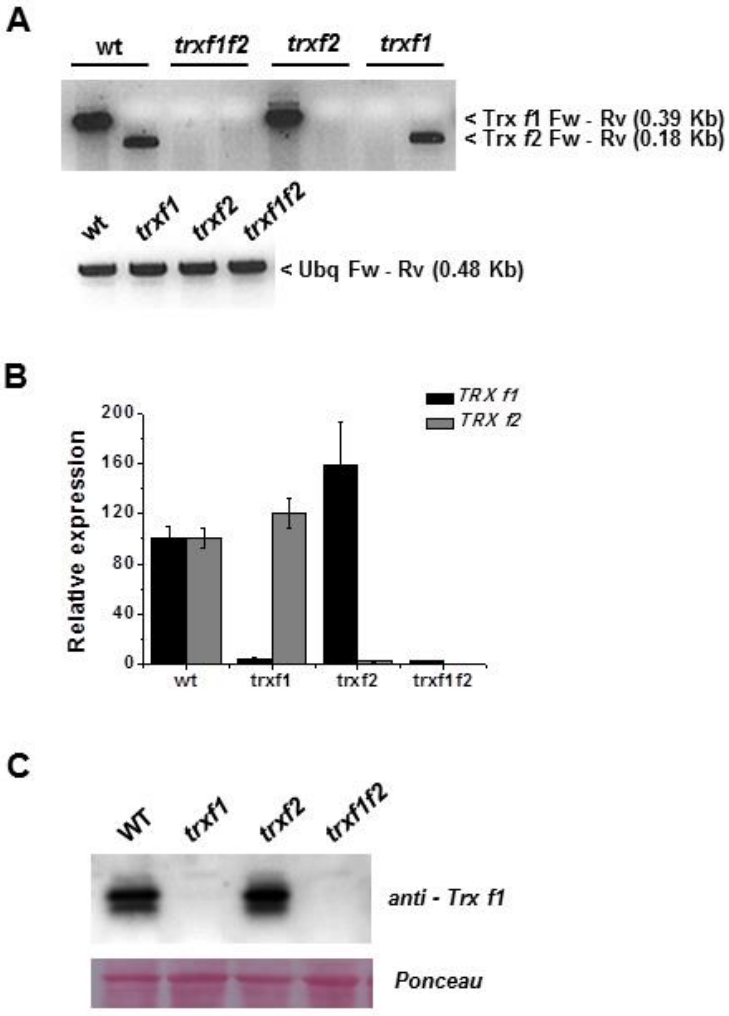

Figure 45. Characterization of *Trx f*-deficient mutants. A) The content of Trx *f*1 and *f*2 transcripts was determined by semiquantitative PCR in total RNA extracted from leaves of wt, *trxf1*, *trxf2* and *trxf1f2* plants grown under long-day conditions for 3 weeks. Amplified DNAs were fractionated in 2% agarose gels and stained with ethidium bromide. Band sizes and the pair of oligonucleotides of each reaction are indicated on the right (and also in Table 2). **B)** The content of Trx *f*1 and *f*2 transcripts was determined by qRT-PCR in total RNA extracted from wild type, *trxf1*, *trxf2* and *trxf1f2* seedlings. The pairs of oligonucleotides used for cDNA amplification are indicated in Table 3. Transcript levels were normalized to *UBIQUITIN* amplification and referred to the level of *TRX f1* and *TRX f2* in wild type plants. Determinations were performed three times and mean values ± SD are represented. **C)** The absence of Trx *f* proteins in mutant lines was analysed by Western blot. Total leaf proteins from wild type, *trxf1*, *trxf2* and *trxf1f2* short-day plants were reduced with 20 mM DTT and precipitated using 10% TCA. Samples in Tris-HCl buffer pH 7.8 containing 2% SDS, 2.5% glycerol and 4 M urea, were subjected to SDS-PAGE (15% polyacrylamide) under reducing conditions and probed with anti-Trx *f* antibody.

4.2.2. Growth of *Trx f*-deficient mutants

To determine the effect of Trxs *f* on plant growth, mutant lines were grown under short- and long-day conditions. The *trxf1f2* double mutant, like the single mutants *trxf1* and *trxf2*, showed wild type phenotype when grown under long-day photoperiod (Figure 46A), as confirmed by the weight of the rosette leaves (Figure 46B) and leaf chlorophyll content (Figure 46C) of mature plants. In contrast, short-day conditions slightly affected the growth of the double mutant (Figure 46D), as shown by the lower weight of rosette leaves (Figure 46E), though the chlorophyll content was unaffected (Figure 46F).

Therefore, despite the central function previously attributed to Trxs *f* in redox regulation of chloroplast metabolism *in vitro*, these Trxs are dispensable for plant growth under short- and long-day photoperiod. Nevertheless, the retarded growth of the *trxf1f2* double mutant under short-day photoperiod confirms the light-dependent participation of *f*-type Trxs in chloroplast photosynthetic metabolism.

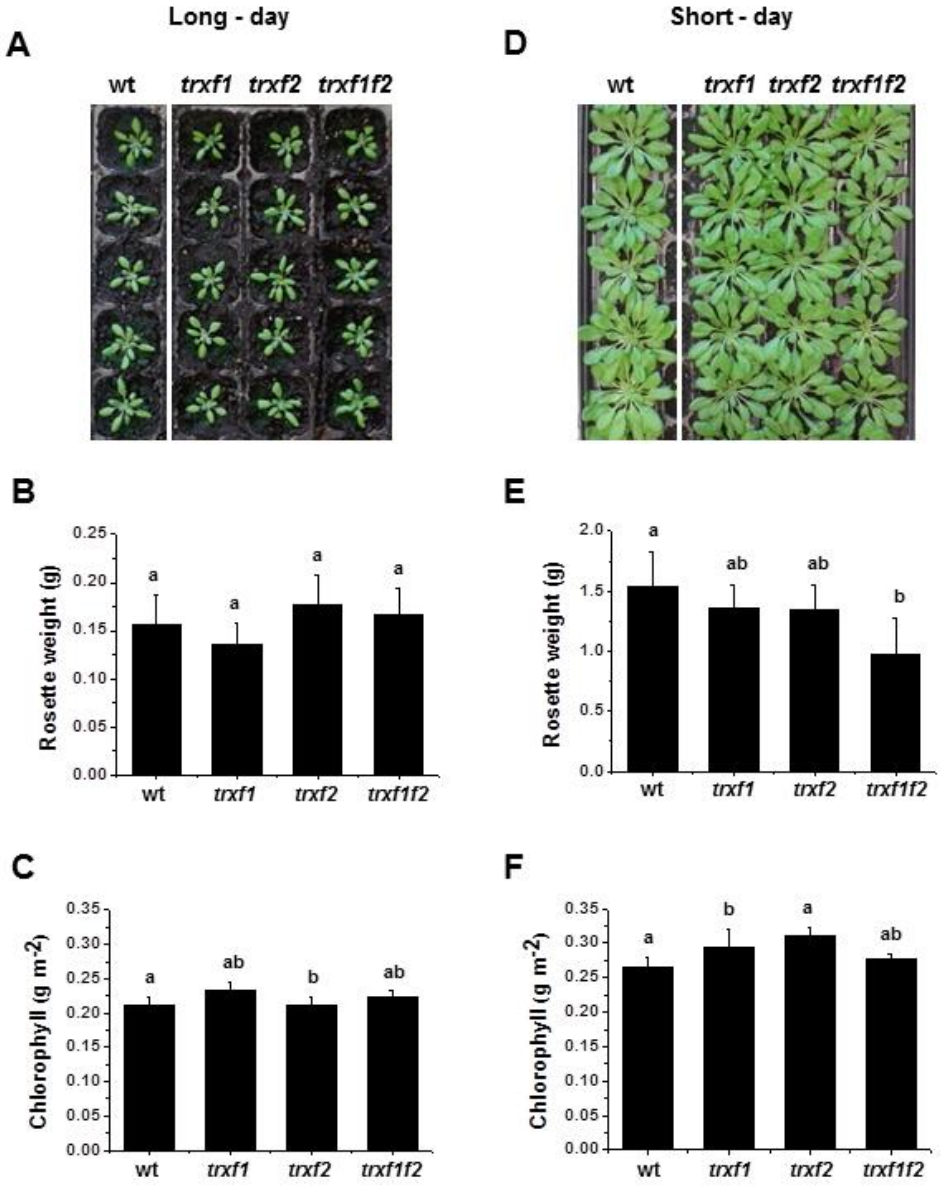

Figure 46. Characterization of *Arabidopsis* lines lacking Trxs *f*. A, D) Wild type and mutant lines were grown under long- and short-day conditions during 3 and 8 weeks, respectively. **B, E)** The weight of the rosette leaves was determined from 9 plants of long-day and 7 plants of short-day conditions, except for the *trxf1f2* double mutant, which was determined from 14 plants. **C, F)** Chlorophyll content was determined from leaf discs (n = 6) and average values ± SD are represented. Letters indicate significant differences with the Tukey-test (ANOVA) and a confidence interval of 99%.

In order to know if the lack of *f*-type Trxs was compensated for an increase in the amounts of other Trxs, which could explain the mild phenotype of the *trxf1f2* mutant, the levels of transcripts of other plastidial Trxs were analysed by qRT-PCR.

Only minor differences of the level of transcripts of genes encoding NTRC, *m*- and *x*-type Trxs were detected (Figure 47), indicating that the absence of *f*-type Trxs has not a significant effect on the expression of these Trxs.

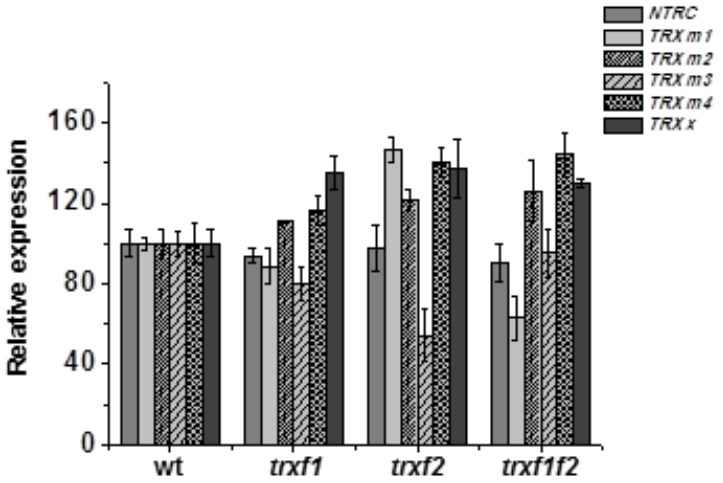

Figure 47. Level of *NTRC*, *m*- and *x*-type *TRX* gene transcripts in Trx *f*-deficient mutants. The content of transcripts of the different genes, as indicated, was determined by qRT-PCR. Total RNA was extracted from leaves of wild type, *trxf1*, *trxf2* and *trxf1f2* plants grown under long-day conditions during 3 weeks and harvested after 3 h illumination. The pairs of oligonucleotides used for cDNA amplification are indicated in Table 3, except for *m*-type Trxs that are described in (Barajas-Lopez Jde *et al.*, 2011). Transcript levels were normalized to *UBIQUITIN* amplification and expressed as percent of the corresponding level in wild type plants. Determinations were performed three times and mean values ± SD are represented.

4.2.3. Effect of Trx *f* deficiency on photosynthetic performance

To explore the function of *f*-type Trxs in photosynthetic metabolism, different photosynthetic parameters of plants lacking either or both Trx *f* enzymes were examined. Using chlorophyll fluorescence, the maximum PSII quantum yield was determined as the ratio of variable to maximal fluorescence (F_v/F_m) in dark-adapted leaves. The result revealed that the integrity of PSII was not affected in the single or double *trxf1f2* mutants (Table 7).

Table 7. Maximum PSII quantum yield in Trx *f* deficient mutants. The integrity of PSII was determined as variable fluorescence (F_v) to maximal fluorescence (F_m), F_v/F_m, in dark adapted leaves of 8-weeks old plants grown under short-day conditions. Each F_v/F_m value is the mean of 12 measurements from 6 different plants ± SD.

Genotype	**wt**	***trxf1***	***trxf2***	***trxf1f2***
F_v/F_m	0.81 ± 0.01	0.82 ± 0.01	0.81 ± 0.01	0.82 ± 0.01

Effective PSII quantum yield, Y(II), and NPQ quantum yield, Y(NPQ), were determined through induction-recovery curves, during 8 min of illumination with actinic light followed by 10 min of darkness. The light intensity applied was 75 µmol quanta m^{-2} s^{-1}, which is slightly lower than the growth light intensity. Since NPQ is a loss of chlorophyll fluorescence that reflects adaptation mechanisms regulating the fraction of absorbed light that reaches the PSII reaction centre, it is typically observed under strong illumination. However, as shown previously (Figure 20A), following the onset of actinic light at low or moderate intensity, a brief peak of NPQ is normally observed in wild type plants due to transient acidification of the thylakoid lumen before activation of photosynthesis (Kalituho *et al.*, 2007). Such an initial peak of NPQ was also found in the *trxf2* mutant and a somewhat broader peak in the *trxf1* mutant (Figures 48A and 49). In contrast, the double mutant displayed an extensive NPQ, which did not relax completely even after 8 min of illumination at 75 µmol quanta m^{-2} s^{-1} (Figures 48A and 49). As a result, the PSII effective quantum yield, Y(II), increased more slowly in the light and remained lower in the *trxf1f2* double mutant and also in the *trxf1* single mutant, although less pronounced (Figures 48A and 49).

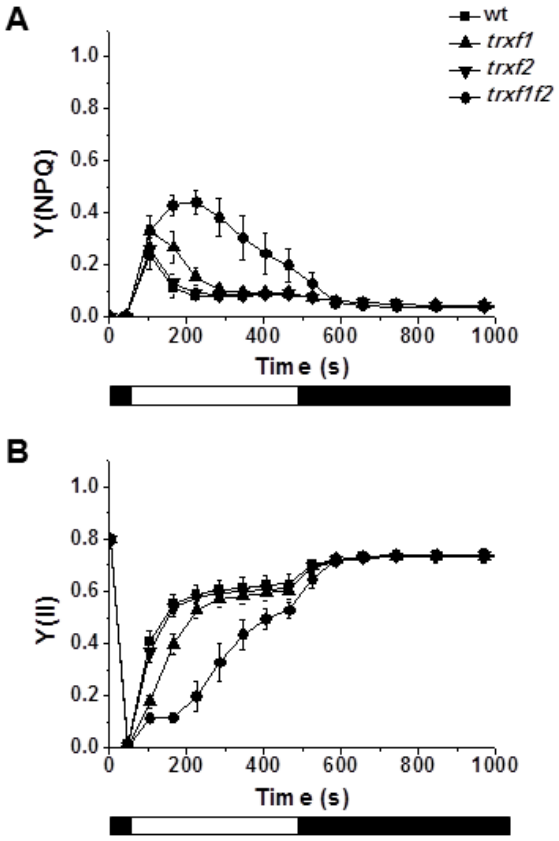

Figure 48. Non-photochemical quenching and photosystem II activity in wild type and Trx *f* deficient mutants. Chlorophyll *a* fluorescence of photosystem II was measured using a pulse-amplitude modulation fluorometer in attached leaves of plants grown for 8 weeks under short-day conditions. After incubation of plants during 30 min in darkness, an induction-recovery curve was performed to determine the quantum yields of non-photochemical quenching, Y(NPQ) (**A**), and photosystem II, Y(II) (**B**). During the 8 min induction period, 75 μmol quanta m^{-2} s^{-1} intensity actinic light was applied. Thereafter, the actinic light was switched off and measurements were continued for another 10 min in the dark. Saturation pulses were applied every 60 s. Each data point is the mean of the values from 6 plants and SDs are indicated by error bars. White and black bars below graphs indicate periods of illumination with actinic light and darkness, respectively.

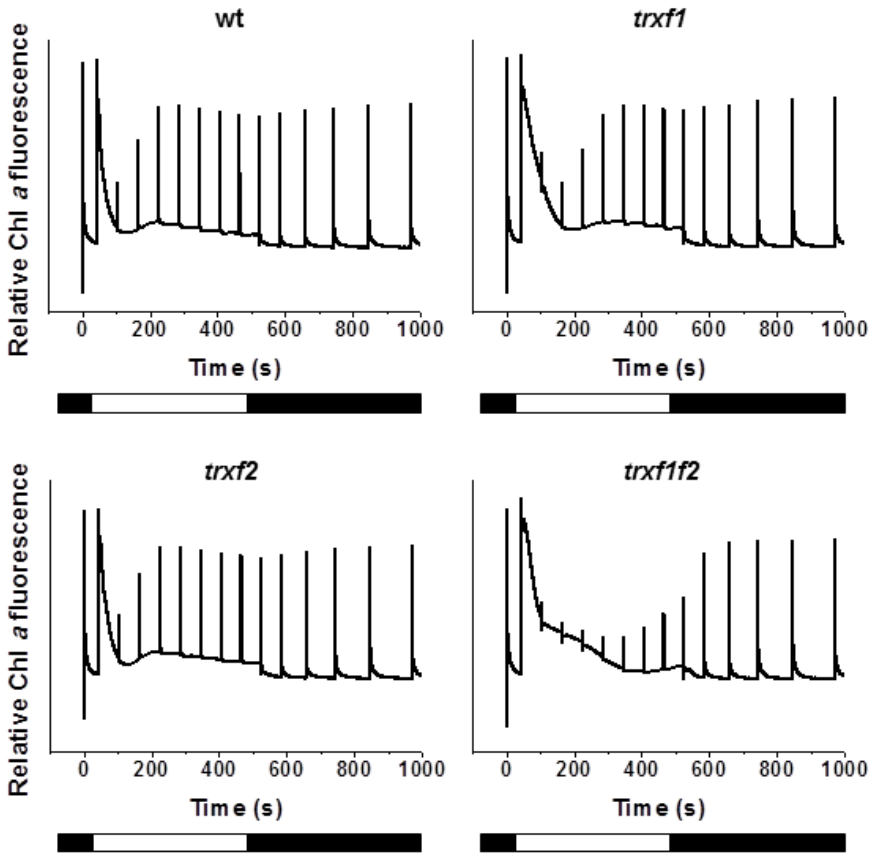

Figure 49. Chlorophyll fluorescence of PSII. Typical chlorophyll *a* fluorescence traces from the experiments represented in Figure 48. The amplitude of the saturation pulses in the light period is proportional to the PSII activity, while the decrease in the fluorescence maxima achieved with the saturation pulses during illumination (F_m') with respect to the fluorescence maxima in the dark (F_m) correspond to the NPQ. Light and dark periods are indicated by white and black bars below graphs.

In agreement with these results, the relative linear photosynthetic electron transport rates of photosystem II (ETR(II)) were considerably lower in the double mutant at all light intensities examined (Figure 50A). In contrast, only a small but significant reduction in photosynthetic electron transport rates was observed in the *trxf1* mutant, whereas the *trxf2* mutant displayed wild type rates (Figure 50A). Notably, the yields of NPQ were higher in *trxf1f2* plants, particularly at low light intensities (Figure 50B).

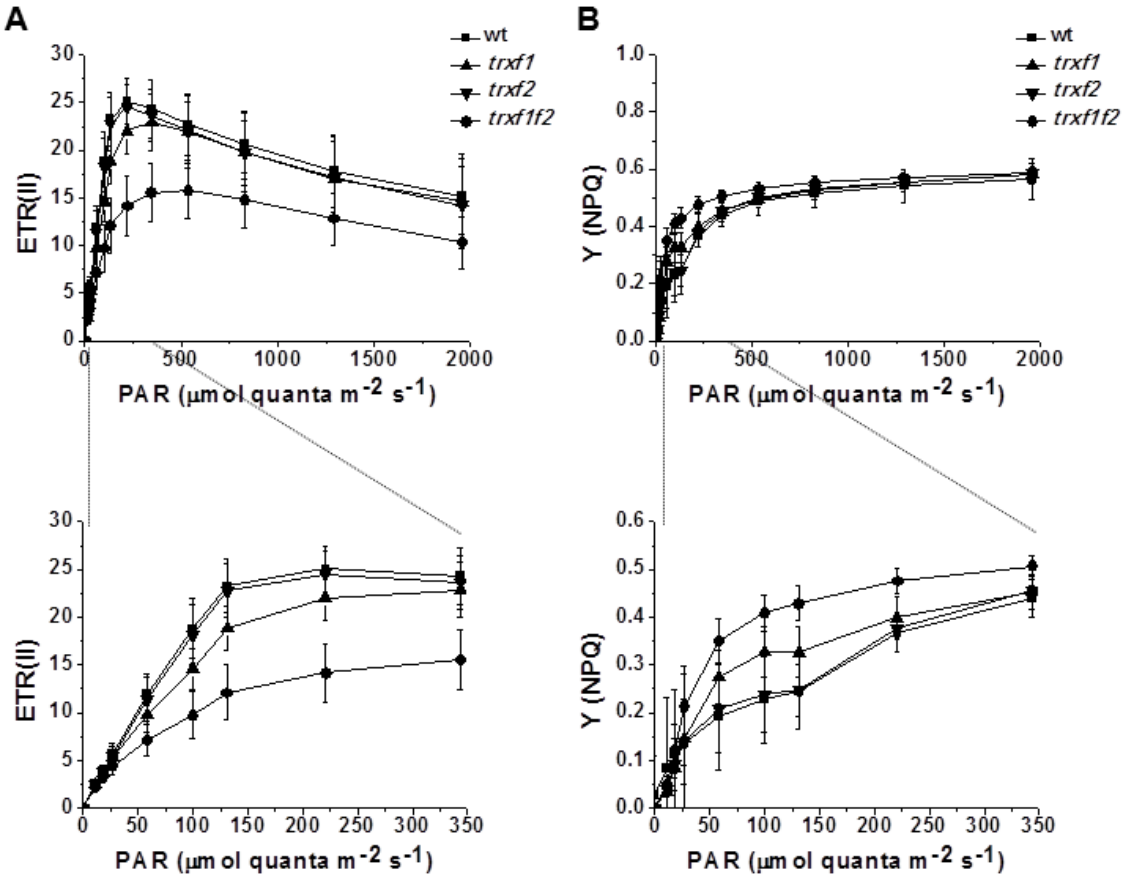

Figure 50. Light-dependent linear photosynthetic electron transport and NPQ in wild type and Trx *f* deficient mutants. A) Relative linear electron transport rates of photosystem II, ETR(II), was measured in pre-illuminated attached leaves of 8-weeks old plants grown at 125 µmol quanta m^{-2} s^{-1} under short-day conditions. Chlorophyll fluorescence of photosystem II was determined using a pulse-amplitude modulation fluorometer. **B)** Quantum yields of NPQ, Y(NPQ), from the corresponding light-titration curves in (A). Each data point is the mean of measures from 8 plants ± SD. PAR (photosynthetically active radiation).

The effect of Trxs *f* on the control of energy quenching and photosynthetic yield might be through direct interaction with the photosynthetic apparatus or an indirect consequence of limited biosynthesis and demand for ATP, leading to lower luminal pH. The latter should be revealed by a lower rate of consumption of electrons from the photosynthetic electron transport. To test this possibility, we measured the PSI quantum yield, Y(I), based on P700 absorbance changes during an induction-recovery curve, in mutant and wild type plants (Figures 51 and 52). Indeed, the double mutant had lower PSI activity due to prolonged limitations on the acceptor side, Y(NA), after turning on the light (Figure 51). This suggests that the NPQ observed during illumination is a

consequence of luminal acidification because of limited demand for ATP, since biosynthetic processes are not completely activated.

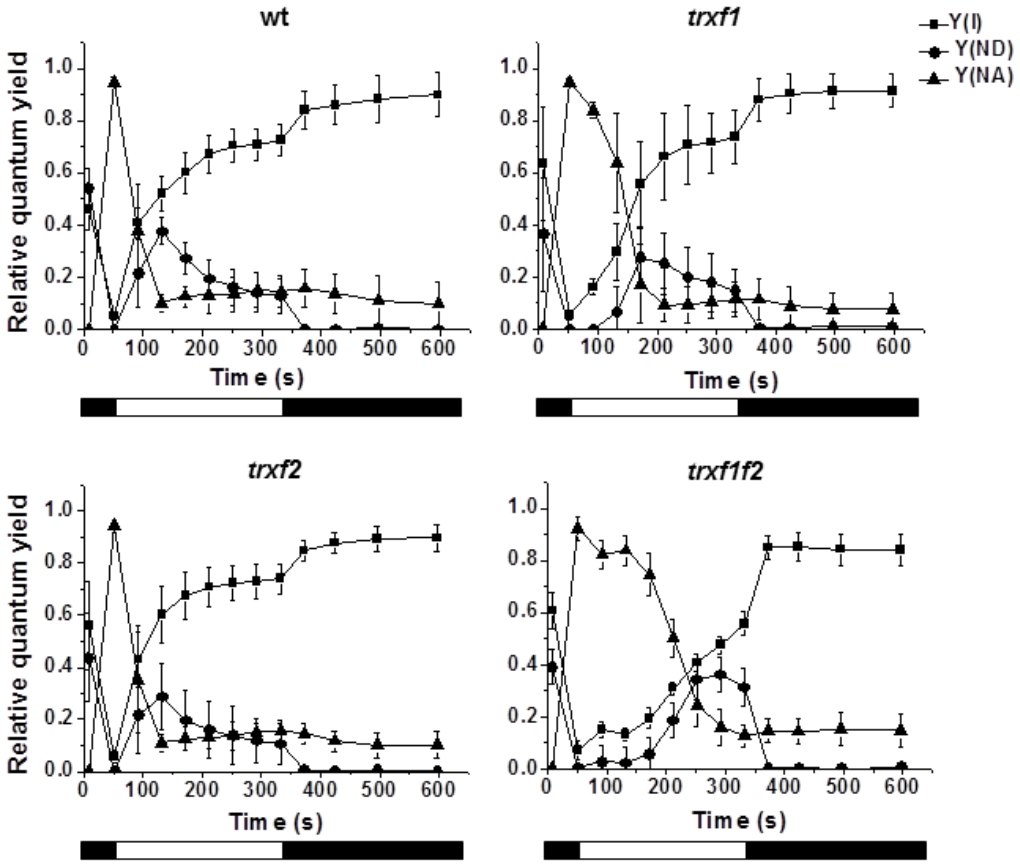

Figure 51. Comparative analysis of photosystem I activity in wild type and Trx *f* deficient mutants. The redox state of P700 was inferred from changes in the absorbance at 830 nm versus 875 nm and monitored during 10 min. Dark adapted leaves from 8-weeks old plants under short-day photoperiod, were illuminated with a saturation pulse after 10 s of far red light to determine the maximum oxidation of P700. Subsequently, actinic light (126 µmol quanta m^{-2} s^{-1}) was kept on during 5 min followed by another 5 min of darkness. White light saturation pulses were applied every 20 s. The quantum yields of PSI, Y(I), donor side limitations, Y(ND), and acceptor side limitations, Y(NA), are based on saturating pulse analysis. Data were collected from 6 plants and mean ± SD are represented. Light and dark periods are indicated by white and black bars below graphs.

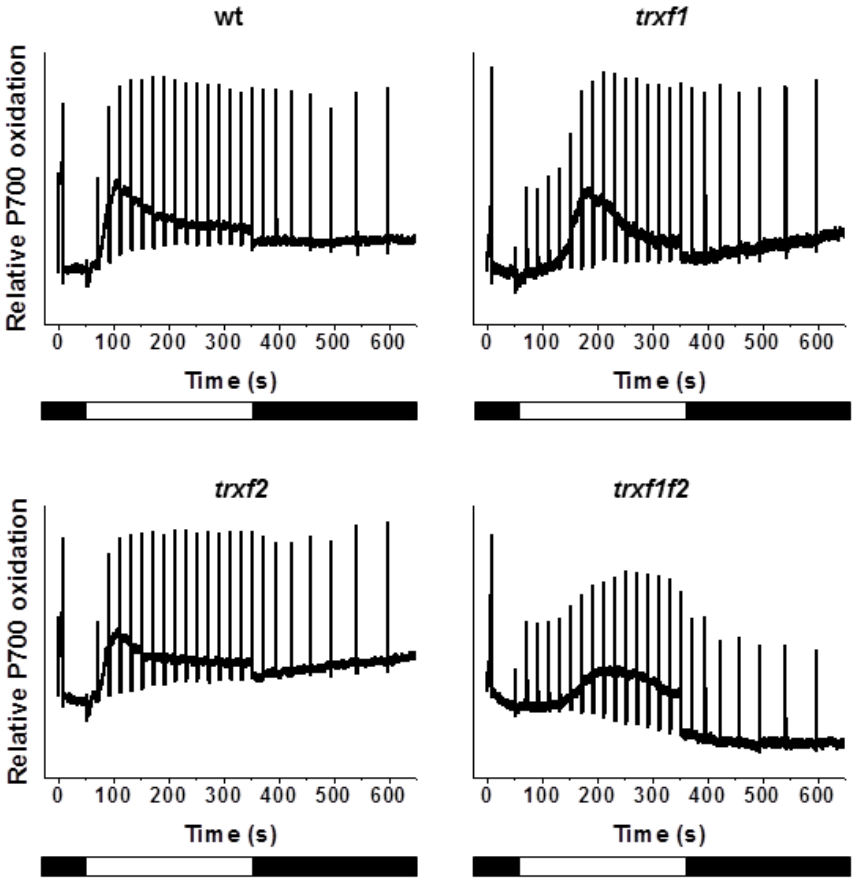

Figure 52. Absorbance of the oxidised form of photosystem I. Typical P700 absorbance traces at 830 nm from the experiments represented in Figure 51. The amplitude of the saturation pulses in the light period is proportional to the PSI activity, while the decreased of the maximal absorbance reached during illumination correspond to a deficit in electron acceptors of PSI, which consequently limits the ability of P700 oxidation. In contrast, the increase of the minimal absorbance is caused by a deficit in electron donors to PSI and therefore, a decrease in P700 reduction. Light and dark periods are indicated by white and black bars below graphs.

The results inferred from chlorophyll *a* fluorescence and P700 absorbance measurements indicate retardation of the activation of the biosynthetic processes, which consume reducing equivalents derived from the photosynthetic electron transport. Therefore, we proceeded to study the response of the rate of CO_2 fixation (A_N) to illumination in plants lacking Trxs *f*.

Despite the similar rates of carbon assimilation (A_N) in wild type and mutant plants (Figure 53), the halftime for reaching the maximal CO_2 fixation rate after turning on the light was more than twice as long in the double mutant as compared to wild type

plants (Table 8). The response of the rate of CO_2 fixation (A_N) to illumination was more retarded in the *trxf1* than in the *trxf2* single mutant while the *trxf1f2* double mutant displayed even slower kinetics (Table 8 and Figure 53). These results suggest the function of *f*-type Trxs in the rapid response of the chloroplast assimilatory metabolism to light.

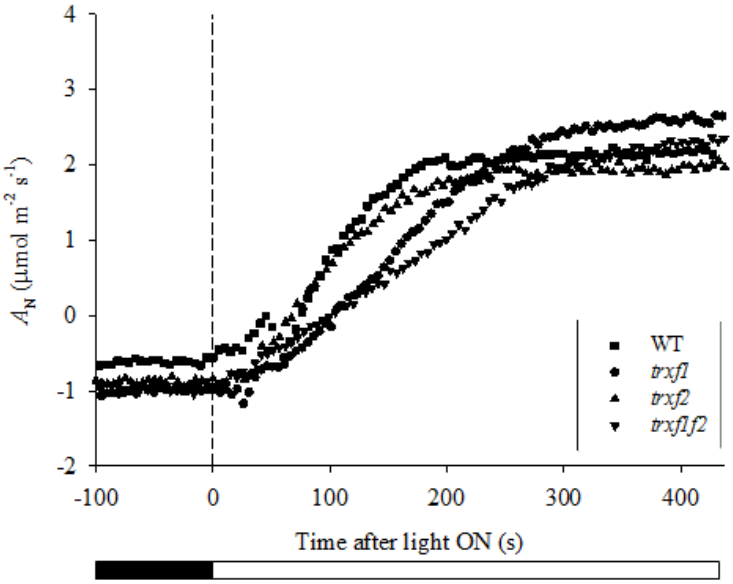

Figure 53. Net CO_2 assimilation rate (A_N) upon a dark-light transition in wild type and Trx *f* deficient plants. The rate of net CO_2 assimilation was determined using an infrared gas analyser in short-day grown plants (7-weeks old) previously adapted to darkness. The vertical dashed line represents when actinic light of 75 µmol quanta m^{-2} s^{-1} was turned on. The kinetic of one leave of each line is represented (statistics are in Table 8).

Table 8. Kinetics of response of net CO_2 assimilation rate to light. $t_{1/2}$ represents the time to achieve 50% of the final rate of CO_2 (Figure 53). Data are the means ± SE of 6 measures from 7-weeks old plants grown under short-day conditions. The significant differences between mutant and the wild type plants are indicated by different letters (ANOVA Tukey-test, P<0.01).

Genotype	**wt**	***trxf1***	***trxf2***	***trxf1f2***
$t_{1/2}$ (s)	106.0 ± 2.3 **a**	187.9 ± 7.5 **b**	134.3 ± 9.5 **a**	237.2 ± 10.1 **c**

4.2.4. Redox state of Calvin-Benson cycle enzymes

The results obtained from measurements of photosynthetic electron transport and CO_2 fixation indicate that activation of the Calvin-Benson cycle is delayed in Trx *f*-deficient plants following a dark-light transition.

Therefore, we proceeded to analyse the redox state of enzymes of the Calvin-Benson cycle. There is extensive evidence *in vitro* supporting the relevant function of *f*-type Trxs in light-dependent reductive activation of different chloroplast enzymes including those of the Calvin-Benson cycle (recently reviewed by (Michelet et al., 2013)). To analyse further the function of *f*-type Trxs *in vivo*, we examined the redox status of two well-known *in vitro* targets of Trxs *f*, FBPase and Rubisco activase, in the mutant lines. To this end, samples were taken at the end of the night period from plants that had been grown at a light intensity of 120 μmol quanta m^{-2} s^{-1} and then subjected to illumination with the same or higher (500 μmol quanta m^{-2} s^{-1}) light intensity. Short-term changes of the redox status of these enzymes was analysed by Western blot with the aid of the thiol-alkylating agent $MM(PEG)_{24}$, which adds 1.24 kDa per thiolic group, thus producing a shift of the electrophoretic mobility of the labelled proteins that reflects their redox status.

In dark-adapted plants FBPase was detected as a single band indicating that, as expected, the enzyme is present in the oxidised form under these conditions (Figure 54). In wild type plants, FBPase becomes rapidly reduced in response to light within the first minute after illumination (Figure 54). The level of reduction of FBPase proved to be dependent on light intensity, since the enzyme becomes fully reduced after 10 min at 500 μmol quanta m^{-2} s^{-1}, whereas the growth light intensity of 120 μmol quanta m^{-2} s^{-1} only promoted a partial reduction, approximately 50%, of the enzyme (Figure 54). While the lack of Trx *f*2 exerted almost no effect on FBPase reduction in response to light, the lack of Trx *f*1 significantly impaired the level of reduction of the enzyme at both light intensities (Figure 54). The *trxf1f2* double mutant showed not only a pronounced delay of FBPase reduction in response to light, but also a lower level of reduction of the enzyme after 10 min of illumination even at the higher light intensity (Figure 54). A similar pattern of reduction in response to light was observed for another prominent redox-regulated enzyme of the Calvin-Benson cycle, the Rubisco activase (Figure 55).

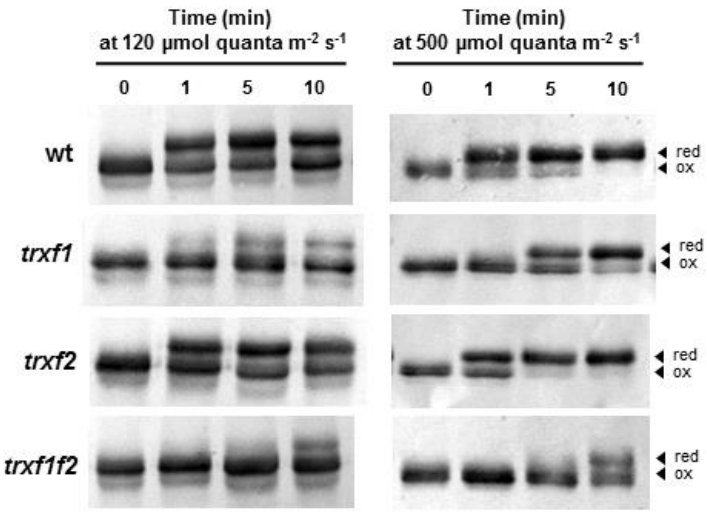

Figure 54. *In vivo* redox state of FBPase in response to light in wild type and Trx *f* mutant lines. The redox state of FBPase from the different lines under analysis, as indicated on the left, was determined in leaf extracts from 7-weeks old plants grown under short-day conditions and harvested at the end of the dark period (time 0), and after 1, 5 and 10 min of illumination at the indicated light intensities. Total leaf proteins were extracted in the presence of 10% TCA and protein thiols were alkylated with 10 mM $MM(PEG)_{24}$. Proteins were resolved in SDS-PAGE (9.5% polyacrylamide) under non-reducing conditions and probed with an anti-FBPase antibody. red, reduced; ox, oxidised.

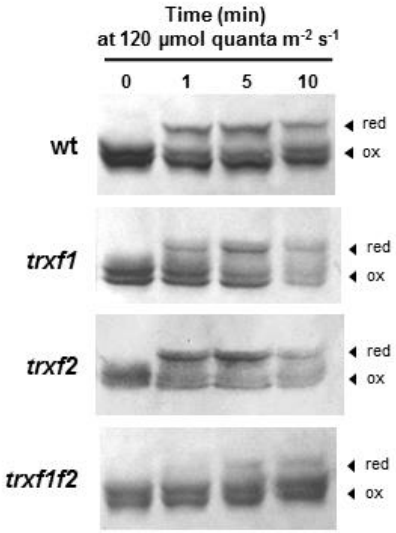

Figure 55. *In vivo* redox state of Rubisco activase in response to light in wild type and Trx *f* mutant lines. The redox state of Rubisco activase from the different lines under analysis, as indicated on the left, was determined in leaf extracts from 7-weeks old plants grown under short-day conditions and harvested at the end of the dark period (time 0), and after 1, 5 and 10 min of illumination. Total leaf proteins were extracted in the presence of 10% TCA and protein thiols were alkylated with 10 mM $MM(PEG)_{24}$. Samples were fractionated in SDS-PAGE (9.5% polyacrylamide) under non-reducing conditions and probed with an anti-Rubisco activase antibody. red, reduced; ox, oxidised.

Quantification of the reduction of FBPase and Rubisco activase from three experiments, such as those presented in (Figures 54 and 55), revealed that reduction of these enzymes is slower in the *trxf1f2* double mutant and even in the *trxf1* single mutant. Moreover, the levels of reduction of both enzymes remained half of the wild type level in the *trxf1f2* double mutant after 10 min illumination at growth light intensity (Figure 56A and B).

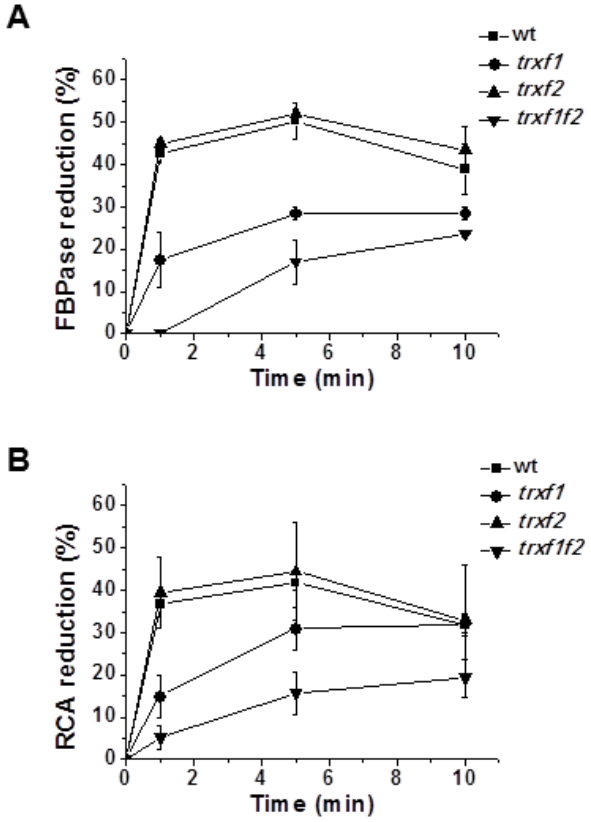

Figure 56. Light-dependent reduction FBPase and Rubisco activase. The redox state of FBPase and Rubisco activase (RCA) was determined by alkylation experiments followed by Western blot analyses. Band intensities were quantified and the percentage of reduced proteins was calculated as the ratio between the shifted band (reduced form) and the sum of reduced and oxidised forms. Each value is the mean of three independent experiments, such as Figures 54 and 55, ± SE.

Furthermore, we analysed the change of the redox status of FBPase following a light-dark transition. Re-oxidation of the FBPase in the dark was faster in all three Trx *f* deficient mutants than in wild type plants (Figure 57). After 5 min in darkness the

FBPase was nearly completely oxidised in the wild type and also in the *trxf* mutants (Figure 57).

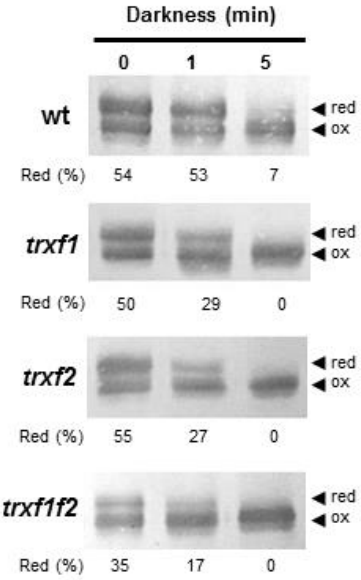

Figure 57. Re-oxidation of FBPase in response to darkness. The redox state of FBPase from the different lines under analysis, as indicated on the left, was determined in leaf extracts from plants grown for 7 weeks under short-day conditions and harvested at the end of the light period (time 0), and after 1 and 5 min of darkness. Total leaf proteins were extracted in the presence of 10% TCA and protein thiols were alkylated with 10 mM $MM(PEG)_{24}$. Proteins were resolved in SDS-PAGE (9.5% polyacrylamide) under non-reducing conditions and probed with an anti-FBPase antibody. red, reduced; ox, oxidised. Band intensities were quantified and the percentage of reduced FBPase is indicated.

4.2.5. Starch content

Given the lower photosynthetic electron transport rates and the incomplete reductive activation of the Calvin-Benson cycle observed in *trxf1* and *trxf1f2* mutants, we proceeded to determine the starch content of plants devoid of *f*-type Trxs. In addition, single *trxf1* mutants have previously been reported to contain 22% less starch than wild type plants (Thormahlen *et al.*, 2013). Thus, starch quantifications in leaves from long-day grown plants showed that the content of starch in leaves of the *trxf1f2* double mutant was significantly lower than those in the wild type and *trxf2* single mutant, being the levels in *trxf1* mutant slightly higher (Figure 58).

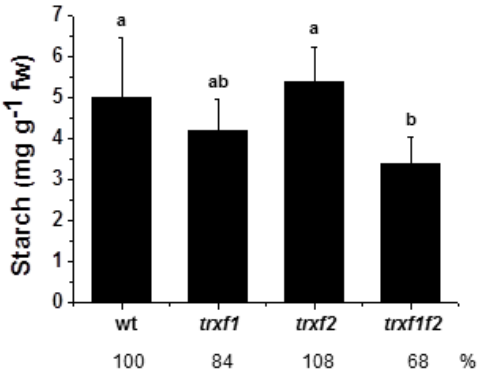

Figure 58. Starch content in leaves of wild type and Trx *f* mutant lines. Starch content was determined at the end of the day in leaves from plants grown under long-day conditions during 3 weeks. Data are the mean ± SD of at least 5 replicates from two different experiments (with a total of 3 starch extractions). Letters indicate significant differences with the Tukey-test (ANOVA) and a confidence interval of 99%.

4.2.6. Interactions between the redox systems of NTRC and *f*-type thioredoxins

An intriguing result of the characterization of the *trxf1f2* double mutant was the finding of a significant reduction of FBPase and Rubisco activase despite the absence of *f*-type Trxs. This result was unexpected based on previously reported extensive biochemical analysis, which suggested a central role of these Trxs in redox regulation of the Calvin-Benson cycle enzymes and suggested that additional chloroplast redox systems might be involved in light-dependent regulation of these enzymes. To address this issue, we have analysed in this work the function of NTRC.

Surprisingly, experiments using alkylation with $MM(PEG)_{24}$ revealed that typical Trx *f* targets, such as FBPase and Rubisco activase, were more oxidised in the *ntrc* mutant (Figure 59). This raises several possibilities regarding the nature of the chloroplast regulatory system. One possibility is that NTRC exerts a direct effect on the reduction of these enzymes *in vivo*, i.e., FBPase and Rubisco activase might be substrates for NTRC. Alternatively, the lower rates of photosynthetic electron transport in the *ntrc* mutant could lead to lower degree of reduction of the Trxs *f*, leading to less efficient reduction of their targets. There is still another possibility, which is that NTRC and Trxs *f* have redox interaction. To test this possibility, we have studied the possible transfer of electrons between NTRC and Trx *f*1 *in vitro.*

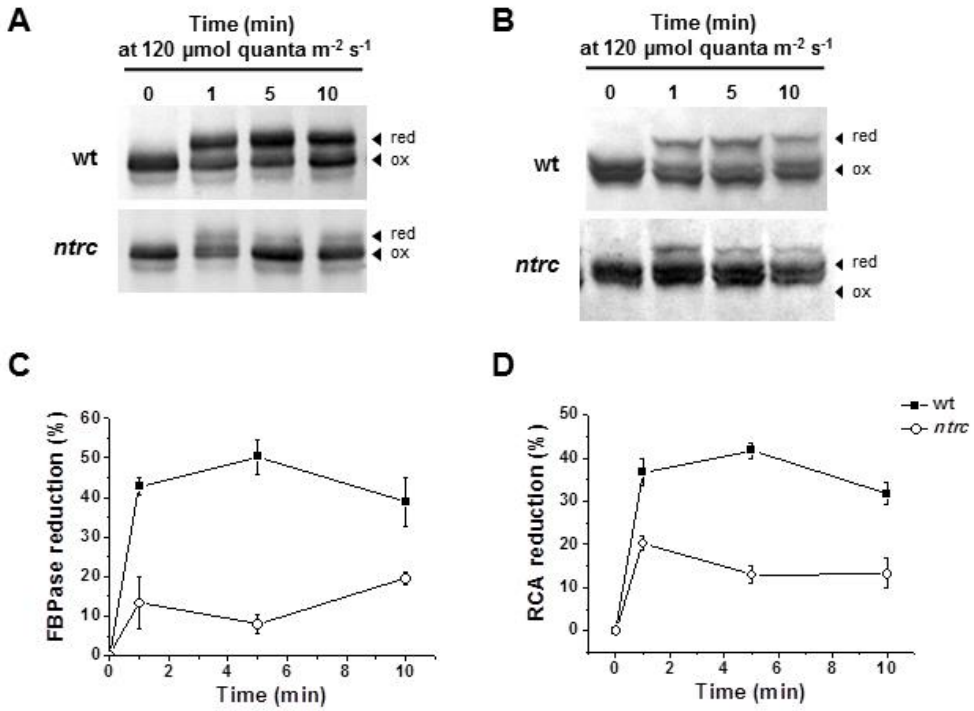

Figure 59. *In vivo* redox state of FBPase and Rubisco activase in wild type and *ntrc* mutant plants. The redox state of FBPase and Rubisco activase (RCA) was determined in leaf extracts from 7-weeks old plants grown under short-day conditions at 120 µmol quanta m^{-2} s^{-1} and harvested at the end of the dark period (time 0), and after 1, 5 and 10 min of illumination at growth light intensity. Total leaf proteins were extracted in the presence of 10% TCA and protein thiols were alkylated with 10 mM $MM(PEG)_{24}$. **A, B)** Proteins were resolved in SDS-PAGE (9.5% polyacrylamide) under non-reducing conditions and probed with anti-FBPase (A) and anti-RCA (B) antibodies. red, reduced; ox, oxidised. **C, D)** Band intensities were quantified and the percentage of reduced proteins was calculated as the ratio between the shifted band (reduced form) and the sum of reduced and oxidised forms. Each value is the mean of three independent experiments, such as (A) and (B), ± SE.

Purified untreated Trx *f*1 was detected as three major bands after alkylation with $MM(PEG)_{24}$ in SDS-PAGE (Figure 60). Treatment with increasing concentrations of DTT led to the appearance of a slower migrating band, while the fast migrating band disappeared, revealing the mobility of the reduced form of Trx *f*1 (Figure 60). In contrast, treatment with the oxidising agent $CuCl_2$ caused the disappearance of the upper band and an increase in the fast migrating band, revealing the electrophoretic mobility of the fully oxidised form of Trx *f*1 (Figure 60). Treatment with NADPH did not show any significant effect (Figure 60).

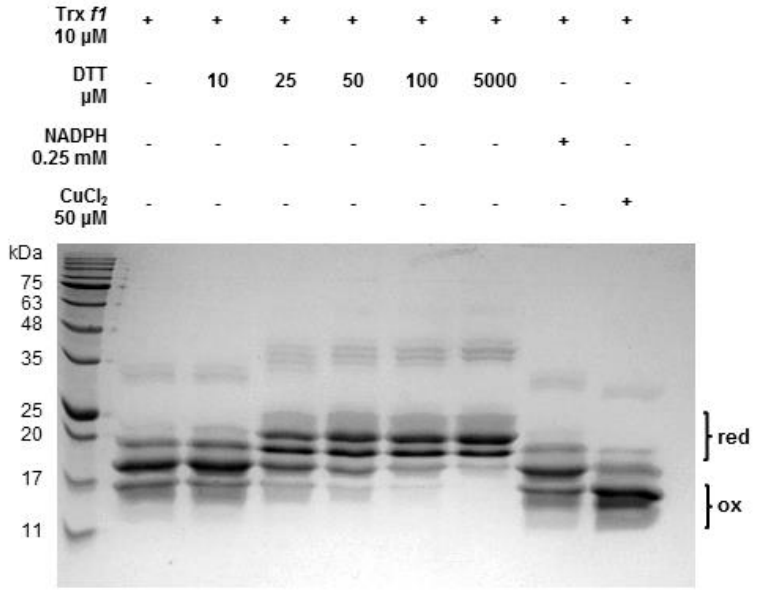

Figure 60. Reduction of Trx *f*1 recombinant protein. Purified Trx *f*1 protein in their mature form (without transit peptide) was incubated as indicated above each lane during 20 min at room temperature in a 10 mM phosphate buffer pH 7.4. After reactions, proteins were precipitated with 10% TCA, alkylated with 10 mM $MM(PEG)_{24}$ and electrophoresed under reducing conditions in a 15% polyacrylamide gel (5 µg of Trx *f*1 were loaded). Gels were stained with Coomassie Brilliant Blue. DTT and NADPH were used as reductants and $CuCl_2$ as oxidant agent. red, reduced; ox, oxidised.

Once established the electrophoretic mobility of reduced and oxidised Trx *f*1, we tested the effect of NTRC on the redox state of Trx *f*1 *in vitro*. In the presence of a low concentration of DTT (25 µM), which reduced Trx *f*1 (Figure 61), incubation with NTRC led to a decrease in the intensity of the upper band while the fast migrating band increased, thus, indicating oxidation of Trx *f*1 (Figure 61). Incubation in the presence of NTRC and NADPH, but not NTRC alone, led to reduction of Trx *f*1 in the absence of DTT (Figure 61). Taken together, these results suggest that NTRC and Trx *f*1 are able to exchange electrons at least *in vitro*.

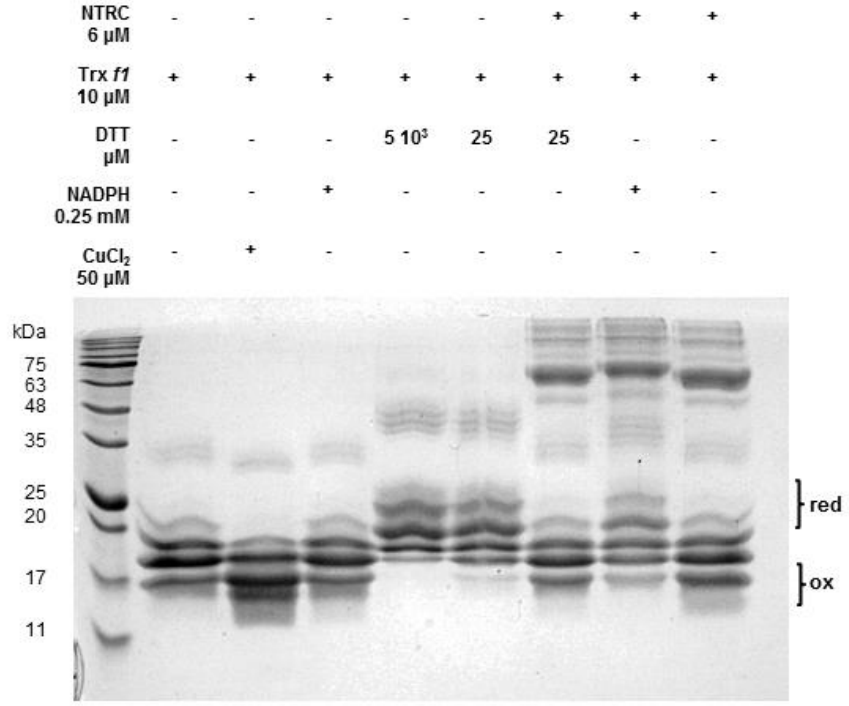

Figure 61. Redox exchange between Trx *f*1 and NTRC recombinant proteins. Purified proteins in their mature forms (without transit peptides) were incubated as indicated above each lane during 20 min at room temperature in a 10 mM phosphate buffer pH 7.4. After reactions, proteins were precipitated with 10% TCA, alkylated with 10 mM $MM(PEG)_{24}$ and electrophoresed under reducing conditions in a 15% polyacrylamide gel (5 µg of Trx *f*1 were loaded). Gels were stained with Coomassie Brilliant Blue. DTT and NADPH were used as reductants and $CuCl_2$ as oxidant agent. red, reduced; ox, oxidised.

After establishing the redox interaction between NTRC and Trx *f*1, we tested the involvement of the two domains of NTRC in this interaction. Neither the NTR nor the Trx domains of NTRC were efficient in Trx *f*1 oxidation (Figure 62A). Thereafter, two mutant variants of NTRC, C140S and C380S, with Cys at the active site of the NTR and Trx domains of the enzyme, respectively, replaced by Ser, were tested for their efficiency in exchanging electrons with Trx *f*1. Figure 62B shows that both mutants were unable to affect the redox state of Trx *f*1, thus indicating that a fully functional NTRC is required for redox interaction with Trx *f*1.

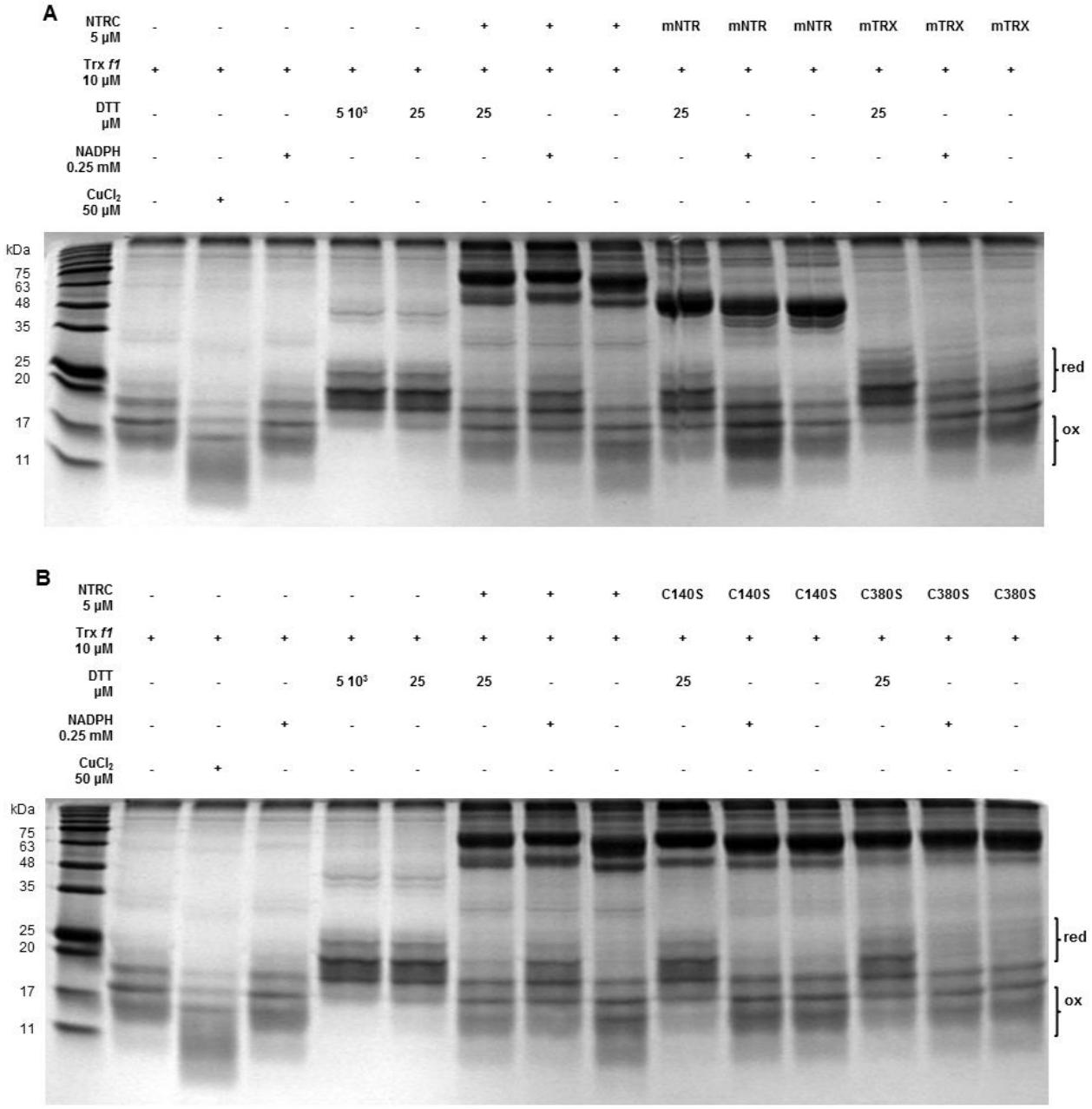

Figure 62. Reduction of Trx *f*1 recombinant protein by each domain of NTRC, NTR and Trx. Purified proteins in their mature forms (without transit peptides) were incubated as indicated above each lane during 20 min at room temperature in a 10 mM phosphate buffer pH 7.4. After reactions, proteins were precipitated with 10% TCA, alkylated with 10 mM $MM(PEG)_{24}$ and electrophoresed under reducing conditions. **A)** Five µg of Trx *f*1 in a 15% polyacrylamide gel. **B)** Ten µg of NTRC in a 9% polyacrylamide gel. Gels were stained with Coomassie Brilliant Blue. DTT and NADPH were used as reductants and $CuCl_2$ as oxidant agent. red, reduced; ox, oxidised.

4.3. The ability of NTRC to reduce $NADP^+$

The finding described in the previous section showing that NTRC is able to oxidise reduced Trx *f*1 suggests that NTRC is able to act as oxidant. This result raises the question of the fate of the electrons in this redox interchange. In this work we have performed preliminary experiments to address this issue. In the presence of a reductant such as DTT, at a concentration of 1 mM, NTRC efficiently catalysed the reduction of $NADP^+$ in a concentration-dependent manner (Figure 63A). Moreover, NTRC was able to catalyse the reduction of $NADP^+$ in the presence of Trx *f*1 reduced by a low concentration of DTT (0.1 mM) (Figure 63B). DTT alone at this lower concentration was not sufficient to support production of NADPH catalysed by NTRC. These results confirm the redox interaction of NTRC and Trx *f*1 and uncover the ability of NTRC to catalyse the reverse reaction.

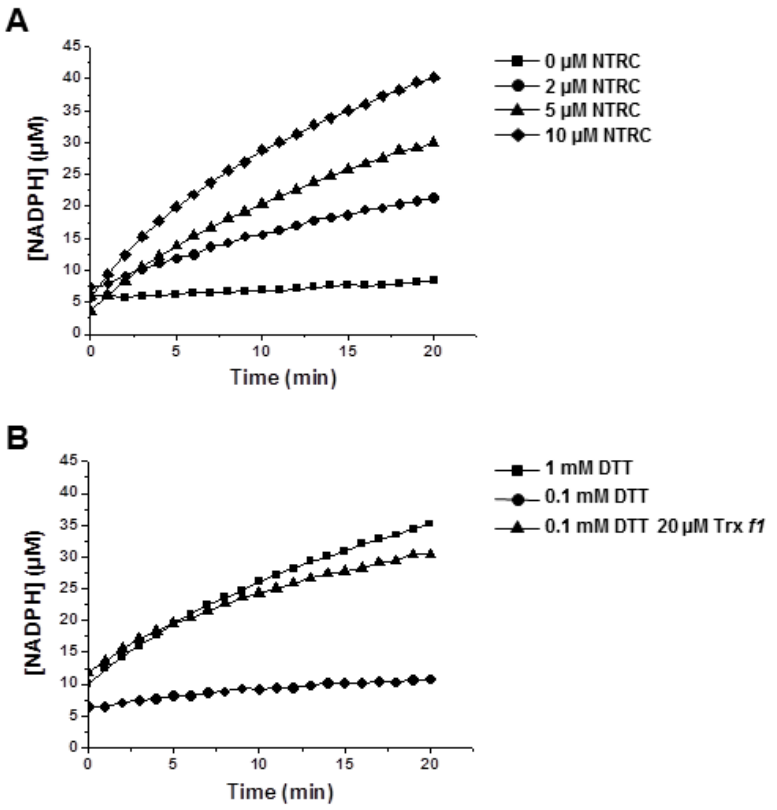

Figure 63. Production of NADPH catalysed by NTRC. The reduction of $NADP^+$ to NADPH was monitored through the absorbance increase at 340 nm during 20 min. **A)** Different concentrations of NTRC in the presence of 1 mM DTT and 1 mM $NADP^+$. **B)** Five μM NTRC with DTT and Trx *f*1, and 1 mM $NADP^+$.

DISCUSSION

5. DISCUSSION

Photosynthesis is the process in which light energy is converted into chemical energy, ATP, and reducing power in the forms of reduced Fd and NADPH, which are used for chloroplast biosynthetic processes. Photosynthesis is essential for plants and, thus, it is carefully controlled in response to changes in light intensity. At lower light intensities, plants need an efficient absorption of energy, which is necessary for proper plant growth and development. However, the absorption of excess light leads to the production of ROS, which may be harmful (Li *et al.*, 2009; Ruban *et al.*, 2012).

To prevent damage to the photosynthetic apparatus or photoinhibition caused by ROS (Krieger-Liszkay *et al.*, 2008; Tyystjarvi, 2013), plants have evolved different mechanisms to cope with high light intensities (Li et al., 2009; Spetea et al., 2014; Dietz, 2015). These mechanisms operate at different time scales. Thus, at the molecular level, long-term acclimation mechanisms comprise mainly changes in the expression of genes encoding antenna proteins and enzymes with antioxidant functions. In contrast, short-term acclimation mechanisms are mostly based on post-translational protein modifications and may involve dissipation of the excess energy absorbed as heat through the process known as NPQ (Li et al., 2009; Dietz, 2015). In plants, the major component of NPQ is the energy-dependent quenching, qE, which allows a rapid and reversible response to light stress (Muller et al., 2001; Szabo et al., 2005; Baker, 2008).

The ability to induce and revert acclimation mechanisms, such as qE, allows plants to survive and grow under the continuous light fluctuations that they face in nature. Trxs have been proposed to be redox sensors mediating plant responses to light stress, since their redox state is intimately linked to the photosynthetic electron transport and can exhibit significant changes depending on light intensity (Li et al., 2009; Nikkanen and Rintamaki, 2014). Beside the Fd-dependent Trxs, the chloroplast contains an NTR with a joint Trx domain at the C-terminus, which is termed NTRC. NTRC shows a high affinity for NADPH and, thus, allows the use of this nucleotide for chloroplast redox regulation (Spinola et al., 2008; Cejudo et al., 2012). Redox regulation based on disulphide-dithiol interchange would be a suitable regulatory mechanism in this context, since it allows the rapid and reversible adaptation of proteins function to environmental stimuli. Based on these premises, the hypothesis that redox regulation might be important in chloroplast acclimation to light was postulated. In this

work, we have addressed this issue by analysing the effect of two important chloroplast redox systems, NTRC and *f*-type Trxs, in chloroplast performance in response to different light conditions.

5.1. The role of NTRC in plant acclimation to changes in light intensity

The *Arabidopsis thaliana ntrc* knockout mutant displays pale leaves and retarded growth as compared to the wild type (Serrato *et al.*, 2004) and this phenotype is particularly pronounced under short-day conditions (Perez-Ruiz et al., 2006; Lepisto et al., 2009). Moreover, *Arabidopsis* plants lacking NTRC have been reported to be hypersensitive to several kinds of abiotic stresses, such as high salinity and drought (Serrato *et al.*, 2004), prolonged darkness (Perez-Ruiz *et al.*, 2006) and heat (Chae *et al.*, 2013). Under these conditions the already low growth rate of the *ntrc* mutant is further reduced in comparison to wild type plants (Serrato et al., 2004; Perez-Ruiz et al., 2006). In this context and given the possible redox control of light acclimation mechanisms (Li *et al.*, 2009), we have investigated the putative role of NTRC in photoprotection.

Previous results showing the implication of NTRC in abiotic stress tolerance and peroxide detoxification suggested that NTRC might also participate in adaptation to high light stress. Surprisingly, we found that plants lacking NTRC are not hypersensitive to high light stress. In contrast, the *ntrc* mutant tolerates light intensities up to 1000 μmol quanta m^{-2} s^{-1}, maintaining the proportion of their rosette size and chlorophyll content to those of wild type plants (Figure 15). This is in agreement with a recent report showing that growth of the *ntrc* mutant at 600 μmol quanta m^{-2} s^{-1} was not further compromised (Toivola *et al.*, 2013), and confirms that NTRC is not involved in molecular mechanisms controlling long-term acclimation to high light intensities.

NTRC is the most relevant reductant of chloroplast 2-Cys Prxs (Moon et al., 2006; Perez-Ruiz et al., 2006; Alkhalfioui et al., 2007; Puerto-Galan et al., 2013). A double knockout mutant devoid of 2-Cys Prxs A and B was recently reported to be hypersensitive to photoinhibition upon a transfer from low to high irradiances (Awad *et al.*, 2015), suggesting that plants devoid of NTRC might suffer increased photoinhibition. However, *ntrc* plants grown to adult stage at 120 μmol quanta m^{-2} s^{-1}

and transferred to 800 μmol quanta m^{-2} s^{-1} light intensity did not show exacerbated photoinhibition (Figure 16). This indicates that NTRC is not required for short-term acclimation to high light and suggests that the 2-Cys Prx benefits from electron donors other than NTRC at high light intensities. In support of this notion, we found also that NTRC is not required for peroxide detoxification in high light. The hydrogen peroxide content in *ntrc* leaves after 1 h at 500 μmol quanta m^{-2} s^{-1} was indistinguishable from that in wild type leaves (Figure 18), while hydrogen peroxide accumulated in plants devoid of 2-Cys Prxs under high light conditions (Awad *et al.*, 2015). However, the absence of NTRC results in higher hydrogen peroxide levels under growth light and in darkness (Figure 18), in agreement with the protective role attributed to NTRC against oxidative stress as the main reductant of 2-Cys Prxs in normal light and especially, in darkness, when NTRC becomes the most relevant redox system using NADPH produced from sugars through the oxidative pentose phosphate pathway (Perez-Ruiz *et al.*, 2006; Pulido *et al.*, 2010).

While exploring the light responses of the *ntrc* mutant a new distinctive feature was uncovered. At light intensities equal to the irradiance applied during growth, or even lower light intensities, these plants present drastically elevated levels of NPQ, which are retained throughout the illumination period. This characteristic is unique to the plants lacking NTRC and is not found in wild type plants or the *Δ2cp* and *trxx* mutants (Figure 23). NPQ is usually observed in wild type plants after a sudden increase in light intensity (Figure 19) that exceeds their capacity for utilization in metabolic processes (Li *et al.*, 2009; Ruban *et al.*, 2012).

As expected, the high NPQ in plants lacking NTRC was accompanied by a decrease in PSII yield (Figure 20), which shows that these plants are not able to use the energy properly and this could be a factor contributing to the retarded growth of the *ntrc* mutant. Indeed, the increase of NPQ in *ntrc* plants was more pronounced in the youngest leaves (Figure 22), suggesting that down-regulation of NPQ by NTRC, to maximize light energy utilization, could be especially important during early leaf development. Moreover, it could affect the synthesis of chlorophylls since leaves with higher levels of NPQ are the most pale.

To understand the influence of NTRC on NPQ, the factors contributing to different elements of dissipation of the light energy have been considered. NPQ

comprises at least three components: qT, qI and qE, which are distinguishable according to induction and relaxation times. The qT component is the quenching resulting from state transitions, which is particularly important in algae, while the qI component is related to photoinhibition and occurs on a time scale of hours (Szabo et al., 2005; Baker, 2008). The major and most rapid NPQ component in plant leaves is qE, which is also referred to as ΔpH-dependent quenching (Szabo *et al.*, 2005) or energy-dependent quenching (Kramer et al., 2004a; Baker, 2008) and occurs within seconds. The fast dark-light induction and light-dark relaxation kinetics of NPQ in *ntrc* plants suggested that the qE component is specifically induced in this mutant (Figure 20).

qE is triggered it by the acidification of the thylakoid lumen which activates VDE leading to production of the xanthophyll zeaxanthin, and the protonation of the PSII subunit PsbS. The factors involved in qE are intimately related. Thus, the trans-thylakoid pH gradient alone was previously proven not to be sufficient to maintain NPQ in the absence of zeaxanthin (Gilmore *et al.*, 1994), and constitutively high concentrations of zeaxanthin in a ZE knockout mutant, *npq2-1*, were not sufficient to produce NPQ in the absence of ΔpH (Niyogi *et al.*, 1998). Moreover, PsbS is necessary in order to produce qE at physiological levels of lumen pH (Li et al., 2000; Johnson and Ruban, 2011), and the content of this protein determines the extent of maximal NPQ (Li *et al.*, 2002).

In this study, we found that the elevated NPQ at low light intensities in the *ntrc* mutant correlates with high levels of zeaxanthin (Figure 26). Furthermore, DTT inhibited NPQ *in vivo* in *ntrc* plants, which again links the NPQ observed to the zeaxanthin formation, since DTT is known to inhibit VDE (Yamamoto and Kamite, 1972), and confirms a redox component in the regulation of NPQ. The inhibition of NPQ by DTT was accompanied by recovery of effective PSII quantum yield (Figure 27D), showing the integrity of the photosynthetic machinery in plants lacking NTRC. In addition, the abnormally high level of NPQ in the *ntrc* mutant was also inhibited by nigericin (Figure 27A), and therefore, is dependent on ΔpH. All these data indicate that qE is the NPQ component specifically affected by the deficiency of NTRC. Additional evidence in support of this notion was obtained by analysing a double mutant of *Arabidopsis* devoid of both NTRC and PsbS, which have very low NPQ and lack the characteristic initial peak of qE in wild type plants upon a dark-light transition (Figure

36A). The double mutant *ntrc-psbs* was unable to induce qE and, therefore, partially recovered the PSII and PSI yields, which led to higher rates of LEF (Figures 36 and 41). Moreover, since these plants are larger and have higher chlorophyll content than the single *ntrc* mutant (Figure 34), it may be concluded that part of the retarded growth and low level of chlorophyll in this mutant is due to its enhanced energy dissipation and low PET rates under moderate light intensities.

A possible redox control of the xanthophyll cycle mediated by NTRC

The two enzymes that participate in the xanthophyll cycle, VDE and ZE, were present in equal amounts in the *ntrc* mutant and in wild type plants (Figure 25). Hence, the large differences regarding xanthophyll composition during illumination in *ntrc* mutant and wild type plants (Figure 26) must be due to alterations of the activities of either one or both enzymes in the mutant. Therefore, we tested the possibility that NTRC exerts a redox control on the enzymatic activities of VDE and/or ZE.

VDE, which is located in the thylakoid lumen, is activated by the decrease in the luminal pH (Pfundel and Dilley, 1993; Bratt et al., 1995; Jahns et al., 2009). Recently, the thylakoid lumen has attracted interest as a compartment where a number of regulatory proteins reside, many of which are plausible targets for redox regulation (Buchanan and Luan, 2005; Hall et al., 2010; Jarvi et al., 2013). Notably, VDE is a Trx target *in vitro* and inhibited by disulphide reduction (Hall *et al.*, 2010; Simionato *et al.*, 2015). A putative interaction between NTRC, located in the chloroplast stroma, and VDE might occur through a transmembrane pathway for disulphide-dithiol exchange, such as the DsbD-like system that involves HCF164 and CcdA (Motohashi and Hisabori, 2006, 2010; Karamoko et al., 2013). Thus, we tested whether NTRC is responsible for the reduction and inactivation of VDE. However, no significant differences of the redox state of VDE were observed in wt and *ntrc* plants in the light, which could explain the high zeaxanthin levels in the latter (Figure 28B).

Regarding ZE, previous reports indicate that this enzyme is inactivated by oxidation. Treatment of plants with cadmium ions results in inhibition of its activity (Latowski *et al.*, 2005) and ZE is also inhibited *in vivo* by photo-oxidative stress under high light conditions (Reinhold *et al.*, 2008). We found that ZE is prone to thiol

oxidation, which causes the protein to form multimeric aggregates of high molecular mass (Figure 29B). NTRC was able to reduce these ZE aggregates *in vitro* (Figure 29C), suggesting a function in the activation of zeaxanthin epoxidation converting this xanthophyll back to violaxanthin, which would lead to cessation of NPQ. Nevertheless, under normal light conditions the *in vivo* redox state of ZE did not change in either wild type or *ntrc* plants (Figure 30) and could therefore not contribute to explaining the high zeaxanthin levels of the *ntrc* mutant.

In summary, no significant changes of the redox state of VDE and ZE were observed in the *ntrc* mutant plants that could explain its high levels of zeaxanthin. Thus, another factor involved in the regulation of the xanthophyll cycle must be controlled by NTRC. Since the activity of VDE is strictly controlled by pH (Pfundel and Dilley, 1993; Kramer et al., 2003) and the high NPQ observed in *ntrc* plants was inhibited *in vivo* by the uncoupler nigericin (Figure 27A), we focused on the formation of the trans-thylakoid proton gradient.

The involvement of NTRC in the formation of the trans-thylakoid proton gradient

The electrochromic shift experiments demonstrated that the trans-thylakoid proton gradient, ΔpH, is larger under low and medium light intensities in plants devoid of NTRC (Figure 31). This is most likely the underlying cause for the elevated qE and is sufficient to explain the high zeaxanthin levels found in the *ntrc* mutant under moderate light intensities (Figure 26) as a consequence of activation of VDE.

The regulation of electron flow through the photosynthetic electron transport chain is a feed-back control mechanism. The proton gradient formed is the key for ATP synthesis. However, limitations of ATP consumption during photosynthesis will cause accumulation of protons in the thylakoid lumen leading to activation of NPQ and even inhibition of key enzymes involved in PET, such as Cyt b_6f and the oxygen evolving complex, which consequently reduces the electron transport rate (Kramer *et al.*, 2003; Ruban *et al.*, 2012).

Proton accumulation in the thylakoid lumen is produced during PET by water-splitting activity and PQ shuttle, and is relieved by the use of the proton motive force by the ATP synthase. Thus, acidification of the lumen indicates that proton accumulation

exceeds the requirement for ATP synthesis and this is what happens under excess light conditions or upon a transition from darkness to light before the metabolic machinery is activated. Hence, wild type plants transferred from darkness to low or moderate light intensity display a brief initial peak of NPQ that relaxes within less than 2 min and has been suggested to reflect the light-induced activation of the ATP synthase (Kalituho *et al.*, 2007). Moreover, plants with a defective chloroplast ATP synthase have high constitutive NPQ at low light intensities (Dal Bosco *et al.*, 2004). Hence, the trans-thylakoid proton gradient has a double function, driving the synthesis of ATP and triggering NPQ and, therefore, plays a key role in the balance of photoprotection and photochemical efficiency.

It is essential for chloroplasts to maintain the equilibrium of the ATP to NADPH production ratio (Allen, 2003; Kramer *et al.*, 2004a). Thus, an attractive hypothesis would be that NADPH, the substrate for NTRC, might regulate ATP synthesis through NTRC-mediated reduction of the ATP synthase γ-subunit, which is well known to be redox-regulated (Hisabori *et al.*, 2013; Kohzuma *et al.*, 2013). Light-induced reduction of the ATP synthase γ-subunit *in vivo* proved to be somewhat less efficient in the *ntrc* mutant than in wt plants (Figure 32). However, it is uncertain whether this alone would account for the increase in ΔpH observed in the *ntrc* mutant and it is obvious that there are other enzymes contributing to the redox regulation of this reaction *in vivo*.

The distribution of photosynthetic electron flow between LEF and CEF is crucial for balancing the synthesis of ATP and NADPH and for acclimation of plants to fluctuating light conditions (Kramer et al., 2004a; Allahverdiyeva et al., 2015). Interestingly, measurements of constitutive high qE under moderate light conditions have been applied previously to screen for high CEF (*hcef*) mutants, which have higher rates of proton translocation and larger proton motive force (Livingston *et al.*, 2010). The Trx *m*4 has recently been shown *in vivo* to inhibit CEF dependent on the NDH (Courteille *et al.*, 2013). However, mutants lacking Trx *m*4, with high CEF, did not show enhanced NPQ or lower effective PSII quantum yield in the light (Courteille *et al.*, 2013).

The *ntrc* mutant displays elevated and stable post-illumination chlorophyll fluorescence (Figure 42), indicative of an enhanced NDH activity (Shikanai *et al.*, 1998). In addition, the shift of the thermoluminescence AG-band towards a lower

temperature (Figure 43) suggests an increased back transfer of electrons to the acceptor side of PSII (Ducruet and Vass, 2009). Both results are usually related to high CEF, which contributes to an increase in ΔpH (Munekage et al., 2002; Livingston et al., 2010). Nevertheless, the lower PSI activity in the *ntrc* mutant in comparison to wild type plants (Figure 40) indicates that there is not more CEF around PSI in the mutant. Hence, CEF is not causing the larger ΔpH found in the *ntrc* plants.

The higher levels of reduced PQs in *ntrc* plants (Figures 42 and 43) could be due to higher concentrations of reducing power in the form of NADPH in the stroma or, alternatively, higher NDH activity. However, these electrons do not reach PSI, which could be because of a slower rate of PQH_2 oxidation at the Q_o site of Cyt b_6f originated by the high proton gradient formed.

The CEF has been reported to increase under strong illumination, although a large population of P700 also appears to become oxidised under these conditions. This is related to a decrease in the electron flow through the Cyt b_6f after the generation of a ΔpH, which is essential for protection of PSI from light stress, the photoinhibition of which is practically irreversible (Joliot and Johnson, 2011). PGR5 is a protein, which contributes strongly to the acidification of the thylakoid lumen and is involved in the transfer of electrons from Fd to PQ in one of the CEF pathways (Munekage *et al.*, 2002). Plants lacking this protein, *pgr5* mutants, are unable to induce qE and show more damage to PSI due to their inability to downregulate PSII and Cyt b_6f activities (Suorsa *et al.*, 2012).

It is feasible that NTRC could regulate other components, which would contribute to the ΔpH formation in addition to the ATP synthase. Plants devoid of the thylakoid H^+/K^+ antiporter KEA3 that allows proton efflux from the thylakoid lumen, display retardation of NPQ recovery after transfer from high to low light, suggesting a role for KEA3 in this process through direct control of the trans-thylakoid proton gradient (Armbruster *et al.*, 2014). In addition, mutants affected in the two pore K^+ channel TPK3 have been shown to be deficient in NPQ (Carraretto *et al.*, 2013).

The fact that NTRC is the only chloroplast Trx dependent on NADPH instead of Fd makes this protein a possible sensor of the NADPH levels in the chloroplast. The control of PET by NTRC found in this study could function as a positive feedback

regulation of the NADPH level in the chloroplast under moderate light conditions. The NADPH concentration in isolated chloroplasts has been reported to increase under illumination and decrease in darkness (Latouche et al., 2000; Schreiber and Klughammer, 2009). However, so far the specific chloroplast NADPH levels have not been determined *in vivo*.

NTRC has been reported to reduce and activate AGPase, a key enzyme in starch synthesis (Michalska *et al.*, 2009). Moreover, NTRC functions in the synthesis of chlorophyll (Richter et al., 2013; Perez-Ruiz et al., 2014) and in the shikimate pathway (Lepisto *et al.*, 2009). Thus, it seemed plausible that deficiencies in biosynthetic pathways would lead to lack of electron acceptors, poor utilisation of ATP and, consequently, increased acidification of the thylakoid lumen during illumination. This in turn would result in the high and stable levels of NPQ observed. However, a mutant lacking the regulatory small subunit of the AGPase, *aps1* (Ventriglia *et al.*, 2008) that is devoid of leaf starch, shows a pattern of NPQ identical to wild type plants (Figure 38). Moreover, our determinations of PSI activity based on P700 absorbance show that the *ntrc* mutant does not suffer more limitations on the acceptor side of PSI than the wild type. In contrast, whereas the PSI donor side limitations are gradually relieved after a dark-light transition in the wild type, these limitations persist in plants lacking NTRC during the entire period of illumination (Figure 39 and 40B). These results speak against the idea that limited activation of chloroplast biosynthetic processes would contribute to the high-qE phenotype of *ntrc* plants. Figure 64 outlines a model for the photosynthetic electron flows under steady state photosynthesis at low or moderate light intensities in wild type and *ntrc* plants, based on the experimental data presented in this work. Plants devoid of NTRC show high qE at low light intensities caused by an increase in the trans-thylakoid ΔpH, which leads to synthesis of high levels of zeaxanthin. However, electron flow from the stroma keeps the PQ-pool more reduced than in wild type plants, despite the lower PSII activity, although these electrons do not reach the PSI, which presents a deficit of electron donors.

In summary, our results show that plants lacking NTRC accumulate more protons in the thylakoid lumen at low and moderate light intensities, which results in rapid synthesis of zeaxanthin and high levels of dissipation of the light energy absorbed by LHCII. This, in turn, leads to low effective quantum yield of PSII and, thus, to

shortage of electron donors for PSI. A further implication of this enhanced dissipation and slow electron transport is that less energy is available for biosynthesis. Hence, the low starch content in *ntrc* plants (Michalska *et al.*, 2009; Toivola *et al.*, 2013) may also reflect the modest production of photosynthates. Indeed, this view affords an explanation to several aspects of the *ntrc* mutant phenotype. Plants that are continuously starved for light energy should be undersized and grow slowly (Serrato et al., 2004; Perez-Ruiz et al., 2006; Lepisto et al., 2009). Furthermore, longer days should promote growth of such plants by adding to the quantity of total energy absorbed and this is also true for plants lacking NTRC (Perez-Ruiz et al., 2006; Lepisto et al., 2009; Lepisto et al., 2013). Here we show that more electrons can be forced through the LEF pathway in plants lacking both NTRC and PsbS than in plants lacking NTRC alone. This rescues part of the *ntrc* phenotype with respect to growth and pigmentation (Figure 34).

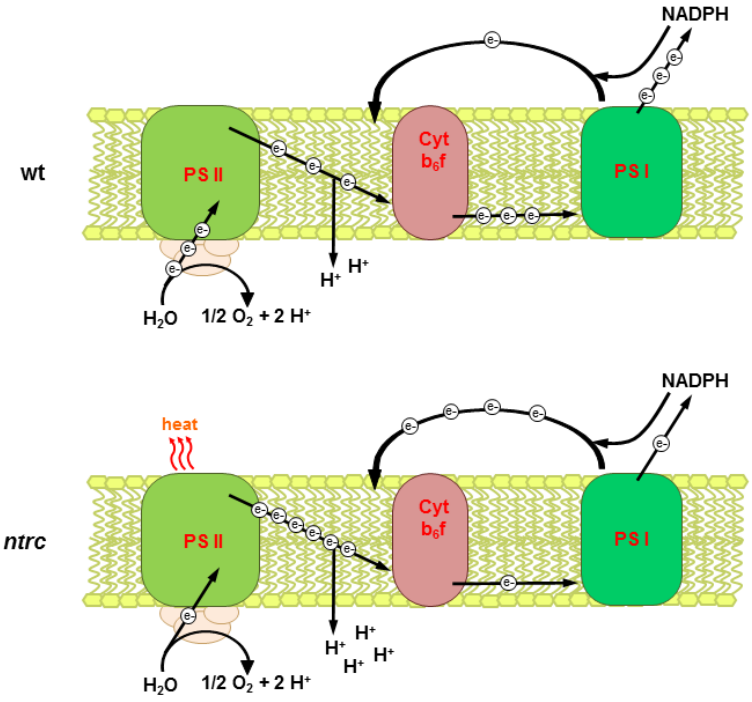

Figure 64. Model of the effect of NTRC on photosynthetic electron flow. Under steady state photosynthetic conditions at low or moderate light intensity, plants lacking NTRC build up a larger pH gradient. Hence, the *ntrc* mutant has lower rates of linear electron flow, due to extensive dissipation of light energy as heat through qE, and PSI suffers shortage of electron donors. In addition, the PQs receive more reducing equivalents from the stroma.

In conclusion, NTRC is required for down-regulation of qE-mediated energy dissipation and stimulation of LEF, which is essential for plant growth, particularly during early leaf development. NTRC is not involved in long- or short-term high light tolerance, nor is implied in peroxide detoxification at high light intensities. On the contrary, plants lacking NTRC are over-protected against light even at low and moderate irradiances leading to a state of permanent starvation for light energy.

5.2. The role of *f*-type Trxs in photosynthetic performance

The *f*-type Trxs have been considered the main reductants responsible for the light-dependent regulation of enzymes involved in carbohydrate metabolism. Extensive biochemical and proteomic work has shown the central role of *f*-type Trxs in the reductive activation of most of the Calvin-Benson cycle enzymes. Indeed, *in vitro* studies have shown that Trxs *f* are the most efficient catalysts for disulphide reduction of several Calvin-Benson enzymes (Collin *et al.*, 2003). The *Arabidopsis f*-type Trxs are also the most efficient in reducing NADP-MDH in comparison to the *m*-type Trxs, as well as the *x*- and *y*-type Trxs (Collin *et al.*, 2003; Collin *et al.*, 2004) and spinach Trx *f* is a better reductant for the enzyme α-glucan water dikinase than spinach Trx *m* (Mikkelsen et al., 2005). However, unless examined *in vivo* the true physiological function of each type of Trx could not be established and, until now, knockout mutants devoid of Trxs *f* have not been available. Two *f*-type Trxs are present in *Arabidopsis*. Both isoforms are very similar, and their functions might be redundant (Collin *et al.*, 2003; Thormahlen *et al.*, 2013). With the aim of analysing the function of these Trxs *in vivo*, in this study we have generated a double mutant of *Arabidopsis*, here termed *trxf1f2*, lacking both Trx *f*1 and Trx *f*2 (Figures 44 and 45).

The growth of the single mutants, *trxf1* and *trxf2*, was indistinguishable from that of the wild type plants. This was consistent with previous studies on *trxf1* mutants which suggest that the low content of the remaining Trx *f*2, either alone or in conjunction with other plastidial redox systems, may be sufficient to support the redox regulation that allows plant growth (Thormahlen *et al.*, 2013). However, plant growth was still similar to that of the wild type plants when both Trxs *f* were absent. Thus, the *trxf1f2* double mutant displayed wild type phenotype when grown under long day conditions, as shown for *f*-type null mutants recently reported (Yoshida *et al.*, 2015), but

showed growth inhibition under short-day conditions (Figure 46). Therefore, despite the central function attributed for Trxs *f* in chloroplast redox regulation based on biochemical *in vitro* analyses, the *in vivo* approach reported here show that these Trxs are dispensable for plant growth at least under the standard long-day conditions. However, it should be noted that short-day conditions have a negative effect on growth of the double mutant indicating that the function of Trxs *f* becomes more relevant when the light is a limiting factor.

Analysis of chlorophyll fluorescence shows that the integrity of PSII remains in the absence of either or both Trxs *f* (Table 5) and, therefore, the different mutants still have the same maximum capacity to perform photochemistry as wild type plants. However, the PSII effective quantum yield was lower in the *trxf1f2* mutant after a dark-light transition with a concomitant increase of NPQ that was maintained during a few minutes of illumination (Figures 48 and 49). As mentioned above, an initial increase of NPQ just after a dark-light transition, that relaxes within less than 2 min, is typical in wild type plants and reflects the light-dependent activation of metabolic reactions (Kalituho *et al.*, 2007). In the double mutant, *trxf1f2*, this initial NPQ was extended during illumination, suggesting retarded activation of the ATP synthase, or subsequent reactions, in plants lacking Trxs *f*.

Nevertheless, there are clear differences between plants lacking NTRC and plants lacking Trxs *f*. In contrast to the stable NPQ of the *ntrc* mutant, the energy dissipation observed in *trxf1f2* plants starts relaxing already in the light. This suggests that the pH of the lumen begins to recover even during illumination and, therefore, that the carbon assimilation could work properly although its activation might be slower.

However, the key to distinguish between the functions of NTRC and Trxs *f* was provided by measurements of PSI activity. The lower PSI activity in the *trxf1f2* mutant proved to be caused by a high deficit of acceptors (Figures 51 and 52). This situates the main function of the Trxs *f* downstream PSI in the photosynthetic reactions, whereas the main function of NTRC, with a high deficit of PSI electron donors, is situated upstream PSI in the photosynthetic electron transport chain.

The saturation of photosynthesis and the concomitant decrease of electron transport rate are intimately related to the capacity for CO_2 assimilation and the subsequent metabolic reactions, which determine the availability of electron acceptors

for PSI. Thus, the light-harvesting efficiency and PET are highly sensitive to changes in carbon assimilation. For example, sub-atmospheric levels of CO_2, which result in limited regeneration of ADP and $NADP^+$, lead to elevated NPQ and decreased effective PSII quantum yield at low or moderate light intensities (Kramer *et al.*, 2004b; Takizawa *et al.*, 2007). Similarly, inhibition of the Calvin-Benson cycle enzymes *in vivo* by iodoacetamide leads to higher NPQ and slower linear photosynthetic electron transport (Joliot and Alric, 2013). Notably, the qE component of NPQ ensures safe dissipation of the light energy absorbed and prevents excess excitation of PSII (Szabo et al., 2005; Baker, 2008; Ruban et al., 2012). Such a negative feedback control arisen from hampered CO_2 fixation is the most likely explanation for the results concerning the activities of PSII and PSI in the *trxf1f2* mutant. Indeed, the activation rate of CO_2 fixation was also retarded in the double mutant after a dark-light transition (Table 6 and Figure 53).

To address this issue, we proceeded to study the redox state *in vivo* of two Calvin-Benson cycle enzymes, FBPase and Rubisco activase, well-known *in vitro* targets of *f*-type Trxs (Schurmann and Buchanan, 2008). This analysis shows that reduction of both FBPase and Rubisco activase upon illumination was impaired in the *trxf1f2* knockout mutant, which presented a slower reduction of both enzymes (Figures 54, 55 and 56). Nevertheless, despite the complete absence of Trx *f*, both enzymes became partially reduced during illumination.

The light-dependent reduction of FBPase and Rubisco activase show very similar patterns in wild type plants on one hand and in Trx *f*-deficient plants on the other, suggesting common regulatory mechanisms for the two enzymes. This may be significant since both enzymes are involved in the pathway of CO_2 fixation in the chloroplast.

A relevant question concerning chloroplast redox regulation is the level of redundancy or specificity among the many different types of Trxs of this organelle. In this regard, the redox status *in vivo* of the Mg chelatase CHLI subunit from pea plants was affected by the simultaneous silencing of the *TRX f* and *TRX m* genes, but not by the silencing of the *TRX f* gene alone (Luo *et al.*, 2012), showing the compensatory effect of Trx *m* on the regulation of this enzyme of the chlorophyll biosynthesis pathway. Therefore, *m*-type Trxs could substitute for *f*-type Trxs in the light-dependent

redox regulation of the Calvin-Benson cycle enzymes. However, comparative analyses *in vitro* of a large number of the *Arabidopsis* plastid Trxs (*f*1, *f*2, *m*1, *m*2, *m*3, *m*4, *x*, *y*1 and *y*2) confirmed that only the *f*-type Trxs are capable of activating FBPase using recombinant enzymes (Collin *et al.*, 2003; Collin *et al.*, 2004). In addition, purified Rubisco activase has been shown to be readily reduced and activated by spinach Trx *f*, whereas spinach Trx *m* is unable to reduce this enzyme (Zhang and Portis, 1999).

The results obtained in this study showing partial reduction of FBPase and Rubisco activase after a dark-light transition in the *trxf1f2* mutant, attribute a specific function to the Trxs *f* that is not compensated for by other Trxs. In addition, the ability of the double mutant, *trxf1f2*, to partially reduce FBPase and Rubisco activase, indicates that another redox system is involved in the reduction of these enzymes, which until now have been considered specific targets of *f*-type Trxs. Therefore, *in vitro* studies showing the predominant function of Trxs *f* in redox regulation of the Calvin-Benson enzymes cannot be extrapolated to the physiological situation and show that the double mutant relies on alternative system(s), yet to be discovered, capable of limited reductive activation of these enzymes in response to light.

In addition, an interesting observation regarding the redox state of FBPase and Rubisco activase is that these enzymes do not become fully reduced under the growth light intensity used routinely in this work even in wild type plants. This is in agreement with recent reports (Yoshida et al., 2014; Yoshida et al., 2015) showing that *Arabidopsis* plants display only partial reduction of the FBPase when illuminated at low light intensity. However, we observe complete reduction of the FBPase in wild type plants after 10 min illumination with higher light intensity, 500 μmol quanta m^{-2} s^{-1} (Figure 54). A remarkable implication of these results is that plants that have been adapted to low light conditions have a significant pool of inactive, oxidised enzymes. A possible advantage of this seemingly wasteful synthesis of excess Calvin-Benson cycle enzymes is that after a sudden increase in photon flux leading to higher rates of photosynthetic electron transport, the ATP and NADPH generated would immediately be utilised for carbon dioxide fixation and, thus, would not pose a problem of light stress. Obviously, a prerequisite for this to occur is that there are sufficiently high amounts of Trxs *f* to catalyse the reductive activation of these enzymes. Moreover, we have analysed the changes of redox status of FBPase in light-dark transitions. Re-

oxidation of FBPase in response to darkness is again a very rapid process, which is essentially completed in 5 minutes in wild type plants (Figure 26). The fact that re-oxidation is faster in the mutants could indicate that, until exhausted, a pool of reduced Trxs *f* continues to catalyse reduction in the dark.

It should be noted that plant chloroplasts contain two types of FBPase, termed FBPase I and II, but only one of them, FBPase I, is redox-regulated (Serrato *et al.*, 2009). The result obtained after illumination with 500 μmol quanta m^{-2} s^{-1}, that shows FBPase fully reduced (Figure 54), indicates that the redox-insensitive form, FBPase II, is present in minor amounts in chloroplasts, in agreement with previous results (Rojas-Gonzalez *et al.*, 2015).

Despite the delayed response of carbon assimilation to light of plants devoid of Trxs *f*, these plants reached carbon assimilation rates similar to those of wild type plants (Figure 53). However, the content of starch was diminished in the *trxf1f2* mutant by more than 30% with respect to the wild type (Figure 58). This is in agreement with previous reports showing that overexpression of Trx *f*, but not Trx *m*, enhanced starch accumulation and increased the content of sugars in tobacco leaves (Sanz-Barrio *et al.*, 2013) and that *Arabidopsis* mutants knockout for Trx *f*1 display impairment of AGPase redox regulation and leaf diurnal starch turnover alterations (Thormahlen *et al.*, 2013). The redox regulation of AGPase by Trx *f*, could be a direct cause for the low starch content in the *trxf1f2* double mutant. In any case, the leaf starch accumulated during the day under a long-day light regime seems sufficient to endure the correspondingly short night and to support wild type growth rates (Figure 46). Only in short days the growth of the Trx *f*-null mutant was reduced by approximately one third (Figure 46).

The genes encoding Trx *f*1 and Trx *f*2 isoforms are subject to different regulation in *Arabidopsis*. The expression of the *TRX f1* gene responds to light, whereas the *TRX f2* gene is under circadian control (Barajas-Lopez Jde *et al.*, 2011). The differential pattern of expression of these genes might indicate different functions for the respective Trx *f* isoforms. However, all the photosynthetic parameters analysed in this study, such as photosynthetic electron transport and response to illumination of the rate of CO_2 fixation (A_N), as well as reduction of Calvin-Benson cycle enzymes and starch content, were more affected in the *trxf1* than the *trxf2* mutant, which displayed a pattern similar to that of the wild type plants, while the double mutant showed an additive effect. Most

probably, these results reflect the higher content of Trx *f*1 (Figure 45C) and support a redundant function for both *f*-type Trxs in *Arabidopsis*.

In summary, the *in vivo* approach undertaken in this work identifies the impact of Trxs *f* on photosynthetic performance in *Arabidopsis*, such as the rapid response of the rate of carbon assimilation and redox status of Calvin-Benson cycle enzymes upon a dark-light transition, and the control of photosynthetic electron transport. The fact that these parameters were impaired in plants devoid of Trxs *f* indicates that the functions of these Trxs are specific and are not compensated for by other Trxs or chloroplast redox systems. On the other hand, FBPase and Rubisco activase showed a significant level of reduction upon dark-light transition in the *trxf1f2* double mutant indicating that additional chloroplast redox systems participate in light-dependent reduction of these Calvin-Benson cycle enzymes. This stands out against the well-established notion, based on biochemical *in vitro* analyses, of the almost exclusive role attributed to Trxs *f* in redox regulation of these enzymes. Surprisingly, the growth of plants devoid of Trxs *f* was indistinguishable from wild type plants when grown under standard conditions with long-day photoperiod, indicating that the function of Trxs *f* are dispensable for growth. However, the growth inhibition of the *trxf1f2* null mutant under short-day conditions supports the idea that these Trxs may be essential for the continuous adaptations to variable irradiance under natural environmental conditions.

5.3. NTRC - Trx *f* interaction

As stated above, the results revealing partial reduction of FBPase and Rubisco activase in the *trxf1f2* double mutant indicate that additional redox systems participate in this regulation. Beside the Fd-dependent Trxs, the chloroplast also contains a redox system, NTRC, which depends on NADPH (Serrato et al., 2004). Several recent studies indicate a previously unpredicted relevance of NTRC in chloroplast redox regulation. Therefore, in search for an additional redox system contributing to the redox regulation of the Calvin-Benson enzymes we focused on NTRC.

In this study, we present evidence showing that both Trx *f* and NTRC participate in regulation of photosynthesis, although with different functions. Trxs *f* are involved in regulation of electron acceptors, which act as sinks for the PET, while NTRC seem to

exert an important effect in the control of the input of electrons from light energy into the PET chain. Interestingly, both FBPase and Rubisco activase, despite being Trx *f* targets were found to have impaired redox state in plants devoid of NTRC, suggesting a possible interaction between these redox systems. In line with this notion, it has been reported that enzymes such as 2-Cys Prx and AGPase are regulated by both redox systems, NTRC and Trx *x* (Pulido *et al.*, 2010) or Trx *f*1 (Michalska et al., 2009; Lepisto et al., 2013; Thormahlen et al., 2013), respectively.

The impairment of the redox state of FBPase and Rubisco activase in the *ntrc* mutant could have different reasons. First, this might be the indirect consequence of the lower electron transport rate resulting in defective regulation of the redox targets. Alternatively, impairment of the redox state of these enzymes in the *ntrc* mutant might suggest a direct participation of NTRC in the redox regulation of FBPase and Rubisco activase. Though not yet tested, this possibility is unlikely due to that fact that neither of these enzymes was identified as NTRC target *in vitro* (Ferrández, González and Cejudo, manuscript in preparation). Here, we have addressed an alternative possibility, which is the interaction between NTRC and Trx *f*. This was addressed by *in vitro* assays with purified enzymes. The results show that NTRC is able to oxidise reduced Trx *f*1, but the redox system is operative also in the opposite direction, that is, that NTRC is able to reduce oxidised Trx *f*1. Evidence in favour of the redox interaction between NTRC and Trx *f*1, which was based on alkylating assays (Figure 61) was further confirmed by the finding that NTRC is able to catalyse the reduction of $NADP^+$ using electrons from DTT or reduced Trx *f*1 (Figure 63).

In this regard, transgenic lines over-expressing each of the NTRC domains, or mutated versions of NTRC with one of the domains mutated, in the *ntrc* mutant background were recently reported to partially recover wild type phenotype (Toivola *et al.*, 2013). These results are in agreement with the possible interaction of NTRC with other Trxs. However, our *in vitro* approach indicates that the conformation of NTRC is essential for a proper redox interaction with Trxs *f* (Figure 62). These results reflect the complexity of chloroplast redox regulation and suggest that many more mechanisms remain to be discovered.

CONCLUSIONS

6. CONCLUSIONS

1. Plants lacking NTRC are not hypersensitive to high light. On the contrary, NTRC is necessary for the efficient use of the absorbed light energy in photochemistry. This is particularly relevant during early leaf development.
2. NTRC down-regulates the energy-dependent component of NPQ through control of the trans-thylakoid proton gradient.
3. A double mutant devoid of NTRC and the photosystem II subunit PsbS, which is unable to induce energy-dependent quenching, recovers partially photosynthetic capacity and growth.
4. *f*-type Trxs are dispensable for plant growth when light is not a limiting factor.
5. The Calvin-Benson cycle enzymes FBPase and Rubisco activase are rapidly activated by *f*-type Trxs after a dark-light transition *in vivo*. However, additional chloroplast redox systems are also involved in their regulation.
6. NTRC and Trx *f*1 show redox interaction *in vitro*.

BIBLIOGRAPHY

7. BIBLIOGRAPHY

Adamiec, M., Drath, M., and Jackowski, G. (2008). Redox state of plastoquinone pool regulates expression of Arabidopsis thaliana genes in response to elevated irradiance. Acta Biochim Pol 55**,** 161-173.

Alkhalfioui, F., Renard, M., and Montrichard, F. (2007). Unique properties of NADP-thioredoxin reductase C in legumes. J Exp Bot 58**,** 969-978.

Allahverdiyeva, Y., Suorsa, M., Tikkanen, M., and Aro, E.M. (2015). Photoprotection of photosystems in fluctuating light intensities. J Exp Bot 66**,** 2427-2436.

Allen, J.F. (2003). Cyclic, pseudocyclic and noncyclic photophosphorylation: new links in the chain. Trends Plant Sci 8**,** 15-19.

Armbruster, U., Carrillo, L.R., Venema, K., Pavlovic, L., Schmidtmann, E., Kornfeld, A., Jahns, P., Berry, J.A., Kramer, D.M., and Jonikas, M.C. (2014). Ion antiport accelerates photosynthetic acclimation in fluctuating light environments. Nat Commun 5**,** 5439.

Arnoux, P., Morosinotto, T., Saga, G., Bassi, R., and Pignol, D. (2009). A structural basis for the pH-dependent xanthophyll cycle in Arabidopsis thaliana. Plant Cell 21**,** 2036-2044.

Aro, E.M., Virgin, I., and Andersson, B. (1993). Photoinhibition of Photosystem II. Inactivation, protein damage and turnover. Biochim Biophys Acta 1143**,** 113-134.

Arsova, B., Hoja, U., Wimmelbacher, M., Greiner, E., Ustun, S., Melzer, M., Petersen, K., Lein, W., and Bornke, F. (2010). Plastidial thioredoxin z interacts with two fructokinase-like proteins in a thiol-dependent manner: evidence for an essential role in chloroplast development in Arabidopsis and Nicotiana benthamiana. Plant Cell 22**,** 1498-1515.

Awad, J., Stotz, H.U., Fekete, A., Krischke, M., Engert, C., Havaux, M., Berger, S., and Mueller, M.J. (2015). 2-Cysteine Peroxiredoxins and Thylakoid Ascorbate Peroxidase Create a Water-Water Cycle That Is Essential to Protect the Photosynthetic Apparatus under High Light Stress Conditions. Plant Physiol 167**,** 1592-1603.

Bailleul, B., Cardol, P., Breyton, C., and Finazzi, G. (2010). Electrochromism: a useful probe to study algal photosynthesis. Photosynth Res 106**,** 179-189.

Baker, N.R. (2008). Chlorophyll fluorescence: a probe of photosynthesis in vivo. Annu Rev Plant Biol 59**,** 89-113.

Baniulis, D., Yamashita, E., Zhang, H., Hasan, S.S., and Cramer, W.A. (2008). Structure-function of the cytochrome b6f complex. Photochem Photobiol 84**,** 1349-1358.

Barajas-Lopez Jde, D., Serrato, A.J., Cazalis, R., Meyer, Y., Chueca, A., Reichheld, J.P., and Sahrawy, M. (2011). Circadian regulation of chloroplastic f and m thioredoxins through control of the CCA1 transcription factor. J Exp Bot 62**,** 2039-2051.

Barber, J. (2006). Photosystem II: an enzyme of global significance. Biochem Soc Trans 34**,** 619-631.

Bellafiore, S., Barneche, F., Peltier, G., and Rochaix, J.D. (2005). State transitions and light adaptation require chloroplast thylakoid protein kinase STN7. Nature 433**,** 892-895.

Bernal-Bayard, P., Hervas, M., Cejudo, F.J., and Navarro, J.A. (2012). Electron transfer pathways and dynamics of chloroplast NADPH-dependent thioredoxin reductase C (NTRC). J Biol Chem 287**,** 33865-33872.

Betterle, N., Ballottari, M., Zorzan, S., de Bianchi, S., Cazzaniga, S., Dall'osto, L., Morosinotto, T., and Bassi, R. (2009). Light-induced dissociation of an antenna hetero-oligomer is needed for non-photochemical quenching induction. J Biol Chem 284**,** 15255-15266.

Bohrer, A.S., Massot, V., Innocenti, G., Reichheld, J.P., Issakidis-Bourguet, E., and Vanacker, H. (2012). New insights into the reduction systems of plastidial thioredoxins point out the unique properties of thioredoxin z from Arabidopsis. J Exp Bot 63**,** 6315-6323.

Bouvier, F., d'Harlingue, A., Hugueney, P., Marin, E., Marion-Poll, A., and Camara, B. (1996). Xanthophyll biosynthesis. Cloning, expression, functional reconstitution, and regulation of beta-cyclohexenyl carotenoid epoxidase from pepper (Capsicum annuum). J Biol Chem 271**,** 28861-28867.

Bratt, C.E., Arvidsson, P.O., Carlsson, M., and Akerlund, H.E. (1995). Regulation of violaxanthin de-epoxidase activity by pH and ascorbate concentration. Photosynth Res 45**,** 169-175.

Broin, M., Cuine, S., Eymery, F., and Rey, P. (2002). The plastidic 2-cysteine peroxiredoxin is a target for a thioredoxin involved in the protection of the photosynthetic apparatus against oxidative damage. Plant Cell 14**,** 1417-1432.

Buchanan, B.B., and Luan, S. (2005). Redox regulation in the chloroplast thylakoid lumen: a new frontier in photosynthesis research. J Exp Bot 56**,** 1439-1447.

Buchanan, B.B., and Balmer, Y. (2005). Redox regulation: a broadening horizon. Annu Rev Plant Biol 56**,** 187-220.

Bugos, R.C., and Yamamoto, H.Y. (1996). Molecular cloning of violaxanthin de-epoxidase from romaine lettuce and expression in Escherichia coli. Proc Natl Acad Sci U S A 93**,** 6320-6325.

Carraretto, L., Formentin, E., Teardo, E., Checchetto, V., Tomizioli, M., Morosinotto, T., Giacometti, G.M., Finazzi, G., and Szabo, I. (2013). A thylakoid-located two-pore K+ channel controls photosynthetic light utilization in plants. Science 342**,** 114-118.

Cejudo, F.J., Ferrandez, J., Cano, B., Puerto-Galan, L., and Guinea, M. (2012). The function of the NADPH thioredoxin reductase C-2-Cys peroxiredoxin system in plastid redox regulation and signalling. FEBS Lett 586**,** 2974-2980.

Collin, V., Issakidis-Bourguet, E., Marchand, C., Hirasawa, M., Lancelin, J.M., Knaff, D.B., and Miginiac-Maslow, M. (2003). The Arabidopsis plastidial thioredoxins: new functions and new insights into specificity. J Biol Chem 278**,** 23747-23752.

Collin, V., Lamkemeyer, P., Miginiac-Maslow, M., Hirasawa, M., Knaff, D.B., Dietz, K.J., and Issakidis-Bourguet, E. (2004). Characterization of plastidial thioredoxins from Arabidopsis belonging to the new y-type. Plant Physiol 136**,** 4088-4095.

Courteille, A., Vesa, S., Sanz-Barrio, R., Cazale, A.C., Becuwe-Linka, N., Farran, I., Havaux, M., Rey, P., and Rumeau, D. (2013). Thioredoxin m4 controls photosynthetic alternative electron pathways in Arabidopsis. Plant Physiol 161**,** 508-520.

Crouchman, S., Ruban, A., and Horton, P. (2006). PsbS enhances nonphotochemical fluorescence quenching in the absence of zeaxanthin. FEBS Lett 580**,** 2053-2058.

Chae, H.B., Moon, J.C., Shin, M.R., Chi, Y.H., Jung, Y.J., Lee, S.Y., Nawkar, G.M., Jung, H.S., Hyun, J.K., Kim, W.Y., Kang, C.H., Yun, D.J., and Lee, K.O. (2013). Thioredoxin reductase type C (NTRC) orchestrates enhanced thermotolerance to Arabidopsis by its redox-dependent holdase chaperone function. Mol Plant 6**,** 323-336.

Dai, S., Friemann, R., Glauser, D.A., Bourquin, F., Manieri, W., Schurmann, P., and Eklund, H. (2007). Structural snapshots along the reaction pathway of ferredoxin-thioredoxin reductase. Nature 448**,** 92-96.

Dal Bosco, C., Lezhneva, L., Biehl, A., Leister, D., Strotmann, H., Wanner, G., and Meurer, J. (2004). Inactivation of the chloroplast ATP synthase gamma subunit results in high non-photochemical fluorescence quenching and altered nuclear gene expression in Arabidopsis thaliana. J Biol Chem 279**,** 1060-1069.

DalCorso, G., Pesaresi, P., Masiero, S., Aseeva, E., Schunemann, D., Finazzi, G., Joliot, P., Barbato, R., and Leister, D. (2008). A complex containing PGRL1 and PGR5 is involved in the switch between linear and cyclic electron flow in Arabidopsis. Cell 132**,** 273-285.

Dall'Osto, L., Cazzaniga, S., Havaux, M., and Bassi, R. (2010). Enhanced photoprotection by protein-bound vs free xanthophyll pools: a comparative analysis of chlorophyll b and xanthophyll biosynthesis mutants. Mol Plant 3**,** 576-593.

Dietz, K.J. (2015). Efficient high light acclimation involves rapid processes at multiple mechanistic levels. J Exp Bot.

Ducruet, J.M. (2003). Chlorophyll thermoluminescence of leaf discs: simple instruments and progress in signal interpretation open the way to new ecophysiological indicators. J Exp Bot 54**,** 2419-2430.

Ducruet, J.M., and Miranda, T. (1992). Graphical and numerical analysis of thermoluminescence and fluorescence F0 emission in photosynthetic material. Photosynth Res 33**,** 15-27.

Ducruet, J.M., and Vass, I. (2009). Thermoluminescence: experimental. Photosynth Res 101**,** 195-204.

Foyer, C.H., and Noctor, G. (2009). Redox regulation in photosynthetic organisms: signaling, acclimation, and practical implications. Antioxid Redox Signal 11**,** 861-905.

Galzerano, D., Feilke, K., Schaub, P., Beyer, P., and Krieger-Liszkay, A. (2014). Effect of constitutive expression of bacterial phytoene desaturase CRTI on photosynthetic electron transport in Arabidopsis thaliana. Biochim Biophys Acta 1837**,** 345-353.

Gilmore, A.M., Mohanty, N., and Yamamoto, H.Y. (1994). Epoxidation of zeaxanthin and antheraxanthin reverses non-photochemical quenching of photosystem II chlorophyll a fluorescence in the presence of trans-thylakoid delta pH. FEBS Lett 350**,** 271-274.

Gomez-Cadenas, A., Pozo, O.J., Garcia-Augustin, P., and Sancho, J.V. (2002). Direct analysis of abscisic acid in crude plant extracts by liquid chromatography--electrospray/tandem mass spectrometry. Phytochem Anal 13**,** 228-234.

Hall, M., Mata-Cabana, A., Akerlund, H.E., Florencio, F.J., Schroder, W.P., Lindahl, M., and Kieselbach, T. (2010). Thioredoxin targets of the plant chloroplast lumen and their implications for plastid function. Proteomics 10**,** 987-1001.

Hansen, R.E., and Winther, J.R. (2009). An introduction to methods for analyzing thiols and disulfides: Reactions, reagents, and practical considerations. Anal Biochem 394**,** 147-158.

Havaux, M., and Niyogi, K.K. (1999). The violaxanthin cycle protects plants from photooxidative damage by more than one mechanism. Proc Natl Acad Sci U S A 96**,** 8762-8767.

Havaux, M., Dall'osto, L., and Bassi, R. (2007). Zeaxanthin has enhanced antioxidant capacity with respect to all other xanthophylls in Arabidopsis leaves and functions independent of binding to PSII antennae. Plant Physiol 145**,** 1506-1520.

Hawkins, C.L., and Davies, M.J. (2014). Detection and characterisation of radicals in biological materials using EPR methodology. Biochim Biophys Acta 1840**,** 708-721.

Heber, U. (2002). Irrungen, Wirrungen? The Mehler reaction in relation to cyclic electron transport in C3 plants. Photosynth Res 73**,** 223-231.

Hertle, A.P., Blunder, T., Wunder, T., Pesaresi, P., Pribil, M., Armbruster, U., and Leister, D. (2013). PGRL1 is the elusive ferredoxin-plastoquinone reductase in photosynthetic cyclic electron flow. Mol Cell 49**,** 511-523.

Hisabori, T., Sunamura, E., Kim, Y., and Konno, H. (2013). The chloroplast ATP synthase features the characteristic redox regulation machinery. Antioxid Redox Signal 19**,** 1846-1854.

Hornero-Mendez, D., Gomez-Ladron De Guevara, R., and Minguez-Mosquera, M.I. (2000). Carotenoid biosynthesis changes in five red pepper (Capsicum annuum L.) cultivars during ripening. Cultivar selection for breeding. J Agric Food Chem 48**,** 3857-3864.

Issakidis-Bourguet, E., Mouaheb, N., Meyer, Y., and Miginiac-Maslow, M. (2001). Heterologous complementation of yeast reveals a new putative function for chloroplast m-type thioredoxin. Plant J 25**,** 127-135.

Jahns, P., and Holzwarth, A.R. (2012). The role of the xanthophyll cycle and of lutein in photoprotection of photosystem II. Biochim Biophys Acta 1817**,** 182-193.

Jahns, P., Latowski, D., and Strzalka, K. (2009). Mechanism and regulation of the violaxanthin cycle: the role of antenna proteins and membrane lipids. Biochim Biophys Acta 1787**,** 3-14.

Jarvi, S., Gollan, P.J., and Aro, E.M. (2013). Understanding the roles of the thylakoid lumen in photosynthesis regulation. Front Plant Sci 4**,** 434.

Johnson, G.N. (2011). Physiology of PSI cyclic electron transport in higher plants. Biochim Biophys Acta 1807**,** 384-389.

Johnson, M.P., and Ruban, A.V. (2011). Restoration of rapidly reversible photoprotective energy dissipation in the absence of PsbS protein by enhanced DeltapH. J Biol Chem 286**,** 19973-19981.

Johnson, M.P., Perez-Bueno, M.L., Zia, A., Horton, P., and Ruban, A.V. (2009). The zeaxanthin-independent and zeaxanthin-dependent qE components of nonphotochemical quenching involve common conformational changes within the photosystem II antenna in Arabidopsis. Plant Physiol 149**,** 1061-1075.

Johnson, M.P., Havaux, M., Triantaphylides, C., Ksas, B., Pascal, A.A., Robert, B., Davison, P.A., Ruban, A.V., and Horton, P. (2007). Elevated zeaxanthin bound to oligomeric LHCII enhances the resistance of Arabidopsis to photooxidative stress by a lipid-protective, antioxidant mechanism. J Biol Chem 282**,** 22605-22618.

Joliot, P., and Joliot, A. (2002). Cyclic electron transfer in plant leaf. Proc Natl Acad Sci U S A 99**,** 10209-10214.

Joliot, P., and Johnson, G.N. (2011). Regulation of cyclic and linear electron flow in higher plants. Proc Natl Acad Sci U S A 108**,** 13317-13322.

Joliot, P., and Alric, J. (2013). Inhibition of CO2 fixation by iodoacetamide stimulates cyclic electron flow and non-photochemical quenching upon far-red illumination. Photosynth Res 115**,** 55-63.

Jones, R.L., Ougham, H., Thomas, H., and Waaland, S. (2012). The Molecular Life of Plants. Wiley-Blackwell, Chichester.

Kalituho, L., Beran, K.C., and Jahns, P. (2007). The transiently generated nonphotochemical quenching of excitation energy in Arabidopsis leaves is modulated by zeaxanthin. Plant Physiol 143**,** 1861-1870.

Karamoko, M., Gabilly, S.T., and Hamel, P.P. (2013). Operation of trans-thylakoid thiol-metabolizing pathways in photosynthesis. Front Plant Sci 4**,** 476.

Kirchsteiger, K., Ferrandez, J., Pascual, M.B., Gonzalez, M., and Cejudo, F.J. (2012). NADPH thioredoxin reductase C is localized in plastids of photosynthetic and nonphotosynthetic tissues and is involved in lateral root formation in Arabidopsis. Plant Cell 24**,** 1534-1548.

Klughammer, C., and Schreiber, U. (2008). Saturation Pulse method for assessment of energy conversion in PS I. PAM Application Notes 1**,** 4.

Kohzuma, K., Dal Bosco, C., Meurer, J., and Kramer, D.M. (2013). Light- and metabolism-related regulation of the chloroplast ATP synthase has distinct mechanisms and functions. J Biol Chem 288**,** 13156-13163.

Konno, H., Nakane, T., Yoshida, M., Ueoka-Nakanishi, H., Hara, S., and Hisabori, T. (2012). Thiol modulation of the chloroplast ATP synthase is dependent on the energization of thylakoid membranes. Plant Cell Physiol 53**,** 626-634.

Kramer, D.M., Cruz, J.A., and Kanazawa, A. (2003). Balancing the central roles of the thylakoid proton gradient. Trends Plant Sci 8**,** 27-32.

Kramer, D.M., Avenson, T.J., and Edwards, G.E. (2004a). Dynamic flexibility in the light reactions of photosynthesis governed by both electron and proton transfer reactions. Trends Plant Sci 9**,** 349-357.

Kramer, D.M., Johnson, G., Kiirats, O., and Edwards, G.E. (2004b). New fluorescence parameters for the determination of q(a) redox state and excitation energy fluxes. Photosynth Res 79**,** 209-218.

Krieger-Liszkay, A., Fufezan, C., and Trebst, A. (2008). Singlet oxygen production in photosystem II and related protection mechanism. Photosynth Res 98**,** 551-564.

Laloi, C., Rayapuram, N., Chartier, Y., Grienenberger, J.M., Bonnard, G., and Meyer, Y. (2001). Identification and characterization of a mitochondrial thioredoxin system in plants. Proc Natl Acad Sci U S A 98**,** 14144-14149.

Latouche, G., Cerovic, Z.G., Montagnini, F., and Moya, I. (2000). Light-induced changes of NADPH fluorescence in isolated chloroplasts: a spectral and fluorescence lifetime study. Biochim Biophys Acta 1460**,** 311-329.

Latowski, D., Kruk, J., and Strzalka, K. (2005). Inhibition of zeaxanthin epoxidase activity by cadmium ions in higher plants. J Inorg Biochem 99**,** 2081-2087.

Laughner, B.J., Sehnke, P.C., and Ferl, R.J. (1998). A novel nuclear member of the thioredoxin superfamily. Plant Physiol 118**,** 987-996.

Lepisto, A., Pakula, E., Toivola, J., Krieger-Liszkay, A., Vignols, F., and Rintamaki, E. (2013). Deletion of chloroplast NADPH-dependent thioredoxin reductase results in inability to regulate starch synthesis and causes stunted growth under short-day photoperiods. J Exp Bot 64**,** 3843-3854.

Lepisto, A., Kangasjarvi, S., Luomala, E.M., Brader, G., Sipari, N., Keranen, M., Keinanen, M., and Rintamaki, E. (2009). Chloroplast NADPH-thioredoxin reductase interacts with photoperiodic development in Arabidopsis. Plant Physiol 149**,** 1261-1276.

Li, X.P., Muller-Moule, P., Gilmore, A.M., and Niyogi, K.K. (2002). PsbS-dependent enhancement of feedback de-excitation protects photosystem II from photoinhibition. Proc Natl Acad Sci U S A 99**,** 15222-15227.

Li, X.P., Bjorkman, O., Shih, C., Grossman, A.R., Rosenquist, M., Jansson, S., and Niyogi, K.K. (2000). A pigment-binding protein essential for regulation of photosynthetic light harvesting. Nature 403**,** 391-395.

Li, Z., Wakao, S., Fischer, B.B., and Niyogi, K.K. (2009). Sensing and responding to excess light. Annu Rev Plant Biol 60**,** 239-260.

Lichtenthaler, H.K. (1987). Chlorophylls and carotenoids: Pigments of photosynthetic membranes. Methods Enzymol 148**,** 23.

Lin, T.P., Caspar, T., Somerville, C., and Preiss, J. (1988). Isolation and Characterization of a Starchless Mutant of Arabidopsis thaliana (L.) Heynh Lacking ADPglucose Pyrophosphorylase Activity. Plant Physiol 86**,** 1131-1135.

Lindahl, M., and Kieselbach, T. (2009). Disulphide proteomes and interactions with thioredoxin on the track towards understanding redox regulation in chloroplasts and cyanobacteria. J Proteomics 72**,** 416-438.

Lindahl, M., Mata-Cabana, A., and Kieselbach, T. (2011). The disulfide proteome and other reactive cysteine proteomes: analysis and functional significance. Antioxid Redox Signal 14**,** 2581-2642.

Livingston, A.K., Cruz, J.A., Kohzuma, K., Dhingra, A., and Kramer, D.M. (2010). An Arabidopsis mutant with high cyclic electron flow around photosystem I (hcef) involving the NADPH dehydrogenase complex. Plant Cell 22**,** 221-233.

Luo, T., Fan, T., Liu, Y., Rothbart, M., Yu, J., Zhou, S., Grimm, B., and Luo, M. (2012). Thioredoxin redox regulates ATPase activity of magnesium chelatase CHLI subunit and modulates redox-mediated signaling in tetrapyrrole biosynthesis and homeostasis of reactive oxygen species in pea plants. Plant Physiol 159**,** 118-130.

Marin, E., Nussaume, L., Quesada, A., Gonneau, M., Sotta, B., Hugueney, P., Frey, A., and Marion-Poll, A. (1996). Molecular identification of zeaxanthin epoxidase of Nicotiana plumbaginifolia, a gene involved in abscisic acid biosynthesis and corresponding to the ABA locus of Arabidopsis thaliana. EMBO J 15**,** 2331-2342.

Markwell, M.A., Haas, S.M., Bieber, L.L., and Tolbert, N.E. (1978). A modification of the Lowry procedure to simplify protein determination in membrane and lipoprotein samples. Anal Biochem 87**,** 206-210.

Meyer, Y., Reichheld, J.P., and Vignols, F. (2005). Thioredoxins in Arabidopsis and other plants. Photosynth Res 86**,** 419-433.

Meyer, Y., Buchanan, B.B., Vignols, F., and Reichheld, J.P. (2009). Thioredoxins and glutaredoxins: unifying elements in redox biology. Annu Rev Genet 43**,** 335-367.

Meyer, Y., Belin, C., Delorme-Hinoux, V., Reichheld, J.P., and Riondet, C. (2012). Thioredoxin and glutaredoxin systems in plants: molecular mechanisms, crosstalks, and functional significance. Antioxid Redox Signal 17**,** 1124-1160.

Michalska, J., Zauber, H., Buchanan, B.B., Cejudo, F.J., and Geigenberger, P. (2009). NTRC links built-in thioredoxin to light and sucrose in regulating starch synthesis in chloroplasts and amyloplasts. Proc Natl Acad Sci U S A 106**,** 9908-9913.

Michelet, L., Zaffagnini, M., Morisse, S., Sparla, F., Perez-Perez, M.E., Francia, F., Danon, A., Marchand, C.H., Fermani, S., Trost, P., and Lemaire, S.D. (2013). Redox regulation of the Calvin-Benson cycle: something old, something new. Front Plant Sci 4**,** 470.

Mikkelsen, R., Mutenda, K.E., Mant, A., Schurmann, P., and Blennow, A. (2005). Alpha-glucan, water dikinase (GWD): a plastidic enzyme with redox-regulated and coordinated catalytic activity and binding affinity. Proc Natl Acad Sci U S A 102**,** 1785-1790.

Mills, J.D., Mitchell, P., and Schurmann, P. (1980). Modulation of coupling Factor ATPase Activity in intact chloroplasts, the role of the thioredoxin system. FEBS Lett 112**,** 5.

Moon, J.C., Jang, H.H., Chae, H.B., Lee, J.R., Lee, S.Y., Jung, Y.J., Shin, M.R., Lim, H.S., Chung, W.S., Yun, D.J., and Lee, K.O. (2006). The C-type Arabidopsis thioredoxin reductase ANTR-C acts as an electron donor to 2-Cys peroxiredoxins in chloroplasts. Biochem Biophys Res Commun 348**,** 478-484.

Motohashi, K., and Hisabori, T. (2006). HCF164 receives reducing equivalents from stromal thioredoxin across the thylakoid membrane and mediates reduction of target proteins in the thylakoid lumen. J Biol Chem 281**,** 35039-35047.

Motohashi, K., and Hisabori, T. (2010). CcdA is a thylakoid membrane protein required for the transfer of reducing equivalents from stroma to thylakoid lumen in the higher plant chloroplast. Antioxid Redox Signal 13**,** 1169-1176.

Mubarakshina, M.M., Ivanov, B.N., Naydov, I.A., Hillier, W., Badger, M.R., and Krieger-Liszkay, A. (2010). Production and diffusion of chloroplastic H2O2 and its implication to signalling. J Exp Bot 61**,** 3577-3587.

Muller, P., Li, X.P., and Niyogi, K.K. (2001). Non-photochemical quenching. A response to excess light energy. Plant Physiol 125**,** 1558-1566.

Munekage, Y., Hojo, M., Meurer, J., Endo, T., Tasaka, M., and Shikanai, T. (2002). PGR5 is involved in cyclic electron flow around photosystem I and is essential for photoprotection in Arabidopsis. Cell 110**,** 361-371.

Munekage, Y., Hashimoto, M., Miyake, C., Tomizawa, K., Endo, T., Tasaka, M., and Shikanai, T. (2004). Cyclic electron flow around photosystem I is essential for photosynthesis. Nature 429**,** 579-582.

Murray, M.G., and Thompson, W.F. (1980). Rapid isolation of high molecular weight plant DNA. Nucleic Acids Res 8**,** 4321-4325.

Nambara, E., and Marion-Poll, A. (2005). Abscisic acid biosynthesis and catabolism. Annu Rev Plant Biol 56**,** 165-185.

Nelson, N., and Junge, W. (2015). Structure and Energy Transfer in Photosystems of Oxygenic Photosynthesis. Annu Rev Biochem.

Nevo, R., Charuvi, D., Tsabari, O., and Reich, Z. (2012). Composition, architecture and dynamics of the photosynthetic apparatus in higher plants. Plant J 70**,** 157-176.

Nikkanen, L., and Rintamaki, E. (2014). Thioredoxin-dependent regulatory networks in chloroplasts under fluctuating light conditions. Philos Trans R Soc Lond B Biol Sci 369**,** 20130224.

Nixon, P.J., Michoux, F., Yu, J., Boehm, M., and Komenda, J. (2010). Recent advances in understanding the assembly and repair of photosystem II. Ann Bot 106**,** 1-16.

Niyogi, K.K., Grossman, A.R., and Bjorkman, O. (1998). Arabidopsis mutants define a central role for the xanthophyll cycle in the regulation of photosynthetic energy conversion. Plant Cell 10**,** 1121-1134.

Niyogi, K.K., Li, X.P., Rosenberg, V., and Jung, H.S. (2005). Is PsbS the site of non-photochemical quenching in photosynthesis? J Exp Bot 56**,** 375-382.

op den Camp, R.G., Przybyla, D., Ochsenbein, C., Laloi, C., Kim, C., Danon, A., Wagner, D., Hideg, E., Gobel, C., Feussner, I., Nater, M., and Apel, K. (2003). Rapid induction of distinct stress responses after the release of singlet oxygen in Arabidopsis. Plant Cell 15**,** 2320-2332.

Peng, L., and Shikanai, T. (2011). Supercomplex formation with photosystem I is required for the stabilization of the chloroplast NADH dehydrogenase-like complex in Arabidopsis. Plant Physiol 155**,** 1629-1639.

Peng, L., Shimizu, H., and Shikanai, T. (2008). The chloroplast NAD(P)H dehydrogenase complex interacts with photosystem I in Arabidopsis. J Biol Chem 283**,** 34873-34879.

Peng, L., Fukao, Y., Fujiwara, M., Takami, T., and Shikanai, T. (2009). Efficient operation of NAD(P)H dehydrogenase requires supercomplex formation with photosystem I via minor LHCI in Arabidopsis. Plant Cell 21**,** 3623-3640.

Perez-Ruiz, J.M., and Cejudo, F.J. (2009). A proposed reaction mechanism for rice NADPH thioredoxin reductase C, an enzyme with protein disulfide reductase activity. FEBS Lett 583**,** 1399-1402.

Perez-Ruiz, J.M., Guinea, M., Puerto-Galan, L., and Cejudo, F.J. (2014). NADPH thioredoxin reductase C is involved in redox regulation of the Mg-chelatase I subunit in Arabidopsis thaliana chloroplasts. Mol Plant 7**,** 1252-1255.

Perez-Ruiz, J.M., Spinola, M.C., Kirchsteiger, K., Moreno, J., Sahrawy, M., and Cejudo, F.J. (2006). Rice NTRC is a high-efficiency redox system for chloroplast protection against oxidative damage. Plant Cell 18**,** 2356-2368.

Pfundel, E.E., and Dilley, R.A. (1993). The pH Dependence of Violaxanthin Deepoxidation in Isolated Pea Chloroplasts. Plant Physiol 101**,** 65-71.

Puerto-Galan, L., Perez-Ruiz, J.M., Ferrandez, J., Cano, B., Naranjo, B., Najera, V.A., Gonzalez, M., Lindahl, A.M., and Cejudo, F.J. (2013). Overoxidation of chloroplast 2-Cys peroxiredoxins: balancing toxic and signaling activities of hydrogen peroxide. Front Plant Sci 4**,** 310.

Pulido, P., Spinola, M.C., Kirchsteiger, K., Guinea, M., Pascual, M.B., Sahrawy, M., Sandalio, L.M., Dietz, K.J., Gonzalez, M., and Cejudo, F.J. (2010). Functional analysis of the pathways for 2-Cys peroxiredoxin reduction in Arabidopsis thaliana chloroplasts. J Exp Bot 61**,** 4043-4054.

Reichheld, J.P., Meyer, E., Khafif, M., Bonnard, G., and Meyer, Y. (2005). AtNTRB is the major mitochondrial thioredoxin reductase in Arabidopsis thaliana. FEBS Lett 579**,** 337-342.

Reinhold, C., Niczyporuk, S., Beran, K.C., and Jahns, P. (2008). Short-term down-regulation of zeaxanthin epoxidation in Arabidopsis thaliana in response to photo-oxidative stress conditions. Biochim Biophys Acta 1777**,** 462-469.

Richter, A.S., Peter, E., Rothbart, M., Schlicke, H., Toivola, J., Rintamaki, E., and Grimm, B. (2013). Posttranslational influence of NADPH-dependent thioredoxin reductase C on enzymes in tetrapyrrole synthesis. Plant Physiol 162**,** 63-73.

Roach, T., and Krieger-Liszkay, A. (2012). The role of the PsbS protein in the protection of photosystems I and II against high light in Arabidopsis thaliana. Biochim Biophys Acta 1817**,** 2158-2165.

Rojas-Gonzalez, J.A., Soto-Suarez, M., Garcia-Diaz, A., Romero-Puertas, M.C., Sandalio, L.M., Merida, A., Thormahlen, I., Geigenberger, P., Serrato, A.J., and Sahrawy, M. (2015). Disruption of both chloroplastic and cytosolic FBPase genes results in a dwarf phenotype and important starch and metabolite changes in Arabidopsis thaliana. J Exp Bot 66**,** 2673-2689.

Ruban, A.V., Johnson, M.P., and Duffy, C.D. (2012). The photoprotective molecular switch in the photosystem II antenna. Biochim Biophys Acta 1817**,** 167-181.

Ruban, A.V., Lee, P.J., Wentworth, M., Young, A.J., and Horton, P. (1999). Determination of the stoichiometry and strength of binding of xanthophylls to the photosystem II light harvesting complexes. J Biol Chem 274**,** 10458-10465.

Sanz-Barrio, R., Corral-Martinez, P., Ancin, M., Segui-Simarro, J.M., and Farran, I. (2013). Overexpression of plastidial thioredoxin f leads to enhanced starch accumulation in tobacco leaves. Plant Biotechnol J 11**,** 618-627.

Schreiber, U., and Klughammer, C. (2009). New NADPH/9-AA module for the DUAL-PAM-100: Description, operation and examples of application. PAM Application Notes 2**,** 13.

Schurmann, P., and Buchanan, B.B. (2008). The ferredoxin/thioredoxin system of oxygenic photosynthesis. Antioxid Redox Signal 10**,** 1235-1274.

Serrato, A.J., Perez-Ruiz, J.M., Spinola, M.C., and Cejudo, F.J. (2004). A novel NADPH thioredoxin reductase, localized in the chloroplast, which deficiency causes hypersensitivity to abiotic stress in Arabidopsis thaliana. J Biol Chem 279**,** 43821-43827.

Serrato, A.J., Yubero-Serrano, E.M., Sandalio, L.M., Munoz-Blanco, J., Chueca, A., Caballero, J.L., and Sahrawy, M. (2009). cpFBPaseII, a novel redox-independent chloroplastic isoform of fructose-1,6-bisphosphatase. Plant Cell Environ 32**,** 811-827.

Shikanai, T. (2007). Cyclic electron transport around photosystem I: genetic approaches. Annu Rev Plant Biol 58**,** 199-217.

Shikanai, T. (2014). Central role of cyclic electron transport around photosystem I in the regulation of photosynthesis. Curr Opin Biotechnol 26**,** 25-30.

Shikanai, T., Endo, T., Hashimoto, T., Yamada, Y., Asada, K., and Yokota, A. (1998). Directed disruption of the tobacco ndhB gene impairs cyclic electron flow around photosystem I. Proc Natl Acad Sci U S A 95**,** 9705-9709.

Simionato, D., Basso, S., Zaffagnini, M., Lana, T., Marzotto, F., Trost, P., and Morosinotto, T. (2015). Protein redox regulation in the thylakoid lumen: The importance of disulfide bonds for violaxanthin de-epoxidase. FEBS Lett.

Spetea, C., Rintamaki, E., and Schoefs, B. (2014). Changing the light environment: chloroplast signalling and response mechanisms. Philos Trans R Soc Lond B Biol Sci 369**,** 20130220.

Spinola, M.C., Perez-Ruiz, J.M., Pulido, P., Kirchsteiger, K., Guinea, M., Gonzalez, M., and Cejudo, F.J. (2008). NTRC new ways of using NADPH in the chloroplast. Physiol Plant 133**,** 516-524.

Suorsa, M., Sirpio, S., and Aro, E.M. (2009). Towards characterization of the chloroplast NAD(P)H dehydrogenase complex. Mol Plant 2**,** 1127-1140.

Suorsa, M., Jarvi, S., Grieco, M., Nurmi, M., Pietrzykowska, M., Rantala, M., Kangasjarvi, S., Paakkarinen, V., Tikkanen, M., Jansson, S., and Aro, E.M. (2012). PROTON GRADIENT REGULATION5 is essential for proper acclimation of Arabidopsis photosystem I to naturally and artificially fluctuating light conditions. Plant Cell 24**,** 2934-2948.

Szabo, I., Bergantino, E., and Giacometti, G.M. (2005). Light and oxygenic photosynthesis: energy dissipation as a protection mechanism against photo-oxidation. EMBO Rep 6**,** 629-634.

Takizawa, K., Cruz, J.A., Kanazawa, A., and Kramer, D.M. (2007). The thylakoid proton motive force in vivo. Quantitative, non-invasive probes, energetics, and regulatory consequences of light-induced pmf. Biochim Biophys Acta 1767**,** 1233-1244.

Thapper, A., Mamedov, F., Mokvist, F., Hammarstrom, L., and Styring, S. (2009). Defining the far-red limit of photosystem II in spinach. Plant Cell 21**,** 2391-2401.

Thormahlen, I., Ruber, J., von Roepenack-Lahaye, E., Ehrlich, S.M., Massot, V., Hummer, C., Tezycka, J., Issakidis-Bourguet, E., and Geigenberger, P. (2013). Inactivation of thioredoxin f1 leads to decreased light activation of ADP-glucose pyrophosphorylase and altered diurnal starch turnover in leaves of Arabidopsis plants. Plant Cell Environ 36**,** 16-29.

Toivola, J., Nikkanen, L., Dahlstrom, K.M., Salminen, T.A., Lepisto, A., Vignols, H.F., and Rintamaki, E. (2013). Overexpression of chloroplast NADPH-dependent thioredoxin reductase in Arabidopsis enhances leaf growth and elucidates in vivo function of reductase and thioredoxin domains. Front Plant Sci 4**,** 389.

Tyystjarvi, E. (2013). Photoinhibition of Photosystem II. Int Rev Cell Mol Biol 300**,** 243-303.

Vanderauwera, S., Zimmermann, P., Rombauts, S., Vandenabeele, S., Langebartels, C., Gruissem, W., Inze, D., and Van Breusegem, F. (2005). Genome-wide analysis of hydrogen peroxide-regulated gene expression in Arabidopsis reveals a high light-induced transcriptional cluster involved in anthocyanin biosynthesis. Plant Physiol 139**,** 806-821.

Ventriglia, T., Kuhn, M.L., Ruiz, M.T., Ribeiro-Pedro, M., Valverde, F., Ballicora, M.A., Preiss, J., and Romero, J.M. (2008). Two Arabidopsis ADP-glucose pyrophosphorylase large subunits (APL1 and APL2) are catalytic. Plant Physiol 148**,** 65-76.

Yamamoto, H.Y., and Kamite, L. (1972). The effects of dithiothreitol on violaxanthin de-epoxidation and absorbance changes in the 500-nm region. Biochim Biophys Acta 267**,** 538-543.

Yamamoto, H.Y., Wang, Y., and Kamite, L. (1971). A chloroplast absorbance change from violaxanthin de-epoxidation. A possible component of 515 nm changes. Biochem Biophys Res Commun 42**,** 37-42.

Yoshida, K., Hara, S., and Hisabori, T. (2015). Thioredoxin Selectivity for Thiol-based Redox Regulation of Target Proteins in Chloroplasts. J Biol Chem 290**,** 14278-14288.

Yoshida, K., Matsuoka, Y., Hara, S., Konno, H., and Hisabori, T. (2014). Distinct redox behaviors of chloroplast thiol enzymes and their relationships with photosynthetic electron transport in Arabidopsis thaliana. Plant Cell Physiol 55**,** 1415-1425.

Zhang, H., Whitelegge, J.P., and Cramer, W.A. (2001). Ferredoxin:NADP+ oxidoreductase is a subunit of the chloroplast cytochrome b6f complex. J Biol Chem 276**,** 38159-38165.

Zhang, N., and Portis, A.R., Jr. (1999). Mechanism of light regulation of Rubisco: a specific role for the larger Rubisco activase isoform involving reductive activation by thioredoxin-f. Proc Natl Acad Sci U S A 96**,** 9438-9443.